Airborne measurements of trace gases using a Chemical Ionisation Mass Spectrometer (CIMS) onboard the FAAM BAe-146 research aircraft

A thesis submitted to the University of Manchester for the degree of

Doctor of Philosophy

In the faculty of Engineering and Physical Sciences

2013

Michael Le Breton

School of Earth, Atmospheric and Environmental Sciences

Contents

Abstract 6

Declaration 7

Copyright statement 8

Acknowledgements 9

Rationale for submitting thesis in alternative format 10

Flowchart of thesis progression 11

1 Introduction 12

1.1 Trace gases in the troposphere 12

1.2 Regional and global air quality issues 14

1.2.1 Photochemical pollution 14

1.2.2 Acid rain 15

1.2.3 Biomass burning 15

1.3 Quantifying the global and regional impacts of trace gases 16

1.3.1 Daytime chemistry 16

1.3.2 Nighttime chemistry 17

1.4 Production pathways of trace gases in the troposphere 18

1.4.1 Primary production of trace gases and O_3 19

1.4.2 Secondary production of trace gases such as HC(O)OH by reaction with O_3 20

1.5 Challenges in quantifying trace gas concentration 21

1.5.1 Atmospheric measurements 22

1.5.2 Instrumental challenges and selection criteria in measuring trace gases 23

1.5.2.1 Detection 23

1.5.2.2 Sampling inlet 23

1.5.2.3 Time response 24

1.5.2.4 Operational requirements for use on an aircraft 24

1.6 Measurements of trace gases 25

1.6.1 Nitric acid (HNO_3) 25

1.6.1.1 Filter techniques 25

1.6.1.2 Denuders 25
1.6.1.3 Aqueous scrubber 26
1.6.1.4 Laser Induced Fluorescence (LIF) 26
1.6.1.5 Instrument comparison for HNO_3 detection 26
1.6.1.6 Chemical Ionisation Mass Spectrometer (CIMS) 27
1.6.2 Formic acid (HC(O)OH) 27
1.6.2.1 Ion chromatography 27
1.6.2.2 Infrared spectroscopy (IR) 28
1.6.2.3 Mass spectrometry 28
1.6.3 Hydrogen cyanide (HCN) 29
1.6.3.1 Infrared spectroscopy 29
1.6.3.2 CIMS 29
1.6.3.3 Proton Transfer Mass Spectrometer (PTR MS) 30
1.6.3.4 Gas chromatography 30
1.6.4 Dinitrogen pentoxide (N_2O_5) 30
1.6.4.1 Indirect measurements via NO_3 30
1.7 Chemical Ionisation Mass Spectrometer (CIMS) 31
1.8 Ion chemistry 32
1.9 Aims of thesis 35
2 Paper A 39
3 Paper B 42
4 Paper C 44
5 Paper D 47
6 Conclusions 49
6.1 Instrumental conclusions 49
6.2 Observational conclusions 50
7 Further Work 52
7.1 Instrumental development 52
7.2 HC(O)OH uncertainties 53

7.3 Simultaneous measurements 53
7.4 Detection of new species 54
7.5 Criegee intermediate chemistry 55
8 References 57

List of figures and table

Figure 1. Example pathways for the production of photochemical pollutants. 14

Table 1: Estimated global budget of HC(O)OH sources and sinks to the atmosphere, including both primary and secondary sources (Paulot, *et al*., 2011) 21

Figure 2: A summary of the key atmospheric processes studied in this work. 19

Table 2: Current measurement techniques for nitric acid, formic acid, hydrogen cyanide and dinitrogen pentoxide 34

Table 3: Ionisation reagent gases and detectable species used in situ atmospheric measurements from 2006 to present 34

Figure 3: A schematic diagram of the chemical ionisation mass spectrometer (CIMS) used in this study from paper A. Dimensions are not to scale 32

Word count: 49 257

Abstract

A chemical ionisation mass spectrometer (CIMS) was developed and utilised for measurements onboard the Facility for Atmospheric Airborne Measurements (FAAM) BAe-146 aircraft. The I^- ionisation scheme was implemented to detect nitric acid (HNO_3), formic acid (HC(O)OH), hydrogen cyanide (HCN) and dinitrogen pentoxide (N_2O_5) simultaneously at a sampling frequency of 1 Hz. Sensitivities ranged from 35±6 ion counts $pptv^{-1}$ s^{-1} for HC(O)OH to 4±0.9 ion counts $pptv^{-1}$ s^{-1} for HCN and limits of detection from 37 ppt for HNO_3 and 5 ppt for HCN. Trace gas concentrations of species such as HC(O)OH are currently under predicted in global models. In order to understand their role in controlling air quality, it is crucial that their production pathways and abundance are accurately measured and constrained. To date, airborne measurements of these trace gases have been difficult as a result of instrumental limitations on an aircraft such as limit of detection and sampling frequency.

The first UK airborne measurements of HC(O)OH and HNO_3 confirmed that HC(O)OH is under predicted by up to a factor of 2 in a trajectory model that implements the full Master Chemical Mechanism (MCM) and Common Representative Intermediate Scheme (CRI). The inclusion of a primary vehicle source enabled the model to reproduce the concentrations observed; verifying that direct sources are under represented. Secondary formation of HC(O)OH was observed through its correlation with HNO_3 and ozone (O_3), indicating a strong photochemical production source. Hydroxyl (OH) concentrations were estimated for the first time in a flight around the UK using the HC(O)OH and HNO_3 measurements. A biomass burning (BB) plume identification technique is applied to data obtained from Canadian biomass fires using HCN as a marker. A 6 sigma above background approach to defining a plume resulted in a higher R^2 correlating value for the normalised excess mixing ratio (NEMR) to carbon monoxide (CO) when compared to current methods in the literature. The NEMR obtained from this work; 3.76±0.02 pptv $ppbv^{-1}$, lies within the range found in the literature. This NEMR is then used to calculate a global emission total for HCN of 0.92 Tg (N) yr^{-1} when incorporated into the global tropospheric model STOCHEM CRI. The first direct N_2O_5 airborne measurements on an aircraft at night are compared to indirect measurements taken by a broadband cavity enhancement absorption spectrometer. An average R^2 correlation coefficient of 0.87 observed over 8 flights for 1 Hz measurements indicates the selectiveness of the I^- ionisation scheme to detect N_2O_5 directly, without nitrate (NO_3) interference.

Declaration

I hereby declare that no portion of the work referred to in the thesis has been submitted in support of an application for another degree or learning qualification of this or any other university or any other institute of learning.

Michael Le Breton

Copyright statement

i. The author of this thesis (including any appendices and/or schedules to this thesis) owns any copyright in it (the "Copyright") and s/he has given The University of Manchester the right to use such Copyright for any administrative, promotional, educational and/or teaching purposes.

ii. Copies of this thesis, either in full or in extracts, may be made only in accordance with the regulations of the John Rylands University Library of Manchester. Details of these regulations may be obtained from the Librarian. This page must form part of any such copies made.

iii. The ownership of any patents, designs, trade marks and any and all other intellectual property rights except for the Copyright (the "Intellectual Property Rights") and any reproductions of copyright works, for example graphs and tables ("Reproductions"), which may be described in this thesis, may not be owned by the author and may be owned by third parties. Such Intellectual Property Rights and Reproductions cannot and must not be made available for use without the prior written permission of the owner(s) of the relevant Intellectual Property Rights and/or Reproductions.

iv. Further information on the conditions under which disclosure, publication and exploitation of this thesis, the Copyright and any Intellectual Property Rights and/or Reproductions described in it may take place is available from the Head of School of (*insert name of school*) (or the Vice-President) and the Dean of the Faculty of Life Sciences, for Faculty of Life Sciences' candidates.

Acknowledgements

I would like to thank my supervisor Professor Carl Percival who gave me the opportunity to further develop my academic knowledge and career. He allowed me to personally develop in many areas and was always available to offer his expertise and advice which was essential for my PhD completion. I would also like to thank my collaborators, Professor Dudley Shallcross, Dr Jennifer Muller, Dr Max Mcgillen, Dr Asan Bacak and Dr Murray Booth who allowed me to squeeze out their incredible knowledge to aid my PhD. The people at FAAM helped significantly with preparation for flying and efficiency of campaigns. I would also like to thank NERC for providing my studentship.

Rationale for submitting this thesis in the alternative format

The alternative thesis format was considered suitable as the research had an overall goal of implementing the CIMS for aircraft measurements, but independent themes were addressed and investigated, deeming the publication of papers appropriate. It is therefore considered to be fortuitous that this thesis could be completed in such a way.

The construction of the thesis format follows the progression of the research itself. Overleaf is a flow chart of how the research has developed. The finding from each paper allowed further development to be taken for the following research.

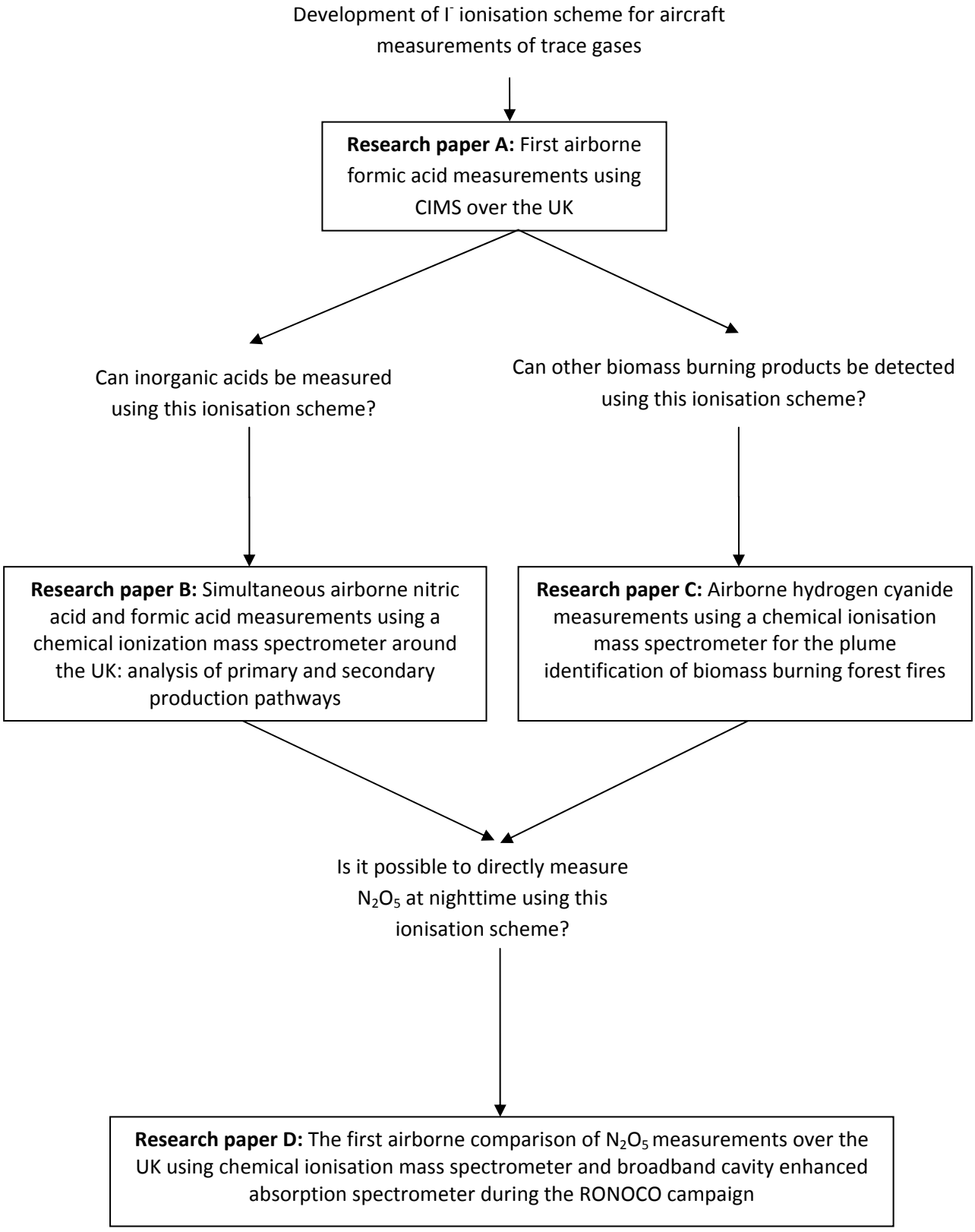

Flowchart showing the progression of the research contributing to this thesis.

1 Introduction

1.1 Trace gases in the troposphere

The troposphere is the lowest section of the Earth's atmosphere and contains approximately 80% of its mass and 99% of its water vapour and aerosols (Barry & Chorley, 1992). Atmospheric phenomena such as convection, turbulence and clouds occur here; consequently making the troposphere the determining factor controlling the atmosphere that supports life. Since the seminal paper of Haagen-Smit (1950) it has been acknowledged that trace gas chemistry and tropospheric concentrations of trace species can play an important role in controlling air quality and climate. A number of pollutants are known to have deleterious effects on humans, plant life and buildings at concentrations often found in polluted air, such as the emissions from highly populated areas (Bascin *et al*., 1996a,b; Xu *et al.*, 2011). Species such as zone (O_3), carbon monoxide (CO) and nitrogen dioxide (NO_2) are known as "criteria pollutants" and are considered good indicators of air quality (WHO, 2000). The World Health Organization provide recommended threshold concentrations of these pollutants which must not be exceeded in order to protect human health. In addition to these criteria pollutants, a wide variety of trace gases have been observed in the polluted troposphere, such as organic acids (Veres *et al*., 2008). These trace gases affect air quality through their own chemical characteristics, but also play a substantial role in the chemical cycling of criteria pollutants. For example, HNO_3 acts as an atmospheric sink for NO_x and therefore controls tropospheric O_3 production; a prominent daytime pollutant (Brown *et al*., 2004), but also can increase cloud water pH; contributing to acid rain (Finlayson-Pitts 2000).

The ubiquitous nature of many trace gases is demonstrated through their partitioning to the aerosol phase and subsequent ability to alter the radiation balance of the atmosphere. Aerosols can scatter and absorb incoming shortwave radiation and absorb outgoing longwave radiation; the aerosol direct effect (McCormick and Ludwig, 1967; Haywood and Boucher, 2000). They can also act as cloud condensation nuclei (CCN), changing the number of droplets which subsequently affects the cloud albedo; the indirect effect (Twomey, 1974; McFiggans *et al*., 2006). Low molecular weight salts, formed by organic acid dissolution, are present in the fine fraction of aerosols. These aerosols possess relatively low critical supersaturations which enable the activation of cloud

droplets and therefore change the total indirect radiative forcing (Yu *et al.,* 2000). The formation of particulate matter can also be governed by the relative concentrations of their gaseous precursors. Ammonium nitrate (NH_4NO_3) aerosol formation is governed by the relative concentrations of HNO_3 and ammonia as shown in R1 and R2, confirming that measurements of HNO_3 are integral to accurately quantify the cooling effect that NH_4NO_3 has on the climate (Forster *et al*., 2003).

$$NO_2 + OH + M \rightarrow HNO_3 + M \quad \textbf{R1}$$

$$HNO_{3(g)} + NH_{3(g)} \leftrightharpoons NH_4NO_{3(s)} \quad \textbf{R2}$$

The concentration of key pollutants, such as NH_4NO_3, can vary regionally and globally as their production and loss is controlled by a number of varying precursor reactions. NO_x levels, which are pertinent to O_3 production, can be influenced by a series of competing chemical pathways initiated by photolysis. The concentration and types of species controlling the production pathways are dependent on geographical location. An example of such variation is seen at nighttime where nitrogen dioxide (NO_2) concentrations increase as a result of the termination of its photolysis, initiating an increase in the following days O_3 production (Atkinson *et al*., 2000), as shown in R3 and R4. However an increase in possible sinks, such as N_2O_5 formation (R5), which could further react with water vapour to form HNO_3, decreases the nighttime NO_x concentration and therefore the following days O_3 production potential (Brown *et al*., 2004). This variation in production results in difficulties in estimating regional and global climatic impacts and air quality.

$$NO_2 + hv \rightarrow NO + O(^3P) \quad \textbf{R3}$$

(*hv*, $\lambda \leq 420$ nm)

$$O(^3P) + O_2 \rightarrow O_3 \quad \textbf{R4}$$

$$NO_3 + NO_2 + M \leftrightharpoons N_2O_5 + M \quad \textbf{R5}$$

1.2 Regional and global air quality issues

Trace gas sources in the troposphere can originate directly from primary emissions or indirectly via atmospheric chemistry creating secondary products. This variation in the emission of trace gases creates a heterogeneous composition of the atmosphere. Varying meteorological conditions and topology affect the distribution of these species and allow global and regional air quality issues to develop.

1.2.1 Photochemical pollution

Anthropogenic activity in major urban areas is an important source of primary pollutants such as NO_x and volatile organic compounds (VOCs) (Kim *et al.*, 2011). Low wind speeds and high incoming solar radiation allows the concentration of pollutants to build up and undergo photochemical reactions to form a variety of secondary pollutants such as O_3, HNO_3, and HC(O)OH (Grosjean *et al.*, 2001) as demonstrated in figure 1.

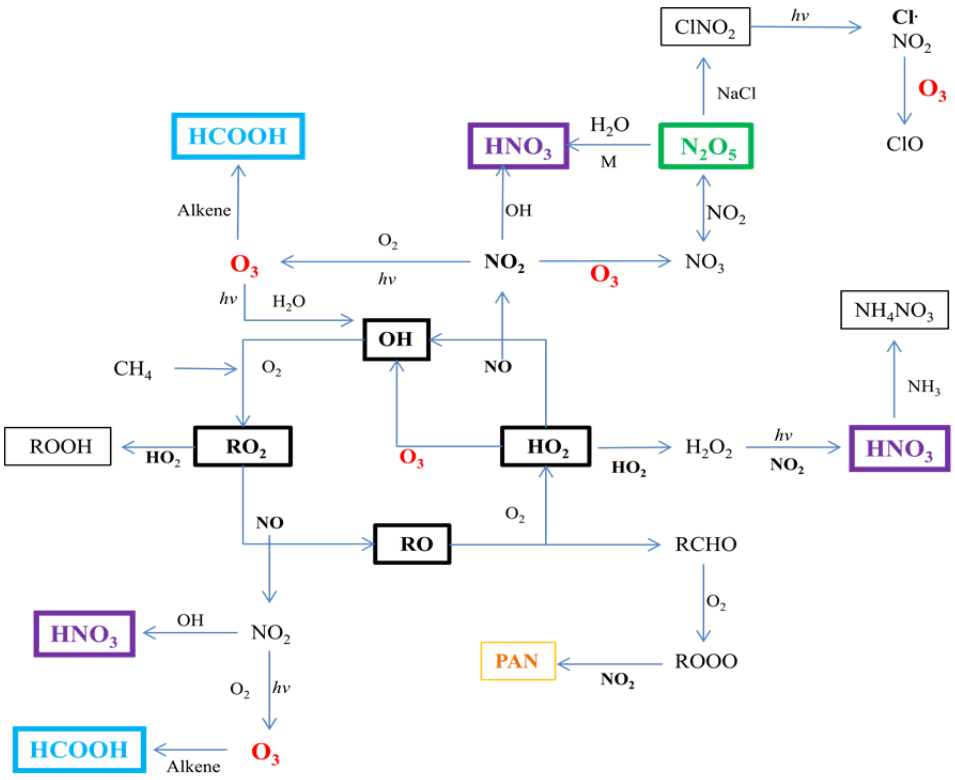

Figure 1: Example pathways for the production of photochemical pollutants. Gases with coloured boxes represent the species measured in this research.

An example of this photochemical pollution is observed in Los Angeles as smog. The smog is especially harmful to the elderly and children as it can inflame breathing passages and interfere with the body's ability to fight infection and trigger asthma (Okwada *et al*., 1979). The production of these pollutants is controlled by the precursors available i.e. the prominent tropospheric pollutant here, O_3, is dependent on NO_2 concentrations present (Stedman and Niki, 1973). NO_2 loss via the creation of N_2O_5 at night by reaction with NO_3, R5, or OH reaction during the day to form HNO_3, as shown by R1, limits the O_3 production (R3 and R4). Therefore knowledge of localised HNO_3 or N_2O_5 production can help evaluate the following days O_3 production potential and therefore the possibility of photochemical smog.

1.2.2 Acid rain

Acid rain predominantly arises from the oxidation of sulphur dioxide (SO_2) and NO_2 in the troposphere to form sulphuric acid (H_2SO_4) and HNO_3 respectively (Finalyson and Pitts, 2000). HNO_3 can dissolve into cloud droplets after being formed by R1, leading to low pH values in fogs and precipitation. Organic acids such as HC(O)OH can also significantly contribute to this rain water acidity (Keene and Galloway, 1997). Acid fogs are known to effect cities such as London and are a major health concern as the water droplets are small enough to be inhaled (Hoffman, 1984; Bowes *et al*., 1995). The deposition of these acidic particles can also cause damage to buildings through the corrosion of stones and metals such as bronze. The addition of this acid rain into water can also disrupt freshwater ecosystems by lowering the pH level. The surrounding soil may not be able to buffer the water to a neutral pH, resulting in a release of aluminium from soils into the water, which is toxic to many aquatic organisms (Kochian, 1995).

1.2.3 Biomass burning (BB)

Naturally occurring events such as forest fires have an important role in determining the composition of the atmosphere. The emissions from forest fires are known to be a major contributor of trace gases and aerosols, with the ability to change air quality on a regional and global scale. Pyrogenic species such as carbon dioxide (CO_2), carbon monoxide (CO), hydrogen cyanide (HCN), HC(O)OH and VOCs are emitted and transformed by photochemical processes within the plumes and can alter the distribution of tropospheric O_3 via the formation and subsequent photolysis of NO_2, changing the

oxidising capacity of the atmosphere (Coheur *et al*., 2007). Many of the species emitted can independently affect air quality, such as HCN. HCN is extremely poisonous as it binds irreversibly to the iron atom in haemoglobin in blood making it unavailable to transport oxygen to the body's cells and tissues (Cummings, 2004). BB plumes can reach the stratosphere and therefore allow the global transport of these important species, impacting regional and global air quality (Levine, 2000). In order to assess the impact these events have on human health and air quality, detailed measurements of their chemical components, development and transport are necessary.

1.3 Quantifying the global and regional impacts of trace gases

In order to accurately represent the roles which trace gas emissions play in the atmosphere and the impact they have on air quality and climate, global emissions calculated by models must not only include accurate emission factors for all production pathways, but also ensure that the variance in their strength and dominance geographically is accounted for as concentrations of these species will vary with latitude, longitude, altitude, temperature, pressure, solar intensity, meteorological conditions and concentration of other reactive species present. The transition between day and night dramatically changes the atmospheric chemistry and therefore allows different mechanisms to control production and loss rate of key tropospheric species.

1.3.1 Daytime chemistry

Oxidation processes in the troposphere initiates the removal of trace gases, subsequently leading to the formation of CO_2 and water vapour. Although oxidation can proceed via halogen chemistry, i.e chlorinated species, tropospheric O_3 is predominantly formed via the photolysis of NO_2. O_3 is a highly reactive species whose concentrations far exceeds that of OH (Knipping and Daddub, 2003), allowing ozonolysis of alkenes to compete to be the dominant sink of alkenes in the troposphere (Goldstein *et al*., 2004). Ozonolysis is thought to be a dominant source of organic acids, which current models underestimate (Leather *et al*., 2012; Paulot *et al*., 2011). As a result of a lack of field measurements, there is considerable uncertainty in the magnitude of this underestimation.

O_3 is photolysed to form O^1D, which then rapidly reacts with water vapour to form OH (Levy, 1971). The OH radical is able to react with a vast array of tropospheric species

such as carbon monoxide (CO), hydrocarbons, VOCs such as methane and formaldehyde, hydrofluorocarbons (replacements of CFCs) and SO_2 (Stone *et al*., 2012). HNO_3 formation via the reaction between OH and nitrogen dioxide (NO_2), R1, plays an important role in controlling the tropospheric O_3 budget (Kita *et al*., 2005) by providing a sink for NO_x. Potential O_3 production is further limited as the OH is no longer available to initiate VOC oxidation and produce RO_2 which further reacts with NO to form NO_2. HNO_3 also condenses to form NH_4NO_3 (Seinfeld and Pandis, 1998), a major component of urban aerosols (Kaneyasu *et al*., 1999, Moya *et al*., 2001) and thought be a key compound in global cooling across Europe (Adams *et al*., 2001; Jacobson, 2001; Liao *et al*., 2004).

1.3.2 Nighttime chemistry

OH concentrations peak during the day (~0.4 ppt) and decrease to near zero at night as O_3 is not photolysed (Hausmann *et al.,* 1997). This decrease in OH concentration enables the nitrate radical (NO_3) to replace OH as the main tropospheric oxidising species (Wayne *et al*., 1991). Nighttime oxidation by NO_3 is comparable to the removal of NO_x by OH during the day (Atkinson, 1991). The termination of O_3 photolysis at night allows the reaction between NO_2 and O_3 dominate and produce NO_3, which can then further react with NO_2 to form N_2O_5, R5. NO_3 and N_2O_5 concentrations therefore increase at nighttime in thermal equilibrium.

N_2O_5 can react with water on the surface of aerosols to form HNO_3 as shown in R6, acting as a sink for NO_3 and NO_x, which subsequently affects the following days O_3 concentrations due to the limitation of NO_2 available for photolysis (Brown *et al*., 2004).

$$N_2O_5 + H_2O_{aerosol} \rightarrow 2HNO_3 \qquad \textbf{R6}$$

Nighttime NO_x termination can also be as a result of N_2O_5 loss onto the surface of aerosols, as observed by the efficient production of $ClNO_2$ on sea salt particles (Osthoff *et al*., 2008). N_2O_5 can react with hydrogen chloride (HCl) on the surface of aerosols producing high yields of $ClNO_2$ at night (Thornton *et al*., 2010). This steady build up produces high $ClNO_2$ concentrations at sunrise which dissociates via photolysis to produce Cl and NO_2. This Cl formation enhances the oxidation rates of VOCs and

subsequently increases photochemical production of O_3 (Simon *et al*., 2009). Halogen activation (from $ClNO_2$ formation) can also affect aerosol formation and the lifetime of important trace gases such as methane. However, the impact of halogen activation on regional air quality is uncertain as a result of limited measurements of N_2O_5 and the halogenated species (Simpson *et al*., 2007).

N_2O_5 formation and its subsequent reactions represent major sinks of NO_3 and NO_x at night. Knowledge of the relationship between NO_3 and N_2O_5, and their nighttime heterogeneous chemistry is crucial to understand the impact that NO_3 chemistry can have on O_3 concentrations and regional air quality (Atkinson, 2000). Therefore accurate measurements of N_2O_5 are necessary to further our understanding of nighttime chemistry.

1.4 Production pathways of trace gases in the troposphere

Trace gases are produced via a number of different primary and secondary pathways which must be accounted for in models to understand their role in the atmosphere. Figure 2 summarises the varying production pathways of the key species for this work. The oxidising capacity of the troposphere and air quality is constrained via many of the mechanisms in figure 2 as they involve the production and loss of O_3 and OH. Constraining the formation pathways of these trace species will provide further insight to the availability of the main oxidants in the troposphere.

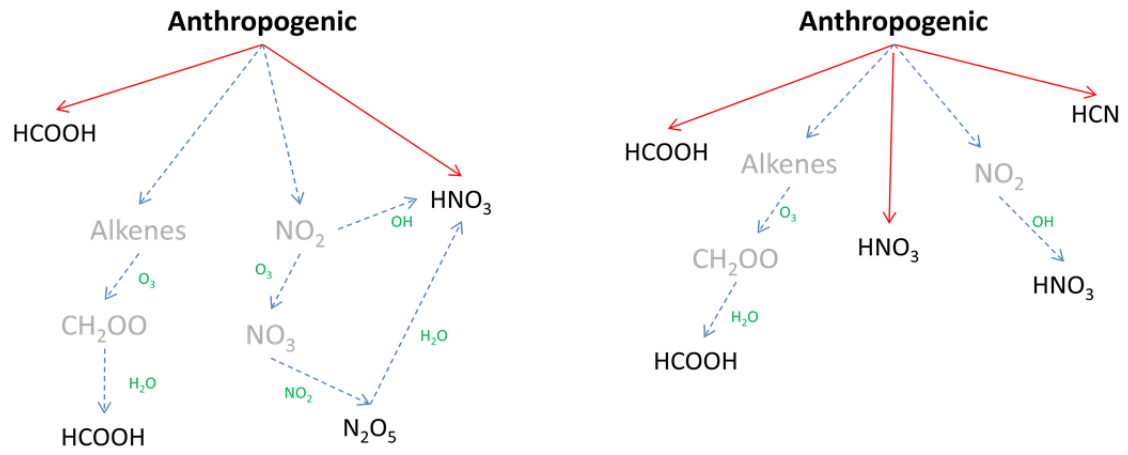

Figure 2: A summary of the key atmospheric processes studied in this work, separated into primary, secondary, natural and anthropogenic pathways. Full red lines represent direct production and dotted blue represents a secondary pathway. The reactive gases producing the species of interest are in green.

1.4.1 Primary production of trace gases and O_3

The lifetime of O_3 can vary from minutes in the troposphere, as a result of photochemical destruction and dry deposition, to weeks in the free troposphere where it can be transported across the globe and therefore affect tropospheric composition and chemistry. O_3 production from the precursors of the outflow from North America are often distributed over the North Atlantic and Europe, (Fehsenfeld *et al*., 2006). In order to understand this outflow; knowledge and quantification of the formation of the precursors are essential. One major source of these precursors is BB fires (Li *et al*., 2000, 2003, 2009; Shim *et al*., 2007). Trace gases emitted directly from BB, such as HC(O)OH and HCN (Burling *et al*., 2010) can be used as markers for BB and can give an insight into how these plumes develop over long distances. HCN has an atmospheric lifetime of 5 months in the troposphere if wet deposition does not occur (Hamm and Warneck, 1990; Li *et al*., 2003) and a few years in the stratosphere (Cicerone and Zellner, 1983; Brasseur *et al*., 1985). As a consequence of the limited sources of HCN in the atmosphere, HCN measurements can be used as a BB plume marker and therefore utilised to estimate global emissions of important VOC`s emitted during BB by deducing normalised excess mixing ratios.

1.4.2 Secondary production of trace gases such as HC(O)OH by reaction with O_3

Trace gas species such as HC(O)OH can be emitted directly (as stated above) or indirectly through a number of different reactions. Table 1 shows the largest emission of HC(O)OH to the atmosphere is via photochemical production and largest sinks are wet and dry deposition. The secondary production of HC(O)OH is currently under-predicted in models as a result of uncertainty in the source strengths of the different formation pathways. For example, ozonolysis of alkenes is thought to be a source of HC(O)OH which is underestimated in current models (Stavrakou *et al*., 2012). A build up of O_3 in the presence of alkenes can lead to the production of the Criegee intermediates (CIs) (Taatjes *et al*., 2008; Leather *et al*., 2011). If the CIs are collisionally stabilised, then the lifetime of CIs with respect to bimolecular reaction becomes comparable to that of decomposition and reaction with water vapour leading to the formation of carboxylic acids such as HC(O)OH, as observed by Wolff *et al*., (1997) and Orzechowska and Paulson, (2005).

Formation of organic acids via the reaction of CIs is an important secondary pathway which is thought to dominate in Savannah regions (Sanhueza *et al*., 1996) creating levels of up to 1 ppbv. All sources must be accurately constrained in global models if the impact of organic acids on acidity of global precipitation (Keene and Galloway, 1983), the influence of organic acids on pH-dependent chemical reactions and OH cloud chemistry (Jacob *et al*., 1986) and the impact of organic acids on oxidising capacity of the atmosphere are to be quantified.

Table 1: Estimated global budget of HC(O)OH sources and sinks to the atmosphere, including both primary and secondary sources (Paulot, *et al*., 2011).

Origin	Process	Global HC(O)OH estimates / Gmol yr^{-1}
Photochemical Production	Biogenic	917
	Anthropogenic + biomass burning	138
Primary Emissions	Fossil fuel	3.5
	Biofuel burning	6.5
	Biomass burning	32.5
	Cattle	39.5
	Soil	39
Primary Emission (Biogenic)	Terrestrial Vegetation	56 (20-130[a] Forest emission)
	Formicine Ants	(10)[a]
	Photochemical	229.5
Sinks	Dry Deposition	536
	Wet Deposition	437.5
	Dust	30

[a] signifies previous data collected by Kesselmeier & Staudt, (1999)

1.5 Challenges in quantifying trace gas concentration

This complex interlinking system of reaction pathways throughout the atmosphere creates a variability which cannot be simply defined within global emission models as a result of the atmospheric chemical cycling and sources, as table 1 highlights for HC(O)OH. (von Kuhlmann *et al*., 2003; Rinsland *et al*., 2004; Paulot *et al*., 2011)**.** Not only must all sources of important atmospheric species be quantified, but the variance in source dominance of trace gases at different locations and in different conditions must be accounted for; e.g. primary emissions from anthropogenic activity to isoprene oxidation in the Amazon rainforest. The lifetime of these species will also vary depending on the air masses composition, age, geographical location horizontally and vertically and meteorological conditions. The knowledge we have about the different source strengths, locations and importance of meteorology is from direct observations. Therefore to capture and quantify the different sources/processes by measurements of a large range of species, the development of instrumentation and design of field

experiments and monitoring schemes must be ongoing to improve our understanding of their relevance to atmospheric chemistry and air quality issues.

1.5.1 Atmospheric measurements

To accurately characterise the individual effects these species have on the global climate and air quality, the quantification of the concentration of these species from all production pathways is crucial. Atmospheric measurements are essential in predicting future changes to the atmosphere and are necessary in the development of government policies and legislation. Understanding trace gas chemical abundance, behaviour and their effect on the global climate is one of the most important challenges facing current and future society.

Although field measurements, laboratory studies and models are all necessary to gain a complete understanding of the complex processes within the atmosphere, field observations have played a role in major breakthroughs in atmospheric science, as observed for the detection of the O_3 hole in the polar stratosphere. Molina and Rowland (1974) suggested that chlorofluorocarbons would destroy O_3 as a result of laboratory measurements; however this would not have been verified without the development of sensitive and accurate field instruments allowing Farman *et al* (1985) to discover a reoccurring springtime O_3 hole. This was confirmed with *in situ* data showing an anti correlation between ClO and O_3 (Anderson *et al*., 1989). This demonstrated the need for field measurements to increase our knowledge of how trace gas chemistry contributes to air quality.

1.5.2 Instrumental challenges and selection criteria in measuring trace gases

Making trace gas measurements in the troposphere brings with it many technological challenges. As concentrations range from a few % to ppq (parts per quadrillion or 1 part in 10^{15}), the measuring instrument must be able to efficiently detect these gases with a limit of detection below the atmospheric variance of the species, but also must not suffer from measurement inaccuracies or low resolutions when encountering high concentrated plumes. Atmospheric concentrations of HNO_3 can range from tens of ppb down to tens of ppt (4 orders of magnitude). Instruments must be able to accurately measure the low

concentrations immediately after the high concentrations without suffering from a high background which is a common problem due to its "sticky" nature (i.e. adsorbing onto surfaces inside the instrument) (Neuman *et al., 1999)*. The importance of trace gases in the troposphere is not dependent on their absolute concentration, as seen for HNO_3, as concentrations of ppt can have considerable implications for atmospheric chemical cycling.

1.5.2.1 Detection

The selection criteria for the measurements of atmospheric species are dependent on the species of interest. The minimum detectable amount must also be significantly less than the atmospheric concentration of the analyte. The detection method must produce a unique signature for the analyte. For example, ethanol and HC(O)OH have similar molecular weight (46.07 and 46.03 respectively), therefore making it difficult to quantify HC(O)OH or ethanol concentrations using PTRMS (Paulot *et al*., 2011) as the masses cannot be separately resolved. Chemical Ionisation Mass Spectrometer (CIMS) does not detect ethanol using the I^- reagent ion and therefore has one unique peak at 173 atomic mass units (amu) (HC(O)OH adduct with I^-).

1.5.2.2 Sampling/inlet

Limiting the interaction of an air sample with the instrument`s artefact is critical as it impedes the accuracy of the measurements by creating an instrumental background which can often be an issue for measurements of "sticky" species such as HNO_3. Detailed research has been taken into possible ways of reducing the wall loss effect that measurements of such species suffer from (Neuman *et al*., 1999). Inlet material and heaters are a determining factor in the magnitude of this loss. A variety of materials have been analysed such as silicone coated quartz (Horri, 2002) and hydrophobic roughened surfaces (Evans *et al*., 2005), although perfluoroalkoxy (PFA) is commonly used in atmospheric research because of its inertness (Neuman *et al*., 1999).

1.5.2.3 Time response

Atmospheric lifetime is defined by the concentration of a species to decay to 1/e (37%) of its original concentration. The time between the collection of the air sample and measurement of a species must be shorter than the atmospheric lifetime of the species of

interest, consequently making measurements of short lived species such as OH extremely difficult as it has a daytime tropospheric lifetime of around 1 second (Monks, 2005). NO_3 measurements must also have a high sampling frequency as it has an average nighttime lifetime of 89 seconds (Li *et al*., 2012) and 5 seconds in the daytime (Monks, 2005). A high measurement frequency also allows for in detail plume measurements to be taken from aircraft. The fast time response of an instrument is crucial if measurements are made on a moving platform, i.e. aircraft. The average science speed of the BAe 146 FAAM research aircraft when acquiring data is 100 ms^{-1}. In order to be able to detect a plume 1 km wide, the time response of an instrument must be better than 10 seconds to acquire 1 data point, which is not extremely useful to extract valuable information from. In reality, many plumes can be much smaller than this, limiting the detection to high frequency measurements. Obtaining knowledge of plume development is only possible with instruments with very high measurement frequencies.

1.5.2.4 Operational requirements for use on an aircraft

The operational requirements of the instrument are important if the species exhibit spatial variation due to different sources, such as altitudinal limits. Instruments on board the aircraft must overcome logistical limitations set by the aircraft itself. The rack which the instrument is positioned and mounted on must not exceed a set weight and size due to the limiting load of the aircraft. Power to the aircraft is only available for a set time before and after a flight. Therefore, instruments must be able to perform at 100% efficiency within a few hours with instrumental necessities such as vacuum pressures being met within this time. Pre and post flight calibrations must also be performed within a short time as the power is not available continuously.

1.6 Measurements of trace gases

The development of trace gas measurements has furthered our knowledge of atmospheric chemical processing, mechanisms and interconnections, but also improved the accuracy of global models by quantifying their under prediction through laboratory and field measurements (Leather *et al*., 2011, Stavrakou *et al.,* 2011). The following section reviews the different methods applied to the measurements of important trace gases and is summarised in table 2.

Table 2. Current measurement techniques for nitric acid, formic acid, hydrogen cyanide and dinitrogen pentoxide.

Species	Instrument	Comments
Nitric acid	Filter techniques	Low time resolution and requires offline analysis
	Denuders	Has converter efficiency issues and time resolution of several hours
	Aqeous scrubbers	Low limits fo detection (10`s ppt) but has interfence with nitrate aerosol
	LIF	High time resolution (seconds) and low limit of detection (90 ppt) but has interference from particulate nitrate
	CIMS	Low limit of detection (10`s ppt) , high sampling frequency (1 Hz) and high sensitivity (10`s counts per ppt per second)
Formic acid	Ion chromatography	High limits of detection and offline analysis
	Infrared spectroscopy	Colum measurements and need of *a-priori* profiles causing large errors
	Mass spectrometry	Low limit of detection (10 ppt) , high sampling frequency (1 Hz) and high sensitivity (10`s counts per ppt per second)
Hydrogen cyanide	Infrared spectroscopy	FTIR can have integration time sof sub 1 Hz, but only for high concentrations > 5 ppb. Lack of resolution with profiles
	CIMS	Low limit of detection (10`s ppt) , high sampling frequency (1 Hz) and high sensitivity (10`s counts per ppt per second)
	PTR MS	High sensitivity and measaurement frequency (1 Hz). Exhibits a high temperature and humidity dependance. Interference with ethene.
	Gas chromatography	Low limit of detection (30 ppt). Requires 5 minute data average merge. High accuracy.
Dinitrogen Pentoxide	Indirect measurements	Fast measurement frequency (1 Hz) and low limit of detection (1 ppt). High sensitivity and proven for accurate aircraft measurements
	CIMS	Low limit of detection (5 ppt) , high sampling frequency (1 Hz) and high sensitivity (10`s counts per ppt per second)

1.6.1 Nitric acid (HNO_3)

1.6.1.1 Filter techniques

HNO_3 measurements are notorious for being difficult to make due to the "sticky" nature of HNO_3 which results in high instrumental background concentrations, interfering with true ambient concentrations (Crosley, 1996; Parrish and Fehsenfeld, 2000). Appel *et al*., (1980) measured HNO_3 using filter packs by sampling the gas on a nylon filter after separation using a Teflon filter and then ion chromatography to determine the concentration. This method suffers from a low time resolution due to the offline analysis and potential inaccuracies caused by adsorption onto the first particle filter (Goldan *et al*. 1983). Further, displacement of particle nitrate on the filter by strong acids may also decrease the accuracy (Finlayson–Pitts 2000).

1.6.1.2 Denuders

Denuders have been implemented for HNO_3 detection via detecting total NO_y by converting all NO_y compounds to NO using a molybdenum converter at 350 °C (Landis *et al*., 2002). Chemiluminescence relies on HNO_3 solely reacting with the KCl (Landis *et al.*, 2002). Denuder measurements suffer from converter efficiency issues (Landis *et al*, 2002) and a low time resolution of several hours.

1.6.1.3 Aqueous scrubbers

Aqueous scrubbers using liquid chromatography measure the sum of nitrous acid (HONO) and HNO_3 (Huang *et al.,* 2002). HNO_3 is calculated by using two separate channels where one will only measure HONO. Although this enables the concentrations of HNO_3 to be calculated, the error on the measurements can increase when ratios of HONO:HNO_3 are high. The limit of detection is useful for tropospheric measurements of HNO_3 (20ppt), but nitrate aerosols interferences with the measurement as they are also scrubbed and low time resolutions (10 minutes) inhibit aircraft use to detect plumes and fluxes.

1.6.1.4 Laser induced fluorescence (LIF)

Laser induced fluorescence (LIF) spectroscopy measures NO_2 after thermally dissociating HNO_3 to NO_2 at 500 $^{\circ}$C (Day *et al*., 2002). This method can be implemented for airborne measurements of HNO_3 (Aruffo *et al* 2012) due to its high time resolution,

1Hz, and low limit of detection (LOD) (90ppt), although interference from particulate nitrate can increase the LOD dramatically up to 1 ppb (Day *et al*., 2002).

1.6.1.5 Instrument comparison for HNO_3 detection

A field intercomparison using a suite of instruments including filter packs, tunable diode laser absorption spectrometers, a mist chamber, laser photolysis and a diffusion scrubber measuring HNO_3 was taken by Gregory *et al*. (1990). Many of the instruments showed poor agreement when measuring low ppt levels of HNO_3 (100 ppt) such as filter pack, tunable diode laser absorption and denuder; common concentrations found in the troposphere. The mist chamber (Talbot *et al*., 1990), diffusion scrubber (Komazaki *et al*., 2001) and laser photolysis fragment fluorescence (Papenbrock and Stuhl, 1990) do not suffer from inaccuracies at low concentrations but were found to take up to 10 minutes to reach such a detection limit due to absorption of HNO_3 onto the walls of the inlet. High frequency online measurements of HNO_3 are limited due to its stickiness to inlet walls and materials, stressing the importance for the choice of inlet material (Neuman *et al*., 1999).

In 1998 the filter pack technique was compared to measurements of HNO_3 using two CIMS instrument (Fehsenfeld 1998). It was found that the two CIMS had a good agreement (within 10%) whereas the filter pack often over estimated concentrations due to the dissociation of NH_4NO_3 on the first filter. This further indicated the ability for CIMS to accurately measure HNO_3 with a low sensitivity and fast time response.

1.6.1.6 Chemical Ionisation Mass Spectrometer (CIMS)

Arnold and Hauck (1985) and Huey *et al*. (1998) developed a CIMS technique to measure HNO_3 with a limit of detection of around 10 ppt and integration time of a few seconds. This was then implemented by Neuman *et al*., (2001) for lower stratospheric and upper tropospheric measurement with a limit of detection of 30 ppt and time response of 1 second. Further campaigns by Neuman *et al*., (2002) allowed boundary layer measurements of HNO_3; indicating the reliability of CIMS HNO_3 measurements at a range of altitudes in the atmosphere with a high sensitivity, low limit of detection at a fast time resolution.

Measurements of HNO_3 using CIMS have been taken by Veres *et al*., (2008, 2011), verifying its proficient ability to sensitively measure HNO_3 at a high frequency. Although CIMS has been proven to be a useful technique for airborne HNO_3 measurements in the United States, no campaigns had taken measurements around the United Kingdom before 2011.

1.6.2 Formic acid (HC(O)OH)

1.6.2.1 Ion chromatography

Initial measurements of HC(O)OH were made using liquid ion chromatography with ultraviolet detection (Grosjean *et al*., 1990) and sodium carbonate denuder tubes (Norton *et al*., 1992) implementing ion chromatography with conductivity detection. Both of these methods suffer from high limits of detection and low time resolution as they require offline analysis.

1.6.2.2 Infrared spectroscopy

Infrared spectroscopy enabled the first airborne measurements of HC(O)OH (Worden *et al*., 1997) which allowed column densities to be taken, although the detection limit was often above the ambient concentrations.

A pulsed quantum cascade laser has been used on board an aircraft over New England which simultaneously measured formaldehyde (HCHO) and HC(O)OH (Herndon *et al*., 2007). This method has a time resolution of 60 seconds and suffers from cross interference with water.

The first satellite measurements by Rinsland *et al*., (2006) using a Fourier Transform Infrared Spectrometer (FTIR) allowed mixing ratios in the upper troposphere to be determined with a 2 second time resolution. However, the accuracy of satellite measurements is limited at altitudes lower than 11 km as an "*a priori*" vertical profile is implemented and can lead to error up to 31% (Zander *et al*., 2010).

Infrared Atmospheric Sounding Interferometer (IASI) has also successfully measured column densities (Coheur *et al*., 2009) to retrieve vertical profiles of HCOOH. FTIR

satellite measurements of HC(O)OH have produced vertical mixing ratios down to 5 km with a statistical error in concentration of 50% (Gonzalez *et al*., 2009).

1.6.2.3 Mass spectrometry

A tandem mass spectrometer was utilised by Chapman (1995) using ratios of parent to daughter ions by successive collisions in order to determine HC(O)OH concentrations. The two quadrupoles are used to ionise then fragment the ions in order to produce unique ions for the species of choice. Collision conditions are often insufficient to fragment the parent ion thus the parent ions intensity is measured. Recently Veres (2008), Roberts *et al*., (2010, 2011) and Bertram *et al*. (2011) have shown how CIMS can be used to selectively detect gas-phase organic acids with a limit of detection below 0.1 ppb for 1 second measurements. This means HC(O)OH can be measured accurately in the troposphere at a high time resolution and with limited interferences. Sensitivities such as 23 counts per second per ppt have been achieved to enable this fast time response at low detection levels (Veres *et al*., 2008).

1.6.3 Hydrogen Cyanide (HCN)

1.6.3.1 Infrared spectroscopy

Column measurements of HCN can be obtained using Infrared Spectroscopy (IR) (Coffey *et al*., 1981; Zhao *et al*., 2002; Kleinbohl *et al*., 2006; Rinsland *et al*., 2007). Accurate tropospheric concentrations are limited using this technique due to the lack of resolution and ability to quantify vertical profile concentrations below 11 km (Rinsland *et al*., 2000). Yokelson *et al.* (2011) measured HCN from forest fires in Mexico onboard an aircraft using an FTIR capable of a time integration period of 0.83 seconds to acquire excess mixing ratios of HCN, but only for concentrations above 5 ppb.

1.6.3.2 CIMS

Negative Ion Chemical Ionisation Mass Spectrometer (NI-CIMS) using $CO_3^-(H_2O)_n$ as the reagent ion has measured HCN in the lower and upper stratosphere (Schneider *et al*., 1997). The CIMS enabled fast time response for measurements but suffered from inaccuracies of up to 30% and was limited to measurements 1km above the tropopause due to the reliability of the reagent ion. The use of CF_3O^- by Crounse *et al*., (2006) allowed HCN to be measured via a cluster ion with a sensitivity of 15 ppt in low water

conditions where hydrolysis of the reagent ion in the presence of above 1% water severely affects the sensitivity due to the formation of water cluster ions obscuring the mass spectra.

1.6.3.3 Proton Transfer Mass Spectrometer (PTR MS)

Recent PTR MS measurements of HCN have been found to exhibit a high temperature and humidity dependence due to the proton affinity being similar to that of water (Knighton *et al*., 2009). There is also an interference with ethene as the cluster $C_2H_4^+$ ion is formed which has the same mass to charge ratio as HCN and therefore causes an interference of ratio 1:0.1ppb.

1.6.3.4 Gas chromatography

A gas chromatography method has been developed and successfully implemented for bottle samples (Singh *et al*., 2003) with a limit of detection of 30 ppt and requires a 5 minute merge (i.e. a running mean) for data precision. The offline analysis of this method inhibits high resolution measurements, although its low limit of detection allows accurate concentrations to be obtained.

1.6.4 Dinitrogen pentoxide (N_2O_5)

1.6.4.1 Indirect measurements via NO_3

N_2O_5 measurements are notoriously difficult in comparison to NO_3 as it does not absorb at visible wavelengths (Smith *et al*., 1995; Allan *et al*., 2000; Geyer *et al*., 2001). Techniques which measure NO_3 have been developed to infer N_2O_5 concentrations using the thermal relationship between NO_3 and N_2O_5, for example high-finesse cavity techniques such as continuous wave cavity ring-down spectroscopy (Simpson *et al*., 2003) and pulsed cavity ring-down spectroscopy (Dube *et al*., 2006). LIF and CIMS have also been employed to measure N_2O_5 indirectly by thermal dissociation to NO_3 (Slusher *et al*., 2004; Matsumoto *et al*., 2005b; Wood *et al*., 2005). LIF was able to detect concentrations up to 800 ppt in Tokyo using these techniques, although this instrument has been shown to have a limit of detection ranging from 80-4 ppt with 10 seconds to 1 minute integrations times respectively (Wood *et al*., 2005; Matsumoto *et al*., 2005b).

Broadband Cavity Enhancement Absorption Spectroscopy (BBCEAS) has recently measured N_2O_5 onboard an aircraft over the UK by using 2 channels to measure NO_3; one heated in order to calculate the difference from dissociation of (Kennedy *et al*., 2012). Although this instruments has proven its accuracy for NO_2 measurements through a comparison with CL (Kennedy *et al.,* 2012), possible measurement accuracies decrease with transmission efficiencies through separate inlets for determination of N_2O_5 concentrations via detection of NO_3.

1.7 Chemical Ionisation Mass Spectrometry (CIMS)

The selectivity, sensitivity and fast time response has enabled CIMS to become a powerful tool to measure a wide variety of atmospheric trace gases. Atmospheric ion composition measurements taken by Arnold and Henschen (1978) and Eisele (1986) led to the development of CIMS, allowing measurements of trace species such as HNO_3 and acetonitrile (CH_3CN) (Arnold *et al*., 1977, 1980, 1986; Arjis and Brasseur, 1986). The development of different ionisation schemes and technological advances has led to a number of different variations of the CIMS technique to be implemented for atmospheric measurements of a variety of compounds.

Although there are variations on the general CIMS method, most consist of the same base components and operate through the same processes as shown in figure 3. The ion which is to be detected by a mass spectral scan is produced through the collision of the species of interest with a chosen reagent ion. For instance Neuman (2003) uses a source of SiF_5^- as the ionisation species to react selectively with HNO_3 creating a cluster ion $SiF_5(HNO_3)^-$ which can be detected. The ion-molecule region often operates at pressures ranging from a few Torr to atmospheric pressure. A Collisional Dissociation Chamber (CDC) at an intermediate pressure (Tanner, 1997) is often used to dissociate weakly bound cluster ions such as hydrated cluster ions via high energy collisions to ensure the signature of the mass spectra produced for the species of interest is not complicated by appearing at several different masses. A quadrupole mass filter in a vacuum pressure chamber then uses the stability of the trajectories in oscillating electric fields to separate ions according to their mass to charge ratio (m/z). An octopole ion guide can also be used to aid the guidance of ions between the intermediate pressure regions (Hagg and Szabo, 1986) which enhances detection signals (Slusher *et al*., 2004; Crounse *et al*.,

2006; Nowak *et al*., 2006a,b). The resulting ions are then detected by an ion multiplier with a gain of up to 1×10^6, producing a signal in units of ion counts per unit time (Hz). Figure 3 is a schematic diagram of the CIMS implemented in this research.

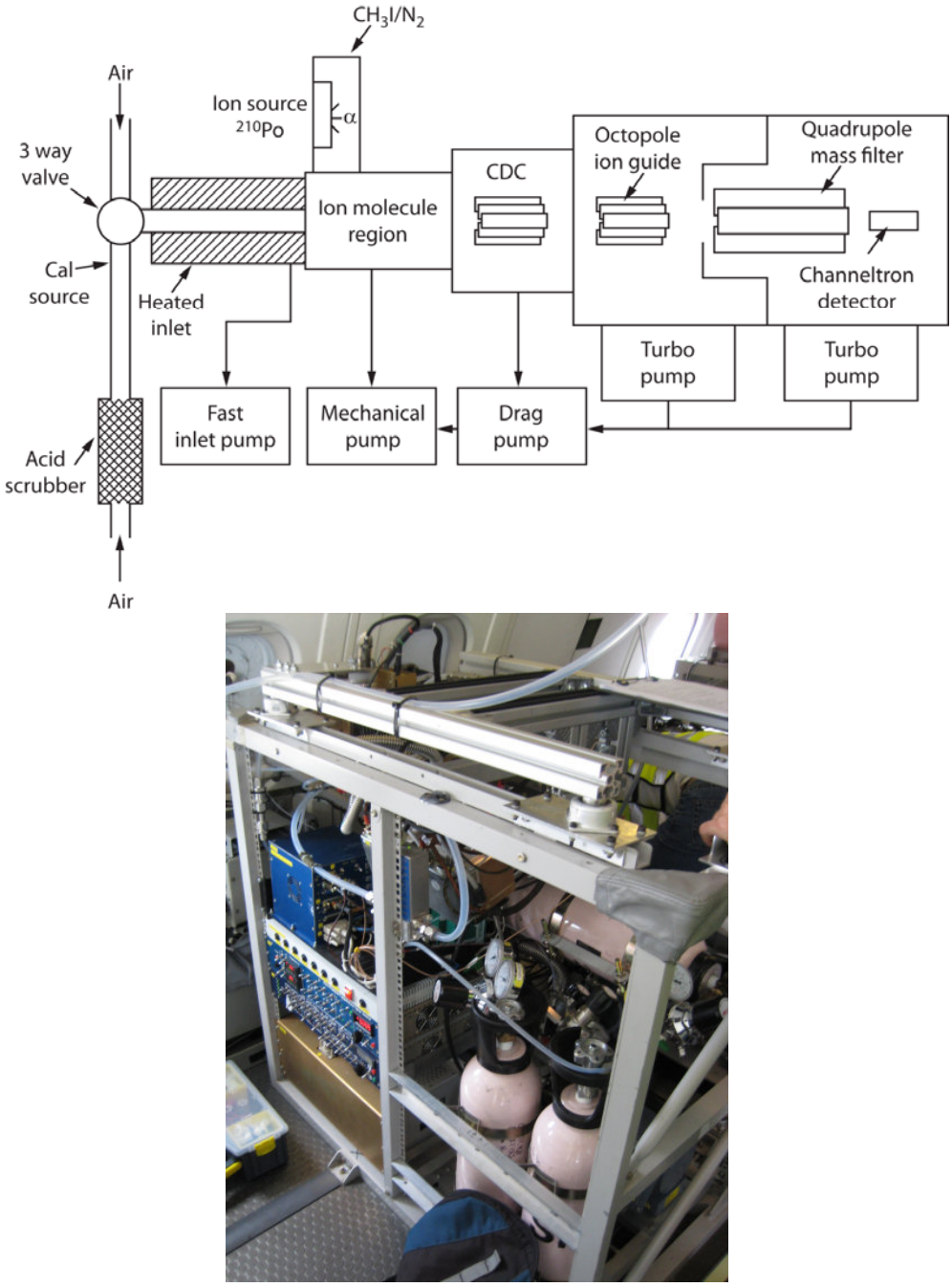

Figure 3: A schematic diagram of the chemical ionisation mass spectrometer (CIMS) developed and implemented n this study (dimensions not to scale) and a photograph of the instrument installed on the aircraft. A permeation source for HNO_3 and diluted HC(O)OH gas mixture in a 3 litre cylinder are installed on the rack for in-flight calibrations.

1.8 Ion chemistry

CIMS differs from other mass spectrometry techniques by the use of ion molecule reactions to selectively ionise the compound of interest in ambient air at low ppt concentrations. A signature ion molecule which is unique to the compound of interest is produced and observed by the mass spectrometer. Certain ions produced may not be unique to the initial compound of interest i.e. the formation of NO_3^- could be a product from NO_3, N_2O_5 or HNO_3 (Huey *et al*., 2006) whereas the I^- ion will give specific mass peaks for HNO_3 and N_2O_5 and NO_3 (Le Breton *et al*., 2012; Paper D).

Product ion stability can be a limiting factor in the choice of the reagent ion. Interference via reactions with atmospheric species would complicate the mass spectrum arising in multiple peaks. Reactions of water vapour with product ions is a common challenge which complicates the mass spectrum as multiple peaks arise (Slusher *et al*., 2001) as observed when measuring pernitric acid (HNO_4) using SF_6^-, limiting the measurements to regions of low water vapour. Certain species may also be in thermal equilibrium with their reactants and therefore split if subjected to a temperature increase. Atmospheric measurements of N_2O_5 are notoriously difficult due to this relationship with NO_3, leading to the development of indirect measurements of N_2O_5 by observing NO_3 concentrations (Dube *et al*., 2006).

Naturally occurring atmospheric ions such as NO_3^-, CO_3^- and H_3O^+ hydrated cluster ions were originally used (Mohler and Arnold, 1991; Tanner *et al*., 1997) as they are atmospherically stable and readily react with acidic and basic trace species of interest such as HNO_3. These ions were found to suffer from issues with water clustering and reagent ion synthesis (Seeley *et al*., 1997; Miller *et al*., 2000) and are therefore confined to high altitude measurements. These constraints on reagent ions lead to the development of reactive ions whose use is more suitable in a wide range of atmospheric conditions; demonstrated by extensive laboratory studies (Hanson and Ravishankara, 1991b; Jensen *et al*., 1994).

The array of reagent ions lead to specific applications for the species of interest and conditions of measurements, whether this is may be high water vapour in the troposphere or high O_3 in the stratosphere as for SF_6^- (Huey *et al*., 1995). The

instrumental operational conditions must also be suitable for the reagent reaction scheme (e.g. pressure, temperature and reaction times). Therefore, the reagent ion must be chosen for its specific use and detection. Table 3 lists the variety of reagent ions used so far for field measurements since the review by Huey (2005) and the trace gases which are detected.

Table 3: Ionisation reagent gases and detectable species used *in situ* atmospheric measurements from 2006 to present.

Reagent ion	***Detected compound***	***Reference***
SiF_5^-	HNO_3	Kita *et al.,* 2006
SF_6^-	HO_2NO_2, HCl	Kim *et al.,* 2007, McNeill *et al.,* 2007
$H^+(C_3H_6O)$	NH_3	Neuman *et al.,* 2002
CO_3^-	SO_2	Speidel *et al.,* 2007
$CH_3CO_2^-$	HC(O)OH, $CH_3COCOOH$, HONO, HNO_3, HNCO, $C_3H_4O_2$, $C_4H_6O_2$, $C_2H_4O_3$, $C_3H_6O_2$, $C_6H_6O_2$	Veres *et al.,* 2008, Roberts *et al.,* 2010
I^-	$ClNO_2$, N_2O_5, PAN, HC(O)OH, CPAN*, MPAN*, HOBr, BRO, HCN, HNO_3	Kercher *et al.,* 2009, Roberts *et al.,* 2009, Slusher *et al.,* 2004, Le Breton *et al.,* 2012, 2013
SO_2Cl^-	HONO	Hirokawa *et al.,* 2009
$(C_2H_5O_2)_n H^+$	NH_4	Benson *et al.,* 2010
$NO_3^-(HNO_3 O)_n$	H_2SO_4	Zheng *et al.,* 2010
NO_3^-	H_2SO_4, HO_2, RO_2	Hornbrook *et al.,* 2011, Kurten *et al.,* 2011

*CPAN – peroxyacetic nitric anhydride

*MPAN – peroxymethacryloyl nitrate

Previous studies have shown the capability of CH_3I ionisation scheme to detect a wide variety of important atmospheric trace gases simultaneously in a range of atmospheric conditions. Recent work has also shown how this scheme is able to detect N_2O_5, HCN and HNO_3 (Papers B, C and D). This enables methyl iodide to measure a variety of important trace gases with high sensitivity (1-50 ion counts $pptv^{-1}$) and at a high frequency (0.8 seconds) on an aircraft.

1.8 Aims of this thesis

Trace gases play an important role in atmospheric chemical cycling and thus have an impact on air quality and climate. They not only effect air quality through their own physical properties but are also often the precursors to the production and destruction of primary oxidants. To accurately constrain the roles these trace gases play in the atmosphere and their contribution to air quality, further knowledge of their production pathways and evolution is needed. The concentration of these species and subsequent effects vary with latitude, longitude, altitude, temperature, pressure, solar intensity, meteorological conditions, anthropogenic activity and concentration of other reactive species present. Airborne measurements are therefore integral to constraining these species within global models and also furthering our knowledge of global circulations of emissions from events such as forest fires. A CIMS has been implemented to measure trace species at low ppt concentrations onboard an aircraft at high measurement frequencies and limits of detection in the low ppt range.

An inlet must be designed that is suitable for the measurement of sticky compounds such as HNO_3, i.e. short length, suitable material and heated. An inlet allowing instrument background measurements in flight must be installed. Varying flight conditions which could impact the sensitivity of the CIMS must be measured and accounted for in the data analysis. Therefore, a calibration system must be developed to allow calibrations of HC(O)OH and HNO_3. Remote access to the valves which control the calibration system is needed as the CIMS is not accessible during a flight. In conjunction with the species specific calibrations, an additional sensitivity assessment of the CIMS relative to additional variations in sampling conditions must be conducted in order to validate the instrument and eliminate any analytical artefacts. Such factors include dependencies of thermodynamic conditions (e.g. temperature and humidity) or pumping volume decreasing as a function of atmospheric pressure.

A software package is needed to process the data acquired during a flight. The analysis necessary for CIMS data must factor in variability in the data observed from flight to flight. The software must be flexible in its analysis as investigated dependencies of sensitivity throughout the development of the instrument must be accounted for and incorporated into the data. The software must allow the processed data to be used in

conjunction with other data acquired in the same time series to allow for a full interpretation of multiple data acquisition from other instruments.

Limited measurements have been acquired in the UK to constrain the sources of HC(O)OH. Therefore the first measurements of HC(O)OH over the UK will help further our knowledge of the current sources and dominant production pathways. Primary and secondary production will be assessed with supporting measurements of CO, NO_x and O_3. Atmospheric chemistry Trajectory models will be implemented to allow a comparison between the data collected from flights around the UK. This will validate both the CIMS measurements and the accuracy of the models in reproducing observed concentrations and confirm if the different sources are constrained accurately.

The correlation of HC(O)OH and HNO_3 observed by Veres *et al.,* (2010) indicates the importance of the photochemical source of these species. Simultaneous measurements of these gases around the UK can validate the magnitude of this production pathway. O_3 and NO_x measurements will be used to infer the photochemical production pathway used as an indication of plume development and aging. Additional HNO_3 measurements further validates the secondary production of HC(O)OH. The sources incorporated into global models will be adjusted to understand where the discrepancies between measured and modelled acid concentrations occur. This work will investigate the link between HNO_3 and HC(O)OH to probe the oxidising capacity of the troposphere.

The efficiency of daytime tropospheric O_3 production and the formation of secondary aerosols are influenced by NO_3 and N_2O_5 levels from the previous night (Johnston *et al*,. 1971). N_2O_5 formation can also act as a sink for NO_3, the strongest night time oxidant, by further reacting with water to form HNO_3, or with sea salt aerosols which activates halogen compounds (Atkinson and Arey, 2003). As N_2O_5 and NO_3 are in equilibrium with each other dependent on temperature, high variability occurs spatially and temporally. Therefore the direct measurement of N_2O_5 can help further our understanding of the availability of NO_3 at night and therefore O_3 production potential the following day.

BB is a major source of trace gases to the atmosphere, with concentrations often high enough to impact regional air quality (Damoah *et al*., 2004). Evolution of BB plumes

plays a crucial role in determining the effects these events have on a global scale. A method of plume identification is needed in order to study this evolution. This work will investigate an ionisation scheme for the detection of HCN. Furthermore, utilising the high sensitivity of CIMS and low detection limits, the data will be used to define what can be classified as "in plume" data.

The overall aims of this thesis are to;

- Develop the Manchester CIMS for simultaneous, high frequency measurements of HC(O)OH, HNO_3, HCN and N_2O_5 using the CH_3I ionisation scheme.
- Develop an analysis toolkit software for the aircraft data collected.
- Utilise the first aircraft measurements of HC(O)OH over the UK to investigate its dominant production pathways and compare to model predictions.
- Investigate photochemical production of HC(O)OH and HNO_3 by simultaneous measurements from CIMS
- Develop the ionisation scheme for N_2O_5 measurements and compare results taken on aircraft with BBCEAS N_2O_5 measurements.
- Develop the ionisation scheme for HCN measurements and utilise the data as a BB plume marker.

2. Paper A

"Airborne measurements of formic acid using a chemical ionisation mass spectrometer"

Atmospheric Measurements Techniques 5, 3029–3039, 2012

Authors: M. Le Breton, M. R. McGillen, J. B. A. Muller, A. Bacak, D. E. Shallcross, P. Xiao, L. G. Huey, D. Tanner, H. Coe, and C. J. Percival.

M. McGillen was integral to initial deployment of CIMS onto the aircraft. J. Muller and A. Bacak helped me with the initial setup for aircraft measurements and laboratory tests. I operated the instrument during this flight and analysed the data using a toolkit developed in the first year of my PhD. S-J. Bauguitte supplied the NO_x data from the core chemistry instrument on the aircraft. I wrote the paper with direction from my supervisor. D. E. Shallcross performed atmospheric modelling. All work was carried out under the supervision of C. J. Percival.

Atmos. Meas. Tech., 5, 3029–3039, 2012
www.atmos-meas-tech.net/5/3029/2012/
doi:10.5194/amt-5-3029-2012

Atmospheric Measurement Techniques

Airborne observations of formic acid using a chemical ionization mass spectrometer

M. Le Breton[1], M. R. McGillen[1,*], J. B. A. Muller[1], A. Bacak[1], D. E. Shallcross[2], P. Xiao[2], L. G. Huey[3], D. Tanner[3], H. Coe[1], and C. J. Percival[1]

[1]Centre for Atmospheric Science, School of Earth, Atmospheric and Environmental Science, University of Manchester, Oxford Road, Manchester, M13 9PL, UK
[2]Biogeochemistry Research Centre, School of Chemistry, University of Bristol, Cantock's Close, Bristol, BS8 1TS, UK
[3]School of Earth and Atmospheric Sciences, Georgia Institute of Technology, Atlanta, Georgia, USA
[*]currently at: Chemical Sciences Division, Earth System Research Laboratory, National Oceanic and Atmospheric Administration (NOAA), 325 Broadway, Boulder, CO 80305, USA

Correspondence to: C. J. Percival (c.percival@manchester.ac.uk)

Received: 5 August 2011 – Published in Atmos. Meas. Tech. Discuss.: 14 September 2011
Revised: 26 October 2012 – Accepted: 27 October 2012 – Published: 7 December 2012

Abstract. The first airborne measurements of formic acid mixing ratios over the United Kingdom were measured on the FAAM BAe-146 research aircraft on 16 March 2010 with a chemical ionization mass spectrometer using I^- reagent ions. The I^- ionization scheme was able to measure formic acid mixing ratios at 1 Hz in the boundary layer.

In-flight standard addition calibrations from a formic acid source were used to determine the instrument sensitivity of 35 ± 6 ion counts $\text{pptv}^{-1}\,\text{s}^{-1}$ and a limit of detection of 25 pptv. Routine measurements were made through a scrubbed inlet to determine the instrumental background. Three plumes of formic acid were observed over the UK, originating from London, Humberside and Tyneside. The London plume had the highest formic acid mixing ratio throughout the flight, peaking at 358 pptv. No significant correlations of formic acid with NO_x and ozone were found, but a positive correlation was observed between CO and HCOOH within the two plumes where coincident data were recorded.

A trajectory model was employed to determine the sources of the plumes and compare modelled mixing ratios with measured values. The model underestimated formic acid concentrations by up to a factor of 2. This is explained by missing sources in the model, which were considered to be both primary emissions of formic acid of mainly anthropogenic origin and a lack of precursor emissions, such as isoprene, from biogenic sources, whose oxidation in situ would lead to formic acid formation.

1 Introduction

Organic acids are ubiquitous in the gas and aerosol phase, common constituents of global precipitation (Keene et al., 1983) and are measured in urban, rural and remote areas (Talbot et al., 1988). The contribution of organic acids to the acidity of precipitation and subsequent effects on aquatic and terrestrial ecosystems has been documented by Keene and Galloway (1986). Formic (HCOOH) acid can dominate free acidity of precipitation, thereby having an influence on pH-dependent chemical reactions and OH cloud chemistry (Jacob, 1986). Low molecular weight organic salts are present in the fine fraction of aerosols, whose physical properties, namely hygroscopicity, include relatively low critical supersaturations, allowing the activation of cloud droplets to occur and subsequently affecting the total indirect forcing (Yu, 2000).

Sources of formic acid include biogenic and anthropogenic primary emissions, e.g. biomass burning (Burling et al., 2010) and in situ production such as hydrocarbon oxidation, though their relative fluxes are poorly constrained (Chebbi and Carlier, 1996). The major sinks of saturated carboxylic acids are dry and wet deposition as a result of their low reactivity towards OH and NO_3. Sanhueza and Andreae (1991) and Hartmann et al. (1991) have shown that forests (acetic acid dominating) and particularly savanna regions (formic acid dominating) in Venezuela are strong sources of formic and acetic acid. These are thought to be

in part from direct emission by plants, but are dominated by in situ production following ozonolysis of alkenes (Sanhueza et al., 1996), where savanna levels for both species peaked around midday with a level of around 1 ppbv. Grosjean (1992) observed high levels of formic at a site in Southern California close to a coastal area, here direct emissions of acetic acid dominated over formic acid by a factor of 2, peaking in the summer at 20.4 and 9.6 metric tons per day, respectively. It was concluded that in situ production was of similar magnitude, with formic acid dominating over acetic acid (25.0 and 10.1 metric tons per day rising to 34.5 for formic acid but dropping for acetic acid to 4.3 at night). Preunkert et al. (2007) also concluded that in situ production was the dominant process for formic and acetic acid production in Europe, based on high-altitude measurements. However, these in situ production rates are based on earlier product data for acid formation from the ozonolysis of alkenes; more recent data (Leather et al., 2012) would suggest that the in situ production has been overestimated.

Johnson and Dawson (1993) carried out ^{13}C and ^{14}C analysis from background sites in the USA and concluded that direct emission of formic acid from C_3 plants was the most likely dominant source. Biomass burning is also a significant source of formic and acetic acid (Dibb et al., 1996; Talbot et al., 1999; Zhong et al., 2001). In Sao Paolo, Fornaro and Gutz (2003) concluded that high acetic acid resulted from direct emissions from ethanol fuelled cars, whilst high formic acid came from in situ production. Ocean sources of these organic acids have been suggested by Baboukas et al. (2000).

Gas-phase concentrations of formic acid in particular have been measured in the low ppb ranges (Talbot et al., 1999), and the modelled atmospheric lifetime has been suggested to be 3.2 days (Paulot et al., 2011). Global models underpredict formic acid budgets (von Kuhlmann et al., 2003; Rinsland et al., 2004; Paulot et al., 2011) by up to a factor of 50 in marine locations. Such discrepancies between perceived source strengths and observed atmospheric concentrations have led many authors to speculate upon the existence of a missing or poorly constrained source term (e.g. Grosjean and Seinfeld, 1989; Talbot et al., 1988, 1995; Granby et al., 1997; Rinsland et al., 2004), and it has been suggested by several of these studies that an unknown anthropogenic, and perhaps secondary source may be responsible, such as higher biogenic emissions during the growing season (Rinsland et al., 2004) and ageing of organic aerosols (Paulot et al., 2011). Also, the oxidation of volatile organic compound (VOC) precursors leading to the production of formic acid has been suggested as a significant source (Arlander et al., 1990), for instance the ozonolysis of ethene, whose emissions have been estimated to be 15 Tg yr^{-1} (Broadgate et al., 1997; Paulot et al., 2011).

Proton transfer reaction mass spectrometry has been used for the detection of organic acids, but has a limit of detection (LOD) of the order of a ppb (de Gouw et al., 2003). However, negative ion chemical ionization mass spectrometry (NI-CIMS) has proven to be a powerful method for sensitive and selective measurements of organic acids at the ppt level (Amelynck et al., 2000; Crounse et al., 2006; Paulot et al., 2009a, b). More recently, Veres et al. (2008), Roberts et al. (2010, 2011) and Bertram et al. (2011) have shown that chemical ionization mass spectrometry can be used to selectively detect gas-phase organic acids with a limit of detection below 0.1 ppbv for 1s measurements of formic acid. Veres et al. (2008) report a limit of detection of 80–90 pptv and sensitivity of 24 ion counts s^{-1} $pptv^{-1}$ using the acetate ionization scheme. Roberts et al. (2010) utilised the same technique for measurements of formic acid and other inorganic acids such as HONO. Although the sensitivity to formic acid is not quoted, the sensitivity for HNCO of 16 ion counts s^{-1} $pptv^{-1}$ is reported. The rapid time response of CIMS is particularly well suited for airborne measurements, and this study focuses on the development of a negative ion chemical ionization mass spectrometer (CIMS) utilising I^- as a method for the on-line measurement of carboxylic acids on an airborne platform.

2 Experimental details

2.1 CIMS apparatus

Chemical ionization mass spectrometry (CIMS) was used for real-time detection of formic acid. The CIMS instrument employed here was built by the Georgia Institute of Technology as previously described by Nowak et al. (2007). The schematic in Fig. 1 shows the setup used and operating conditions of the CIMS on board the FAAM BAe-146 research aircraft.

2.1.1 Inlet

The sample air for the CIMS was obtained by sub-sampling from the aircraft air sampling pipe (ASP). The ASP is a ram air inlet consisting of a 6 cm OD stainless steel pipe, with an internal surface which has been highly electro-polished for inertness. Several 0.6 cm and 1 cm OD Swagelok ports are welded to the ASP, separated by $\sim$ 8.9 cm, providing air to instrumentation in the cabin. Pressure measurements in the ASP were conducted at a flight level of 8230 m with a pitot tube in order to determine the linear air velocity in the ASP during scientific cruise speed, typically 210 knot aircraft-indicated air speed. For an outside static pressure of 261 Torr, the ASP static pressure was 309 Torr, and its ram air pressure was 325 Torr. The derived ASP linear air velocity is 85 m s^{-1}. Given an estimated ASP ID of 45 mm (15.90 cm^2 cross-section), the equivalent volumetric flow rate through the ASP is 135 L s^{-1}. The sub-sample passed through a 1.3 cm diameter PFA (perfluoroalkoxy) inlet line that entered the CIMS body through a 8.9 cm 3-way valve (with internal orifice diameter of 0.63 cm, M-Series Solenoid Valve, TEQCOM). A rotary vane pump (Picolino VTE-3, Gardner

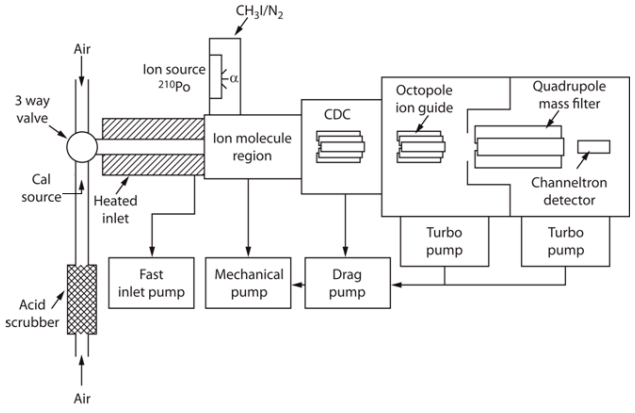

Fig. 1. Schematic of chemical ionization mass spectrometer (CIMS) used in this study. Arrows indicate direction of gas flow. Dimensions are not to scale.

Denver Thomas) allowed a fast inlet flow of 13 L min^{-1}, which corresponded to a residence time of 0.7 s (at standard temperature and pressure) in the total length of inlet tubing. It was not possible to test for loss along the ASP in situ; however, during ground tests only a 3 % loss of HCOOH was observed for a inlet residence time of 0.8 s. Thus, the impact of the ASP losses are assumed to be negligible as they are smaller than the sum of other systematic errors.

2.1.2 Ionization region

Initially the sample passed through a 380 µm diameter sized pinhole to reach the ion-molecule region (IMR) where ionization occurred at a pressure of 22 Torr, maintained by a dry scroll backing pump (UL-DISL 100, ULVAC Industrial). Sample flow through the orifice was 0.8 SLM on the ground. The pressure in the ionization region was set and controlled to 22 Torr, and thus the flow through the orifice changes slightly with ambient pressure. Flows were controlled and measured using a mass flow controller (MKS 1179 and MKS M100 Mass flow controllers, MKS Instruments, UK) and Baratron (1000 Torr range, Pressure Transducer, Model No. 722A, MKS Instruments, UK). At the IMR, N_2 was added at a flow rate of $\sim$ 1.5 SLM, and the ionization gas mixture of $CH_3I/H_2O/N_2$ at a rate of 1 SCCM passed over the ion source (Polonium-210 inline ionizer, NRD Inc Static Solutions Limited), producing an excess of I^- and $I^- \cdot H_2O$ ions in the IMR, which then ionized the organic acid molecules in the air sample.

2.1.3 Ion filtration and detection

The ions are then passed through the pinhole (600 µm) of a charged plate, which entered the mass spectrometer section of the instrument, i.e. the first octopole ion guide chamber which is the collisional dissociation chamber (CDC) where weakly bound ion–water clusters are broken up to simplify the resultant mass spectrum. The pressure in the CDC of 0.24 Torr was achieved by the use of a molecular drag pump (MDP-5011, Adixen Alcatel Vacuum Technology). After the CDC, the ions passed through the second octopole ion guide, which has the effect of collimating the ions. The octopole chamber was held at a pressure of $\sim 10^{-3}$ Torr which was maintained by a turbomolecular pump (V-81M Navigator, Varian Inc. Vacuum Technologies). Past the second octopole chamber, the ions were mass selected by a quadrupole with pre- and post-filters with entrance and exit lenses (Tri-filter Quadrupole Mass Filter, Extrel CMS). The quadrupole section was kept at a pressure of 10^{-4} Torr by a second turbomolecular pump (V-81M Navigator, Varian Inc. Vacuum Technologies). The selected ions were then detected and counted by a continuous dynode electron multiplier (7550 M detector, ITT Power Solutions, Inc.).

2.2 Ionization scheme

The ion-molecule chemistry using iodide ions (I^-) for trace gas detection has been described by Slusher et al. (2004) and was utilised here to detect organic acids. A gas mixture of methyl iodide, CH_3I, and H_2O in N_2 is prepared by gas expansion and used to obtain reagent ions I^- and water clusters $I^- \cdot H_2O$, of which the latter is important for the ionization of formic acid, forming the acid–iodine adducts as seen in the mass spectrum (Fig. 2). Formic acid was ionized by I^- via an adduct reaction,

$$I^- \cdot H_2O_n + HCOOH \rightarrow HCOOH \cdot I^- \cdot H_2O_n \ , \qquad \text{(R1)}$$

which enabled formic acid to be detected selectively at $m/z = 173$. As the ionization efficiency is dependent on the presence of water vapour through the production of $I^- \cdot H_2O$ (Slusher et al., 2004), water vapour was added to the ionization gas mixture so as to produce an excess of $I^- \cdot H_2O$ cluster ions and hence allow operation in the water vapour independent regime. The mix was produced using a manifold by evaporating the liquid deionized H_2O ($\geq$15.0 MΩ cm, obtained from a PURELAB Option-S 7/15, ELGA) and CH_3I sequentially into the manifold to reach the partial pressures of 10 Torr H_2O and 15 Torr CH_3I, before adding 3800 Torr of N_2 to make a ionization gas mixture of 0.39 % CH_3I and 0.26 % H_2O. Methyl iodide CH_3I, $\geq$ 99.5 %, was purchased from Sigma Aldrich and used as provided. Typical reagent ion values were $I^- = 1.5 \times 10^6$ Hz and $I \cdot H_2O = 2.5 \times 10^6$ Hz. The pressure in the CDC was 0.25 Torr, where the local electric field divided by the gas number density (E/N) was 180 Townsend (Td = 10^{-17} V cm^2).

2.3 Formic acid calibrations, sensitivity and LOD

Formic acid calibrations were made pre-flight and in-flight. The calibration cycle involves obtaining the formic acid instrumental background by passing the sample air through an acid scrubber which is made of nylon turnings coated with

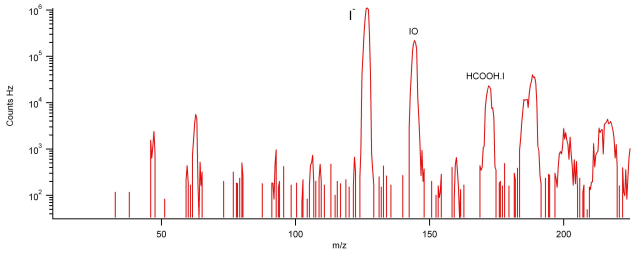

Fig. 2. Mass spectrum of CIMS during flight B518, 16 March 2010 at 16:00. Ionization peaks and formic acid adduct mass are labelled. Peaks at m/z 190, 201, 215 correspond to HNO_3, propanoic and butanoic acid, respectively. The FWHM is 1 amu at $m/z = 173$.

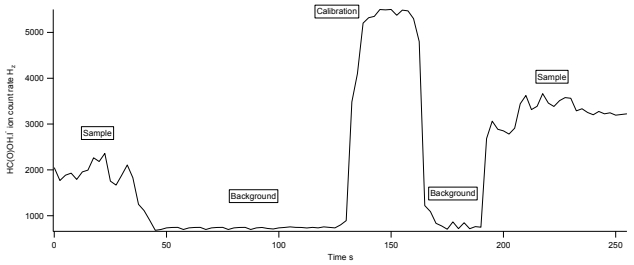

Fig. 3. Typical cycle for background, sampling and calibrations during flight.

sodium bicarbonate. After an effective zero acid air flow for background determination, a known amount of formic acid from a pressurised gas cylinder is added to this scrubbed air flow until a plateau in formic acid signal is achieved. A second background determination is carried out before the 3-way PFA valve is switched back to atmospheric sampling mode (Fig. 1). The organic acid gas mixture that was used for the in-flight calibrations of the CIMS was analysed by flame ionization detection as follows. A liquid standard of the acid (with toluene added) was diluted and then injected directly onto a gas chromatography-flame ionization detector system (GC-FID ADS). The dilution factor was determined by the dilution of the toluene, referenced to a certified synthetic standard (Apel-Riemer Environment, USA) as outlined by Yates et al. (2010). The in-flight standard was then calibrated against this standard mixture, and the formic acid calibration factor was applied to the relative formic acid concentrations during post-flight data processing. During a test flight, the calibration was proven to be invariant with altitude. Calibrations were performed from 15 to 920 m, and the variation in inlet flow was taken into account. The sensitivity determined from the calibrations at these altitudes were within 3 sigma of the error calculated from the statistical noise of the calibration signal in the plateau region.

The sensitivity of the CIMS to formic acid (in units of counts/ppb of formic acid) was calculated as the ratio of the background corrected formic acid calibration counts to the formic acid absolute calibration factor (in units of ppb). The formic acid signal was normalized for $I \cdot H_2O^-$ counts to remove variance caused by changes in reagent ion signal. For this flight the sensitivity was 35 ± 6 ion counts s^{-1} $pptv^{-1}$. The 3σ limit of detection (LOD) for formic acid was calculated to be 25 pptv. The instrument response time was estimated by adding a known amount of formic acid to the instrument for a given period of time, as shown in Fig. 3. The calibration gas is delivered via a 1/8″ diameter PFA tube to the acid-scrubbed air (3/8″ tubing) about 3 cm before the 3-way valve. Total inlet flow was measured and no clear difference between background/calibration flow and flow in sampling mode was observed, and the pressure drop across the scrubber is hence minimal. The instrument has an e-folding time of 1.5 s and a response time, i.e. the time required for a steady-state signal to decay to 10 % of the initial signal when a background measurement is made (Veres et al., 2008), of 4 s. The background was determined in-flight every sixty minutes. The average difference between consecutive backgrounds was 30 ± 5 pptv.

2.4 Data logging, capture and handling

The CIMS can count a number of separate masses in sequence; eight here, with a dwell time of 100 ms each yielding a sampling frequency of 1.67 Hz. Alternatively, spectral scans across the whole mass spectrum can be taken. Spectral scans were performed twice during the flight B518 (Fig. 2). The high-frequency formic acid time series was analysed by removing background counts (averaging to 30 s) and calibrating relative counts using the calibration factor obtained during the in-flight calibration cycle (averaging to 30 s). The formic acid data capture is 86 % for the whole flight, and the 14 % of data loss is a result of the in-flight calibration and background measurements. Data obtained during transit at 3048 m (10 000 feet) are not shown as no calibration was performed at this height and calibration altitude independence was only confirmed for heights up to 914 m (3000 feet, see previous text).

2.5 FAAM BAe-146 onboard instruments

In addition to formic acid data, observations of CO, NO_2 and O_3 are used in the analysis. Nitric oxide (NO) and nitrogen dioxide (NO_2) were measured using separate channels of a chemiluminescence detector and were reported every 10 s with an uncertainty of ±6 % ppbv (Stewart et al., 2008). CO data are reported at 1 Hz using as fast fluorescence CO analyser with an uncertainty of ±5 % (Gerbig et al., 1999). Ozone was measured using a UV Photometric Ozone Analyser at 1 Hz with an uncertainty of ±3 ppbv (Real et al., 2007).

2.6 Trajectory model

A trajectory model has been used to estimate formic acid concentrations along the B518 flight path. The trajectory

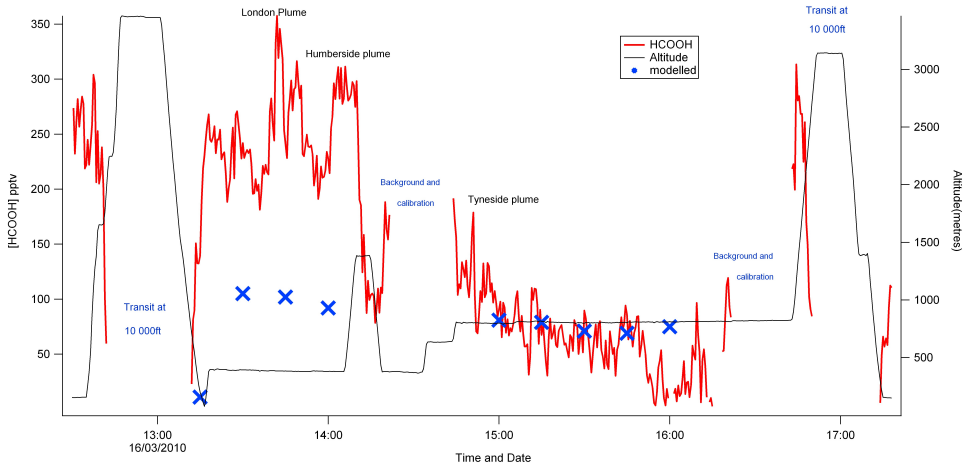

Fig. 4. Time series of 30-s averaged formic acid observations (left axis) with altitude (right axis) from the 16 March 2011 flight. The London, Humberside and Tyneside plumes have been labelled. Sections of the flight where there are backgrounds, calibrations and transits are set to zero, and comparison with back trajectory modelled data is shown.

model used for this purpose has been described in previous papers (Derwent et al., 1991; Derwent and Jenkin, 1996; Johnson et al., 2006a, b; Evans et al., 2000) and will be only briefly described here. The trajectory model simulates the chemical development in a well-mixed air parcel being advected along multi-day trajectories. The air parcel picks up emissions of NO_x, CO, SO_2, methane, anthropogenic VOC and biogenic VOC when in the boundary layer, which are processed using an appropriate description of the chemical and photochemical transformations leading to the formation of ozone and other secondary pollutants. Dry deposition of species also occurs when the air parcel is in the boundary layer.

Two chemistry modules have been integrated into the trajectory mode: the full Master Chemical Mechanism (MCM v3.1; Jenkin et al., 1997) and the Common Representative Intermediates scheme (CRIv2-R5; Jenkin et al., 2008; Watson et al., 2008; Utembe et al., 2009, 2011a, b; Archibald et al., 2010). Trajectories are generated by the Hysplit model and integrated for four days, arriving at a point coincident in time and space with the aircraft flight track (Draxler and Rolph, 2003).

2.7 Field conditions for flight B518

The 1 Hz formic acid data obtained from takeoff until landing on flight B518, 16 March 2010, enabled observations of plumes from a variety of sources. The measurements were taken over the North Sea, aiming to intercept pollution plumes from the UK carried by a south-south-westerly wind with wind speed of 2.8 m s^{-1}. The meteorological conditions for the previous 3 days and the day of the flight were free of precipitation. These conditions favoured the accumulation of carboxylic acids in the vapour phase, since wet deposition would have been reduced.

3 Analysis and discussion

3.1 Observations of formic acid concentrations

The instrumental sensitivity of 35 ± 6 ion counts $pptv^{-1}$ s^{-1} is comparable with previously reported measurements of formic acid using CIMS (Veres et al., 2008; Roberts et al., 2010). Formic acid mixing ratios ranged from 34.4 pptv to 358 pptv, as shown in Fig. 4, intersecting 3 separate major plumes during the flight. The mean mixing ratio during the flight was 142.4 pptv, with a 3-sigma standard deviation of 71.9 pptv. A comparison with previously reported data is difficult due to its scarcity. Satellite and infrared (IR) measurements have been made, but these are mainly at altitudes greater than 2 km. Zander et al. (2010) reported an average mixing of ratio of 110.9 pptv in the 3.58 to 10.6 km region, which is comparable to the concentrations reported here. Satellite-based IR measurements have been made to altitudes of 5 km, where mixing ratios of 157 ± 60 have been recorded (González Abad et al., 2009), similar to the smaller plumes measured on flight B518. A decrease in mixing ratios with altitude is observed, which is most likely a consequence of the increasing distance from direct and indirect sources which results in the dilution of the original plume material and allows time for loss processes (predominantly depositional) to operate. It is difficult to compare the measurements made here with the current data available due to the possible variances in experimental conditions such as different observational regions, times, altitudes and also measurement techniques.

3.2 Urban plumes

Flight B518 intercepted 3 separate plumes of formic acid over the UK. The different plumes detected during the flight were plumes from London, Humberside and Tyneside; these

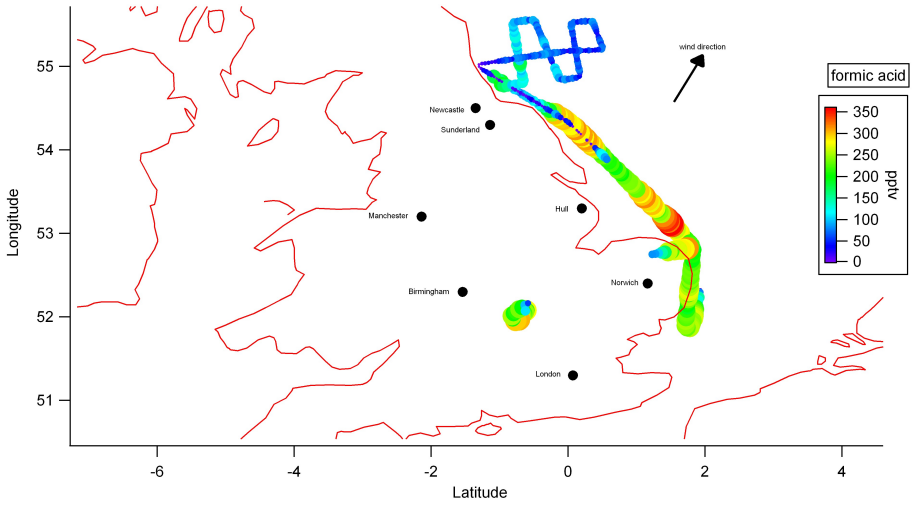

Fig. 5. The FAAM BAe-146 flight track on 16 March 2010 over the UK. Formic acid mixing ratios are reverse rainbow colour coded from 0 ppb to 0.36 ppb. Populated urban areas are indicated and labelled.

are labelled in Fig. 4. The London, Humberside and Tyneside plumes had peak concentrations of 358, 311 and 192 pptv, respectively. The ability to detect these different source areas demonstrates the utility of the instrument for formic acid detection.

The highest formic acid concentration throughout the flight was measured from the London plume. The London metropolitan area is densely populated with a high volume of industrial, domestic and transport activity, a known major source of carboxylic acid emissions (Chebbi and Carlier, 1996). Kawamura and Kaplan (1985) observed formic acid emitted directly from motor vehicle exhausts, which our results show agreement with. The high volume of traffic in the Greater London region is likely to be a major source of formic acid. Important emissions from anthropogenic sources, such as motor exhausts' incomplete combustion of fuel, indicate high levels of formic acid should be emitted from the London area (Kawamura and Kaplan, 1985). Enol formation during combustion has also been noted as a potential source of organic acids (Archibald et al., 2007b). Flight B518 collected data passing through this region. Figure 5 shows the flight track and the concentrations observed on this day. The south-south-westerly wind direction allowed measurements of this plume at an altitude of 700 m, 230 km away from the source. With the average wind speed of 2.8 m s^{-1} on this day, the plume is estimated to have taken around 18 h to reach the location where the CIMS detected it (off the North Norfolk coast). The time series of formic acid concentrations indicates a peak mixing ratio of 358 pptv over this region. No correlations were observed with NO_x and O_3, although NO_x is known to be a marker of traffic and anthropogenic sources. However, restricting ourselves to just data known to be associated with a plume, a positive correlation between CO and HCOOH emerges (see Fig. 6). Although it is tempting to infer a primary source of HCOOH from urban environments,

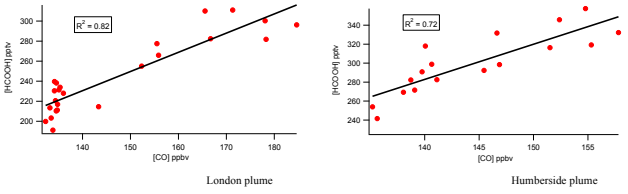

Fig. 6. Correlation plots of HCOOH vs. CO for the London and Humberside plumes.

it is also possible that these data infer that HCOOH precursors are emitted from urban areas and therefore correlate with CO (see later). The different formation and loss processes of NO_x and formic acid may have different time constants, therefore producing a low correlation even if a strong primary emission of HCOOH exists. Since CO is effectively an inert tracer of pollution on the timescales considered here, a correlation with HCOOH is strong evidence of an urban source.

The second plume detected during the flight was from the Humberside region. This is an urban area but with lower population and industrial activity than London; the lower concentrations observed may reflect this difference, but dilution will also be a factor. North of latitude 53°50, the average ambient mixing ratio drops to below 100 pptv, whereas an average concentration before this was 200 pptv. This low ambient concentration allowed the detection of a plume with a peak of 192 pptv from the Tyneside region (Fig. 7). Tyneside is expected to be a heavily polluted area similar to that of Humberside and with similar sources as London. The lower mixing ratios found in the Tyneside plume could be due to a number of reasons: lower direct emissions, lower precursor emissions, more aged plume, greater depositional loss, etc. More data are needed to identify and characterise important source regions over the UK.

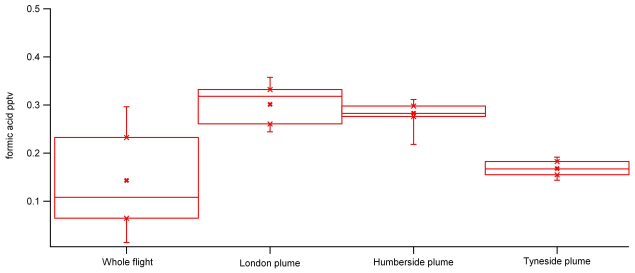

Fig. 7. Box and whisker plots of total flight data and individual plumes detected during flight B518. Whiskers indicate the 5th and 95th percentile.

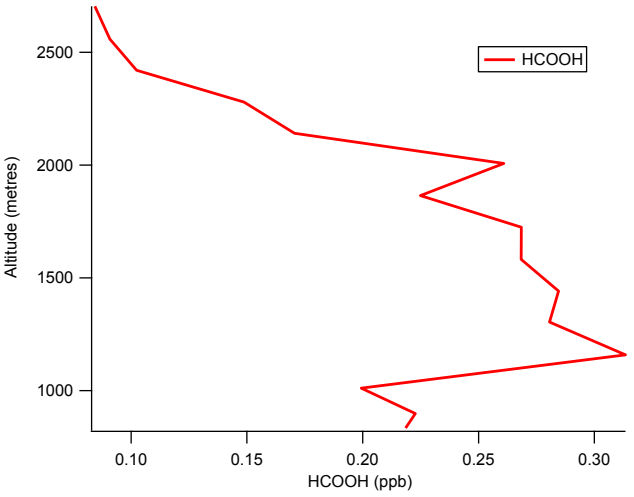

Fig. 8. Vertical profiles of formic acid and NO_x mixing ratios from an altitude of 800 to 2300 m.

3.3 Altitude profile

The correct altitude profile is essential for satellite retrievals and their inference regarding the photochemistry of formic acid. A vertical profile of formic acid from 800 to 2300 m is shown in Fig. 8. The concentration increases up to 1200 m, peaking at a concentration of 313 pptv and then falling off with increasing altitude. Low concentrations were observed below 1000 m. Although Baboukas et al. (2000) observed emissions of formic acid from the ocean, net flux measurements are not well known. Emission rates during this flight may have been lower than the deposition rates, causing the observed lower concentrations. If the only source of formic acid was of primary origin from the surface, then, irrespective of depositional losses, we would imagine that the highest levels would be encountered at the surface and the mixing ratios decrease with altitude. However, it is of course possible to intercept polluted plumes at only higher altitudes and, relative to cleaner surface air, this would give rise to the observations reported. A further explanation of the peak observed at $\sim$ 1000 m is that there are significant secondary sources of formic acid, following oxidation of formic acid precursors within the plume. At 1000 m, air masses rising from anthropogenic and/or biogenic sources (primary and secondary) will be far less susceptible to dry deposition, and so it is possible to imagine that the formic acid altitude profile goes through a maximum at this altitude. A decrease in concentration is observed at 2000 m; this is effectively the top of the boundary layer, and this decrease may simply be dilution of these plumes. The profile in Fig. 8 was measured on the edge of the London plume. Despite the possible higher concentrations in the profile contributed by the plume, it can still provide information concerning the gas as a function of altitude, although it may not be typical of an ambient formic acid profile. Hence, the plume correlation between CO and HCOOH probably indicates that both primary emissions of HCOOH exist and also emissions of HCOOH precursors exist in the urban environment.

Reiner et al. (1999) measured formic acid in the UTLS (standard upper troposphere-lower stratosphere) region from 7–12 km and observed that formic acid concentrations decrease with altitude, which is in agreement with this work. The measured formic acid concentrations ranged from 0–600 ppt, with mean concentrations of 59–215 pptv across the measured altitude range.

3.4 Comparison between model and measurements

The comparison between the trajectory model CO and O_3 and the respective measurements is good, as shown in Fig. 9. The model slightly underestimates O_3 and has a tendency to slightly overestimate CO. We conclude that the dynamics and chemical processing components (oxidising capacity) of the model are operating correctly. If we assume that formic acid is being formed by in situ chemistry, then ozonolysis of 1-alkenes should be the dominant source. Since the model O_3 is reasonably well reproduced, we would conclude that where the model underestimates formic acid significantly (before ca. 02:00 p.m. LT), there is a shortage of 1-alkene precursors. As an example, assuming propene as the 1-alkene, model estimates suggest that an additional 2–5 ppb is required in the model to generate the formic acid observed. Rather than a substantial omission of an emission of a species like propene, we suspect that lower levels of faster reacting 1-alkenes are missing from the model. It is perfectly possible for these fast reacting alkenes to be missing from inventories or for them to be represented by other alkenes that do not lead to formic acid formation. There is no suggestion in the measurement data or the model that a substantial biomass burning source is present at this time (March). A primary emission of HCOOH is also a strong possibility and would increase plume levels of HCOOH.

Although the modelled concentrations do not show as large a variation as the measurements, there is a clear negative gradient with altitude, in keeping with the observations. The model underestimates measurements by a factor of two

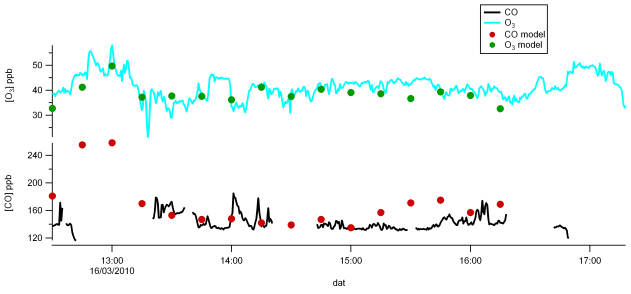

Fig. 9. Ozone and CO concentration time series from flight B518 with back trajectory modelled data.

up to around 02:30 p.m., and from then on agreement between the two is good (Fig. 4). The sources of formic acid in the model are the reaction of CH_2OO (from ethene ozonolysis predominantly but also other sources such as isoprene) with water and the reaction of OH with acetylene, where the former represents over 95 % of the production and the latter the remainder (Taatjes et al., 2008; Welz et al., 2012; Leather et al., 2012). Based on the biogenic emission inventory used, the level of primary emissions from biogenic hydrocarbons into these trajectories is low. The underprediction early on in the time series could be due to missing direct surface emissions or missing extremely reactive formic acid precursors (e.g. Archibald et al., 2007a) such as isoprene. Indeed, inspection of the trajectories shows that at around 02:00 p.m. the aircraft encountered air associated with the plumes from London and Humberside and would have picked up primary surface emissions from combustion sources. Measurements from around 03:00 p.m. onwards are lower; this is a result of an increase in altitude, where air mass back trajectories suggest that direct input from primary surface sources is much weaker. If ozonolysis of terminal olefinic species leads to the formation of CH_2OO (Leather et al., 2012; Taatjes et al., 2008; Welz et al., 2012) and the Criegee intermediate reacts with water to form formic acid, there may be both anthropogenic and biogenic sources (e.g. isoprene and certain terpenes). Inspection of urban isoprene levels from the UK Air Quality (NETCEN) archive (e.g. Rivett et al., 2003a, b; Khan et al., 2008) show that typical levels in March are around 60 pptv, and not all of this will be of biogenic origin. Using these levels of surface isoprene (higher than those predicted by the emission model) as input into the trajectory model would not generate anywhere near enough formic acid to rectify the model underprediction that is seen up to around 02:30 p.m. Increasing primary morning emissions of formic acid from an anthropogenic source increases formic acid in the early afternoon, but has less effect in the late afternoon, consistent with observations. Therefore, based on such a simple analysis, the discrepancy early on is probably due to anthropogenic emissions, either from direct emissions of formic acid or emission of fast producing HCOOH precursors and their reaction with ozone. Therefore, we conclude that anthropogenic sources are probably responsible for the additional formic acid observed before 02:30 p.m., and such a conclusion is consistent with the correlation of HCOOH with CO in these plumes.

4 Conclusions

The first detailed formic acid measurements by chemical ionization mass spectrometer (CIMS) onboard an airborne platform using I^- ionization chemistry are presented. The I^- ionization chemistry has been successfully employed for the detection and measurement of trace amounts of atmospheric formic acid. The sensitivity of CIMS in the detection of formic acid was 35 ± 6 ion counts s^{-1} $pptv^{-1}$, and the limit of detection was 25 pptv. Mean concentrations of formic acid in the UK boundary layer on 16 March 2010 were 142 ± 72 pptv. Higher concentrations were observed in plumes, which could be linked by trajectory analysis to main urban and industrial centres (London, Humberside and Tyneside regions). Formic acid showed no clear correlation with anthropogenic pollution markers such as NO_x, CO and O_3. The highest formic acid mixing ratios were observed at ~ 1000 m; although this could arise from intercepting polluted plumes at higher altitudes only, it may also signal the presence of a significant secondary source of formic acid within the plume. Formic acid levels as estimated by a trajectory model showed an underprediction of concentrations by up to a factor of 2. The model discrepancy can be resolved by the addition of 1-alkene surface emissions that are oxidised to produce formic acid in situ or by addition of a direct emission of HCOOH. Whether the source of the 1-alkene is of anthropogenic or biogenic origin is unclear. More measurements and in-depth modelling studies are needed to validate the current chemical transport models and help identify and quantify formic acid emission sources. This should also improve understanding of the role of formic acid in chemical cycling in the troposphere. Direct measurements of formic acid in the UK boundary layer have shown how variable formic acid levels can be, and that distinct plumes of formic acid can be identified in the horizontal and vertical. The inability of the model to reproduce the observations in the part of the flight before ca. 02:00 p.m. highlights that further studies must aim to improve the understanding and quantification of formic acid sources.

Acknowledgements. The authors would like to thank Alan Knights for analysing the organic acid calibration gas mixture by GC-FID ADS. FAAM staff are also thanked for their assistance in getting the CIMS working onboard the aircraft. CJP and DES thank NERC under whose auspices various elements of this work were carried out.

Edited by: H. Harder

References

Amelynck, C., Schoon, N., and Arijs, E.: Gas phase reactions of CF_3O- and CF_3O-H_2O with nitric, formic, and acetic acid, Int. J. Mass Spectrom., 203, 165–175, 2000.

Archibald, A. T., McGillen, M. R., Taatjes, C. A., Percival, C. J., Shallcross, D. E.: Atmospheric transformation of enols: A potential secondary source of carboxylic acids in the urban troposphere, Geophys. Res. Lett., 34, L21801, doi:10.1029/2007GL031032, 2007a.

Archibald, A. T., McGillen, M. R., Taatjes, C. A., Percival C. J., and Shallcross, D. E.: On the importance of Ethenol in urban atmospheres, Geophys. Res. Lett., 34, L21801, doi:10.1029/2007GL031032, 2007b.

Archibald, A. T., Cooke, M. C., Utembe, S. R., Shallcross, D. E., Derwent, R. G., and Jenkin, M. E.: Impacts of mechanistic changes on HO_x formation and recycling in the oxidation of isoprene, Atmos. Chem. Phys., 10, 8097–8118, doi:10.5194/acp-10-8097-2010, 2010.

Arlander, D. W., Cronn, D. R., Farmer, J. C., Menzia, F. A., and Westberg, H. H.: Gaseous oxygenated hydrocarbons in the remote marine troposphere, J. Geophys. Res.-Atmos., 95, 16391–16403, 1990.

Baboukas, E. D., Kanakidou, M., and Mihalopoulos, N.: Carboxylic acids in gas and particulate phase above the Atlantic Ocean, J. Geophys. Res.-Atmos., 105, 14459–14471, 2000.

Bertram, T. H., Kimmel, J. R., Crisp, T. A., Ryder, O. S., Yatavelli, R. L. N., Thornton, J. A., Cubison, M. J., Gonin, M., and Worsnop, D. R.: A field-deployable, chemical ionization time-of-flight mass spectrometer, Atmos. Meas. Tech., 4, 1471–1479, doi:10.5194/amt-4-1471-2011, 2011.

Burling, I. R., Yokelson, R. J., Griffith, D. W. T., Johnson, T. J., Veres, P., Roberts, J. M., Warneke, C., Urbanski, S. P., Reardon, J., Weise, D. R., Hao, W. M., and de Gouw, J.: Laboratory measurements of trace gas emissions from biomass burning of fuel types from the southeastern and southwestern United States, Atmos. Chem. Phys., 10, 11115–11130, doi:10.5194/acp-10-11115-2010, 2010.

Broadgate, W. J., Liss, P. S., and Penkett, S. A.: Seasonal emissions of isoprene and other reactive hydrocarbon gases from the ocean, Geophy. Res. Lett., 24, 2675–2678,1997.

Chebbi, A. and Carlier, P.: Carboxylic acids in the troposphere, occurrence, sources, and sinks: A review, Atmos. Environ., 30, 4233–4249, 1996.

Crounse, J. D., McKinney, K. A., Kwan, A. J., and Wennberg, P. O.: Measurement of gas-phase hydroperoxides by chemical ionization mass spectrometry, Anal. Chem., 78, 6726–6732, 2006.

de Gouw, J. A., Goldan, P. D., Warneke, C., Kuster, W. C., Roberts, J. M., Marchewka, M., Bertman, S. B., Pszenny, A. A. P., and Keene, W. C.: Validation of proton transfer reaction-mass spectrometry (PTR-MS) measurements of gas-phase organic compounds in the atmosphere during the New England Air Quality Study (NEAQS) in 2002, J. Geophys. Res., 108, 4682, doi:10.1029/2003JD003863, 2003.

Derwent, R. G. and Jenkin, M. E., Hydrocarbons and the long-range transport of ozone and PAN across Europe, Atmos. Environ., 30, 181–199, 1996.

Derwent, R. G., Jenkin, M. E., and Saunders, S. M.: Photochemical ozone creation potentials for a large number of reactive hydrocarbons under European conditions, Atmos. Environ., 25, 1661–1678, 1991.

Dibb, J. E., Talbot, R. W., Whitlow, S. I., Shipham, M. C., Winterle, J., McConnell, J., and Bales, R.: Biomass burning signatures in the atmosphere and snow at Summit, Greenland: An event on 5 August 1994, Atmos. Environ., 30, 553–561, 1996.

Draxler, R. R. and Rolph, G. D.: HYSPLIT (HYbrid Single-Particle Lagrangian Integrated Trajectory) Model access via NOAA ARL READY Website, available at: http://www.arl.noaa.gov/ready/hysplit4.html (last access: 30 November 2012), NOAA Air Resources Laboratory, Silver Spring, MD, 2003.

Evans, M. J., Shallcross, D. E., Law, K. S., Wild, J. O. S., Simmonds, P. G., Spain, T. G., Berrisford, P., Methven, J., Lewis, A. C., McQuaid, J. B., Pilling, M. J., Bandy, B. J., Penkett, S. A., and Pyle, J.: Evaluation of a Lagrangian box model using field measurements from EASE (Eastern Atlantic Summer Experiment) 1996, JA, Atmos. Environ., 34, 3843–3863, 2000.

Fornaro, A. and Gutz, I. G. R.: Wet deposition and related atmospheric chemistry in the Sao Paulo metropolis, Brazil: Part 2 – contribution of formic and acetic acids, Atmos. Environ., 37, 117–128, 2003.

Gerbig, C., Schmitgen, S., Kley, D., and Volz-Thomas, A.: An improved fast-response vacuum-UV resonance fluorescence CO instrument, J. Geophys. Res., 104, 1699–1704, 1999.

González Abad, G., Bernath, P. F., Boone, C. D., McLeod, S. D., Manney, G. L., and Toon, G. C.: Global distribution of upper tropospheric formic acid from the ACE-FTS, Atmos. Chem. Phys., 9, 8039–8047, doi:10.5194/acp-9-8039-2009, 2009.

Granby, K., Christensen, C., and Lohse, C.: Urban and semi-rural observations of carboxylic acids and carbonyls, Atmos. Environ., 31, 1403–1415, 1997.

Grosjean, D.: Formic acid and acetic acid emissions, atmopsheric formication and dry seposition at 2 southern California locations, Atmos. Environ., 26, 3279–3286, 1992.

Grosjean, D. and Seinfeld, J. H.: Parameterization of the formation potential of secondary organic aerosols, Atmos. Environ., 23, 1733–1747, 1989.

Hartmann, W. R., Santana, M., Hermoso, M., Andreae, M. O., and Sanhueza, E.: Diurnal cycles of formic and acetic acids in the northern part of the Guayana shield, Venezuela, J. Atmos. Chem., 13, 63–72, 1991.

Jacob, D.: Chemistry of OH in remote clouds and its role in the production of formic acid and peroxymonosulfate, J. Geophys. Res., 91, 9807–9826, 1986.

Jenkin, M. E., Saunders, S. M., Derwent, R. G., and Pilling, M. J.: Construction and application of a master chemical mechanism (MCM) for modelling tropospheric chemistry, Abstr. Pap. Am. Chem. S., 214, p. 116, 1997.

Jenkin, M. E., Watson, L. A., Utembe, S. R., and Shallcross, D. E.: A Common Representative Intermediates (CRI) mechanism for VOC degradation. Part 1: Gas phase mechanism development, Atmos. Environ., 42, 7185–7195, 2008.

Johnson, B. J. and Dawson, G. A.: A preliminary study of the carbon isotopic content of ambient formic acid and 2 selected sources – automobile exhaust and formicine ants, J. Atmos. Chem., 17, 123–140, 1993.

Johnson, D., Utembe, S. R., Jenkin, M. E., Derwent, R. G., Hayman, G. D., Alfarra, M. R., Coe, H., and McFiggans, G.: Simulating regional scale secondary organic aerosol formation during the TORCH 2003 campaign in the southern UK, Atmos. Chem.

Phys., 6, 403–418, doi:10.5194/acp-6-403-2006, 2006a.

Johnson, D., Utembe, S. R., and Jenkin, M. E.: Simulating the detailed chemical composition of secondary organic aerosol formed on a regional scale during the TORCH 2003 campaign in the southern UK, Atmos. Chem. Phys., 6, 419–431, doi:10.5194/acp-6-419-2006, 2006b.

Kawamura, K. and Kaplan, I. R.: Determination of organic acids (CrC10) in the atmosphere, motor exhausts, and engine oils, Environ. Sci. Technol., 19, 1082–1086, 1985.

Keene, W. C. and Galloway, J. N.: Considerations regarding sources of formic and acetic acids in the troposphere, J. Geophys. Res.-Atmos., 91, 14466–14474, 1986.

Keene, W. C., Galloway, J. N., and Holden, J. D.: Measurement of weak organic acidity in precipitation from remote areas of the world, J. Geophys. Res.-Atmos., 88, 5122–5130, 1983.

Khan, M. A. H., Ashfold, M. J., Nickless, G., Martin, D., Watson, L. A., Hamer, P. D., Wayne, R. P., Canosa-Mas, C. E., and Shallcross, D. E.: Night-time NO_3 and OH radical concentrations in the United Kingdom inferred from hydrocarbon measurements, Atmos. Sci. Lett., 9, 140–146, 2008.

Leather, K. E., McGillen, M. R., Cooke, M. C., Utembe, S. R., Archibald, A. T., Jenkin, M. E., Derwent, R. G., Shallcross, D. E., and Percival, C. J.: Acid-yield measurements of the gas-phase ozonolysis of ethene as a function of humidity using Chemical Ionisation Mass Spectrometry (CIMS), Atmos. Chem. Phys., 12, 469–479, doi:10.5194/acp-12-469-2012, 2012.

Nowak, J. B., Neuman, J. A., Kozai, K., Huey, L. G., Tanner, D. J., Holloway, J. S., Ryerson, T. B., Frost, G. J., McKeen, S. A., and Fehsenfeld, F. C.: A chemical ionization mass spectrometry technique for airborne measurements of ammonia, J. Geophys. Res.-Atmos., 112, D10S02, doi:10.1029/2006JD007589, 2007.

Paulot, F., Crounse, J. D., Kjaergaard, H. G., Kroll, J. H., Seinfeld, J. H., and Wennberg, P. O.: Isoprene photooxidation: new insights into the production of acids and organic nitrates, Atmos. Chem. Phys., 9, 1479–1501, doi:10.5194/acp-9-1479-2009, 2009a.

Paulot, F., Crounse, J. D., Kjaergaard, H. G., Kurten, A., St Clair, J. M., Seinfeld, J. H., and Wennberg, P. O.: Unexpected Epoxide Formation in the Gas-Phase Photooxidation of Isoprene, Science, 325, 730–733, 2009b.

Paulot, F., Wunch, D., Crounse, J. D., Toon, G. C., Millet, D. B., DeCarlo, P. F., Vigouroux, C., Deutscher, N. M., González Abad, G., Notholt, J., Warneke, T., Hannigan, J. W., Warneke, C., de Gouw, J. A., Dunlea, E. J., De Mazière, M., Griffith, D. W. T., Bernath, P., Jimenez, J. L., and Wennberg, P. O.: Importance of secondary sources in the atmospheric budgets of formic and acetic acids, Atmos. Chem. Phys., 11, 1989–2013, doi:10.5194/acp-11-1989-2011, 2011.

Preunkert, S., Legrand, M., Jourdain, B., and Dombrowski-Etchevers, I.: Acidic gases (HCOOH, CH_3COOH, HNO_3, HCl, and SO_2) and related aerosol species at a high mountain Alpine site (4360 m elevation) in Europe, J. Geophys. Res.-Atmos., 112, D23S12, doi:10.1029/2006JD008225, 2007.

Real, E., Law, K. S., Weinzierl, B., Fiebig, M., Petzold, A., Wild, O., Methven, J., Arnold, S., Stohl, A., Huntrieser, H., Roiger, A., Schlager, H., Stewart, D., Avery, M., Sachse, G., Browell, E., Ferrare, R., and Blake, D.: Processes influencing ozone levels in Alaskan forest fire plumes during long-range transport over the North Atlantic, J. Geophys. Res.-Atmos., 112, D10S41, doi:10.1029/2006JD007576, 2007.

Reiner, T., Mohler, O., and Arnold, F.: Measurements of acetone, acetic acid, and formic acid in the northern midlatitude upper troposphere and lower stratosphere, J. Geophys. Res.-Atmos, 104, 13943–13952, 1999.

Rinsland, C. P., Mahieu, E., Zander, R., Goldman, A., Wood, S., and Chiou, L.: Free tropospheric measurements of formic acid (HCOOH) from infrared ground-based solar absorption spectra: Retrieval approach, evidence for a seasonal cycle, and comparison with model calculations, J. Geophys. Res.-Atmos, 109, D18308, doi:10.1029/2004JD004917, 2004.

Rivett, A. C., Martin, D., Gray, D. J., Price, C. S., Nickless, G., Simmonds, P. G., O'Doherty, S. J., Greally, B. R., Knights, A., and Shallcross, D. E.: The role of volatile organic compounds in the polluted urban atmosphere of Bristol, England, Atmos. Chem. Phys., 3, 1165–1176, doi:10.5194/acp-3-1165-2003, 2003a.

Rivett, A. C., Martin, D., Nickless, G., Simmonds, P. G., O'Doherty, S. J., Gray, D. J., and Shallcross, D. E.: In situ gas chromatographic measurements of halocarbons in an urban environment, Atmos. Environ., 37, 2221–2235, 2003b.

Roberts, J. M., Veres, P., Warneke, C., Neuman, J. A., Washenfelder, R. A., Brown, S. S., Baasandorj, M., Burkholder, J. B., Burling, I. R., Johnson, T. J., Yokelson, R. J., and de Gouw, J.: Measurement of HONO, HNCO, and other inorganic acids by negative-ion proton-transfer chemical-ionization mass spectrometry (NI-PT-CIMS): application to biomass burning emissions, Atmos. Meas. Tech., 3, 981–990, doi:10.5194/amt-3-981-2010, 2010.

Roberts, J. M., Veres, P., Cochran, A. K., Warneke, C., Baasandorj, M., Burkholder, J. B., Burling, I. R., Johnson, T. J., Yokelson, R. J., and deGuow, J.: Isocyanic acid in the atmosphere and its possible link to smoke-related health effects, P. Natl. Acad. Sci., 108, 8966–8971, 2011.

Sanhueza, E. and Andreae, M. O.: Emissions of formic and acetic acids from tropical Savanna soils, Geophys. Res. Lett., 18, 1707–1710, 1991.

Sanhueza, E., Figueroa, L., and Santana, M.: Atmospheric formic and acetic acids in Venezuela, Atmos. Environ., 30, 1861–1873, 1996.

Slusher, D. L., Huey, L. G., Tanner, D. J., Flocke, F. M., and Roberts, J. M.: A thermal dissociation-chemical ionization mass spectrometry (TD-CIMS) technique for the simultaneous measurement of peroxyacyl nitrates and dinitrogen pentoxide, J. Geophys. Res.-Atmos., 109, D19315, doi:10.1029/2004JD004670, 2004.

Stewart, D. J., Taylor, C. M., Reeves, C. E., and McQuaid, J. B.: Biogenic nitrogen oxide emissions from soils: impact on NO_x and ozone over west Africa during AMMA (African Monsoon Multidisciplinary Analysis): observational study, Atmos. Chem. Phys., 8, 2285–2297, doi:10.5194/acp-8-2285-2008, 2008.

Taatjes, C. A., Meloni, G., Selby, T. M., Trevitt, A. J., Osborn, D. L., Percival, C. J., and Shallcross, D. E.: Direct observation of the gas-phase Criegee intermediate (CH_2OO), J. Am. Chem. Soc., 130, 11883–11885, 2008.

Talbot, R. W., Beecher, K., and Harriss, R.: Atmospheric geochemistry of formic and acetic acids at a mid-latitude temperate site, J. Geophys. Res., 93, 1638–1652, 1988.

Talbot, R. W., Mosher, B. W., Heikes, B. G., Jacob, D. J., Munger, J. W., Daube, B. C., Keene, W. C., Maben, J. R., and Artz, R. S.: Carboxylic acids in the rural continental atmosphere over the

eastern United States during the Shenandoah cloud and photochemistry experiment. J. Geophys. Res., 100, 9335–9343, 1995.

Talbot, R. W., Dibb, J. E., Scheuer, E. M., Blake, D. R., Blake, N. J., Gregory, G. L., Sachse, G. W., Bradshaw, J. D., Sandholm, S. T., and Singh, H. B.: Influence of biomass combustion emissions on the distribution of acidic trace gases over the southern Pacific basin during austral springtime, J. Geophys. Res.-Atmos., 104, 5623–5634, 1999.

Veres, P., Roberts, J. M., Warneke, C., Welsh-Bon, D., Zahniser, M., Herndon, S., Fall, R., and de Gouw, J.: Development of negative-ion proton-transfer chemical-ionization mass spectrometry (NI-PT-CIMS) for the measurement of gas-phase organic acids in the atmosphere, Int. J. Mass Spectrom., 274, 48–55, 2008.

Von Kuhlmann, R., Lawrence, M. G., Crutzen, P. J., and Rasch, P. J.: A model for studies of tropospheric ozone and nonmethane hydrocarbons: Model evaluation of ozone-related species, J. Geophys. Res.-Atmos, 108, 4729, doi:10.1029/2002JD003348, 2003.

Utembe, S. R., Watson, L. A., Shallcross, D. E., and Jenkin, M. E.: A Common Representative Intermediates (CRI) mechanism for VOC degradation. Part 3: Development of a secondary organic aerosol module, Atmos. Environ., 43, 1982–1990, 2009.

Utembe, S. R., Cooke, M. C., Archibald, A. T., Jenkin, M. E., Derwent, R. J., and Shallcross, D. E.: Using a reduced Common Representative Intermediates (CRIv2-R5) mechanism to simulate tropospheric ozone in a 3-D Lagrangian chemistry transport model, Atmos. Environ., 44, 1609–1622, 2011a.

Utembe, S. R., Cooke, M. C., Archibald, A. T., Shallcross, D. E., Derwent, R. G., and Jenkin, M. E.: Simulating Secondary Organic Aerosol in a 3-D Lagrangian Chemistry Transport Model using the reduced Common Representative Intermediates Mechanism (CRIv2-R5), Atmos. Environ., 45, 1604–1614, 2011b.

Watson, L. A., Shallcross, D. E., Utembe, S. R., and Jenkin, M. E.: A Common Representative Intermediates (CRI) mechanism for VOC degradation. Part 2: Gas phase mechanism reduction, Atmos. Environ., 42, 7196–7204, 2008.

Welz, O., Savee, J. D., Osborn, D. L., Vasu, S., Percival, C. J., Shallcross, D. E., and Taatjes, C. A.: Reaction of CH_2I with O_2 forms Criegee Intermediate: Direct Measurements of CH_2OO Kinetics, Science, 335, 204–207, 2012.

Yates, E. L., Derwent, R. G., Simmonds, P. G., Greally, B. R., O'Doherty, S., and Shallcross, D. E.: The seasonal cycles and photochemistry of C2–C5 alkanes at Mace Head, Atmos. Environ., 44, 2705–2713, 2010.

Yu, S. C.: Role of organic acids (formic, acetic, pyruvic and oxalic) in the formation of cloud condensation nuclei (CCN): a review, Atmos. Res., 53, 185–217, 2000.

Zander, R., Duchatelet, P., Mahieu, E., Demouli, P., Roland, G., Servais, C., Vander Auwera, J., Perrin, A., Rinsland, C. P., and Crutzen, P.: Formic acid above the Jungfraujoch during 1985–2007: observed variability, seasonality, but no long-term background evolution, J. Atmos. Chem. Phys., 10, 10047–10065, 2010,
http://www.atmos-chem-phys.net/10/10047/2010/.

Zhong, Z. C., Victor, T., and Balasubramanian, R.: Measurement of major organic acids in rainwater in Southeast Asia during burning and non-burning period, Water Air Soil Poll., 130, 457–462, 2001.

3. Paper B

"Simultaneous airborne nitric acid and formic acid measurements using a chemical ionisation mass spectrometer around the UK: analysis of primary and secondary production pathways"

Submitted to Atmospheric Environment

Authors: M. Le Breton, A. Bacak, J. B. A. Muller, P. Xiao, B. M. A. Shallcross, R. Batt, M. C. Cooke, D. E. Shallcross, S. J-B. Bauguitte and C. J. Percival.

J. Muller and A. Bacak helped with the initial setup for aircraft measurements and laboratory tests, also assisting with the development of the new inlet. S-J. Bauguitte supplied the NO_x data from the core chemistry instrument on the aircraft. D. E. Shallcross performed the atmospheric modelling and provided the ideas for the NO_x vs O_3 plots and OH estimations. I operated the instrument during this flight and analysed the data using a toolkit developed in the first year of my PhD. The paper was written by myself, with direction from my supervisor and his group. All work was carried out under the supervision of C. J. Percival.

Simultaneous airborne nitric acid and formic acid measurements using a chemical ionization mass spectrometer around the UK: analysis of primary and secondary production pathways

Michael Le Breton[1], Asan Bacak[1], Jennifer B.A. Muller[1], Ping Xiao[2], Beth M. A. Shallcross[2], Rory Batt[2], Michael C. Cooke[2†], Dudley E. Shallcross[2], S. J.-B. Bauguitte[3] and Carl J. Percival[1]*

[1]*The Centre for Atmospheric Science, The School of Earth, Atmospheric and Environmental Sciences, The University of Manchester, Simon Building, Brunswick Street, Manchester, M13 9PL, UK.*

[2]*School of Chemistry, The University of Bristol, Cantock's Close BS8 1TS, UK.*

[3]Facility for Airborne Atmospheric Measurements (FAAM), Building 125, Cranfield University, Cranfield, Bedford, MK43 0AL, UK

[*]Corresponding author Email: carl.percival@manchester.ac.uk

[†] Now at the Met. Office, FitzRoy Road, Exeter, Devon, EX1 3PB.

Abstract

The first simultaneous measurements of formic and nitric acid mixing ratios around the United Kingdom were measured on the FAAM BAe-146 research aircraft with a chemical ionization mass spectrometer using I^- reagent ions at 0.8 Hz. Analysis of the whole dataset shows that formic acid and nitric acid are positively correlated as illustrated by other studies (e.g. Veres *et al*., 2010). However, initial evidence indicates a prominent direct source of formic acid and also a significant source when O_3 levels are high, suggesting the importance of the ozonolysis of 1-alkenes. A trajectory model was able to reproduce the formic acid concentrations by both the inclusion of a primary vehicle source and production via ozonolysis of propene equivalent 1-alkene levels.

Inspection of data archives imply these levels of 1-alkene are possible after 11 am, but formic acid and nitric acid plumes early in the flight are too high for the model to replicate. These data show the relationship between nitric acid and formic acid cannot solely be attributed to related photochemical production. The simultaneous measurement of HCOOH and HNO_3 allows the OH levels along the flight track to be estimated through the assumed relationship between formic acid and nitric in photochemical plumes and a constant source of 1-alkene.

Introduction

Formic acid (HCOOH) has been measured in urban, rural and remote areas (Talbot *et al*., 1988), with its presence in the gas and aerosol phase allowing it to be a common constituent of global precipitation (Keene and Galloway, 1983). Keene and Galloway (1986) have documented the contribution of formic acid to the acidity of precipitation and subsequent affects on aquatic and terrestrial ecosystems. Formic acid can dominate free acidity in precipitation, exerting an influence on pH dependent chemical reactions and OH cloud chemistry (Jacob *et al*., 1986). Organics are often found in the fine fraction of aerosols, encouraging the activation of cloud droplets through the change of their hygroscopicity and therefore affecting their total indirect forcing (Yu, 2000).

The sinks of formic acid are relatively well understood to be wet and dry deposition and are the dominant formic acid loss pathways. Reactivity towards OH and NO_3 is low, leading to an atmospheric lifetime of around 3 days (Paulot *et al*., 2011). However, sources are poorly constrained and many studies (Poisson *et al*., 2000; von Kuhlmann *et al*., 2003a; Ito *et al*., 2007) have found large inconsistencies between measurements and modelled results (Paulot *et al*., 2011). Sources of formic acid include biogenic and anthropogenic primary emissions, for example, biomass burning (Burling *et al*., 2010) and in situ production such as hydrocarbon oxidation, thought their relative fluxes are poorly quantified (Chebbi *et al*., 1996). The emission of acetylene and 1-alkynes from biomass burning can be oxidised by OH to produce formic acid (Hatakeyama et al., 1986, Paulot *et al.*, 2011). The photochemical oxidation of isoprene can also result in the formation of formic acid through the reaction of OH with hydroxycarbonyls,

glycolaldehyde and hydroxyacetone (Butkovskaya *et al*., 20061,b, Paulot *et al*., 2009), yielding up to 18% at room temperature.

Strong sources of formic acid have been reported to originate from forested Savannah regions (Sanhueza and Andreae., 1991; Hartmann *et al*., 1991), as a result of direct emissions by plants, but in situ production via the ozonolysis of alkenes is though to dominate (Sanhueza *et al*., 1996). Formic acid concentrations have reached 1 ppbv in the Savannah with precursor species peaking at midday. High emissions of formic acid have been observed at coastal regions in Southern California, peaking in summer at 9.6 metric tons per day (Grosjean, 1992). *In situ* production was also found to be of similar strength; 10.1 metric tons per day, peaking at 34.5 metric tons per day. However, these *in situ* production rates are based on earlier product data for acid formation from the ozonolysis of alkenes. The dominant reaction between the criegee intermediate and H_2O to form organic acids has been recognised for some time (Atkinson *et al.,* 1994), although more recent data (Leather *et al*., 2011) would suggest that the in situ production has been under-estimated (e.g. Taatjes *et al*., 2008; Verecken *et al*., 2012; Welz *et al*., 2012). Preunkert *et al*. (2007) concluded that *in situ* production was the dominant process for formic acid production in Europe, based on high altitude measurements. Isotopic analysis of ^{13}C and ^{14}C from background locations in the United States by Johnson and Dawson (1993) found that the direct emission of formic acid from C_3 plants was the dominant source. Baboukas *et al.* (2000) also suggests the ocean may be a source of formic acid.

Ground based measurements (Rinsland *et al*., 2004) and airborne measurements (Le Breton *et al*., 2012) have shown that current models underestimate formic acid by a factor of 10-50. Such discrepancies between perceived source strengths and observed atmospheric concentrations have led many authors to speculate upon the existence of a missing or poorly constrained source term (e.g. Grosjean, 1989; Talbot *et al*., 1988; Granby *et al*., 1997; Rinsland, 2004), and it has been suggested by several of these studies that an unknown anthropogenic, and perhaps secondary source may be responsible, such as higher biogenic emissions during the growing season (Rinsland *et*

al., 2004). Paulot *et al.* (2011) report evidence of long-lived missing secondary sources of formic acid which may be associated with the ageing of aerosols. Veres *et al.* (2011) has also shown that organic acids are photochemically and rapidly produced from urban emissions, shown through a correlation with nitric acid (HNO_3). Furthermore, Stavrakou *et al*. (2012) using IASI data have suggested that formic acid levels are under predicted by a factor of 2-3 as a result of oxidation of terpenoids. The oxidation of volatile organic compound (VOC) precursors leading to the production of formic acid has also been suggested as a significant source (Arlander *et al*., 1990). An example of this observed by the ozonolysis of ethene, whose emissions have been estimated to be 15 Tg yr^{-1} (Broadgate *et al*., 1997; Paulot *et al*., 2010).

Le Breton *et al.* (2012) concluded that models under predict formic acid concentrations as a result of the under representation of both primary formic acid emissions of anthropogenic origin and a lack of precursor emissions, such as isoprene, from biogenic sources, which are oxidised to produce formic acid. Further research and analysis into the dominance and representation of such formation pathways is necessary in order to increase the constraint that models have on formic acid production.

Recently, Veres *et al*. (2008, 2011), Roberts *et al*. (2010, 2011), Bertram *et al*. (2011) and Le Breton *et al*. (2012) have shown that chemical ionisation mass spectrometry (CIMS) can selectively detect gas-phase acids with a frequency of 0.8 Hz and a limit of detection below 0.1 ppbv for measurements of formic acid. Here, formic and nitric acid are simultaneously measured using a CIMS on board an aircraft utilising an I^- ionisation scheme to determine the major sources of formic acid around the UK and a Photochemical Trajectory Model will be integrated and compared with the resulting aircraft measurements. The measurements of formic and nitric acid are critically analysed in order to determine the importance and origin of the missing sources. These measurements are then employed to estimate OH concentrations.

Instrumentation

Chemical ionisation mass spectrometry (CIMS) was used for real-time detection of formic acid and nitric acid on board the airborne platform FAAM BAe-146. The CIMS instrument employed here was built by the Georgia Institute of Technology as previously described by Nowak *et al*. (2007). Measurements of formic acid have previously been described in Le Breton *et al*. (2012) with changes only to the inlet which are described in this section. Nitric acid is measured using methyl iodide as the ionisation gas and detected at m/z 189 as shown in equation 1.

$$I.H_2O + HNO_3 \rightarrow HNO_3.I + H_2O \quad (1)$$

The inlet consisted of 3/8" OD diameter PFA tubing of length 580 mm and was heated to 50˚C to reduce surface loss. An orifice of diameter 0.9 mm was positioned at the front of the inlet to restrict the flow to 5.8 SLM. The pressure in the ionisation region was maintained at 19 Torr throughout the flight by controlling the flow of nitrogen into the ionisation region using a mass flow controller (MKS Instruments).

Formic acid calibrations were performed as described in Le Breton *et al* (2012). The nitric acid calibration cycle involves obtaining the nitric acid instrumental background by passing the sample air through an acid scrubber which is made of nylon turnings coated with sodium bicarbonate. After an effective zero acid air flow for background determination, a known amount of nitric acid from a Permeation device (Kin-Tek Laboratories, Inc) is added to this scrubbed air at 75˚C and 20 standard cubic centimetres per minute (sccm) flow until a plateau in formic acid signal is achieved. A second background determination is performed before switching back to atmospheric sampling model. The nitric acid permeation source was calibrated at varying temperatures using a Metrohm 761 Compact Ion Chromatograph to measure NO_3^- ions

after running the permeation source gas through deionised water. The nitric acid calibration factor was applied to the relative formic acid concentrations during post-flight data processing. The average sensitivity (±1σ) for nitric acid was 26 ± 6.5 Hz $pptv^{-1}$ for 1 MHz of reagent ion signal. The average sensitivity for formic acid was 28 ± 7.1 Hz $pptv^{-1}$ for 1 MHz of reagent ion signal. During a test flight, the calibration was proven to be invariant with altitude. Calibrations were performed from 50 feet to 3000 feet. The calibration factor for the range of altitudes was within 3σ of the error calculated from the statistical noise of the calibration signal in the plateau region.

Additional measurements

Ozone (O_3), nitric oxide (NO) and nitrogen dioxide ($NO_{2)}$ were also measured on board the aircraft during flight B547 (0/09/2010). A chemiluminescence detector measured NO and NO_2 every 10 seconds with an uncertainty of ± 6 % ppbv (Stewart *et al*., 2008). O_3 was measured using a UV Photometric Ozone Analyser at 1 Hz with an uncertainty of 3 ppbv (Real *et al*., 2007).

Trajectory model

A particle trajectory model has been used to estimate formic and nitric acid concentrations along the B547 flight path. The trajectory model used for this purpose has been described in detail previously (e.g. Johnson *et al*., 2006; Evans *et al*., 2000) and will be only briefly described here. The trajectory model simulates the chemical development in a well mixed air parcel being advected along multi-day trajectories. The air parcel picks up emissions of NO_x, carbon monoxide (CO), sulphur dioxide (SO_2), methane, anthropogenic VOC and biogenic VOC when in the boundary layer, which are processed using an appropriate description of the chemical and photochemical transformations leading to the formation of ozone and other secondary pollutants such as HCOOH and HNO_3. Dry deposition of species also occurs when the air parcel is in the boundary layer.

Two chemistry modules have been incorporated into the trajectory mode: the full Master Chemical Mechanism (MCM v3.1; Jenkin *et al*., 1997) and the Common Representative Intermediates Scheme (CRIv2-R5; Jenkin *et al*., 2008; Watson *et al*., 2008; Utembe *et al*., 2009, 2010, 2011; Archibald *et al*., 2010). Trajectories are generated by the Hysplit model and integrated for four days, arriving at a point coincident in time and space with the aircraft flight track (Draxler *et al*., 2003).

Results

Overview

Previous aircraft measurements around the UK have allowed national inventories to be validated using a boundary layer budget approach for compounds such as CO, CO_2, CH_4 and N_2O (Polson *et al*., 2011). Formic and nitric acid were measured onboard the BAe-146 on 02/09/2010 around the coast of the UK at 0.8 Hz and are presented here averaged to 30 seconds. A high pressure system and resulting low wind speeds during this flying period allowed the air masses over the UK to age without substantial mixing from Europe as shown in figure 1. The average mixing ratios for this flight were 1478 and 250 pptv for nitric and formic acid respectively. These are comparable of that measured on the ground by Veres *et al.* (2011) in Californian urban plumes, with peak concentrations of 4384 and 710 pptv for nitric and formic acid respectively. The peak concentration ratio of nitric to formic acid from both campaigns are also similar; 5.9:1 for the work presented in this paper and 6.2:1 for Veres *et al.* (2011).

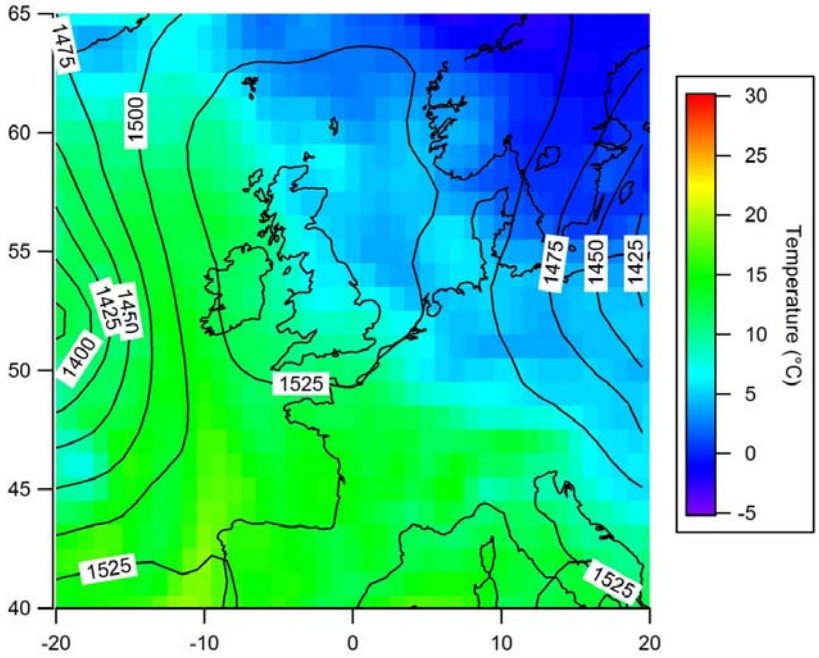

Figure 1. The potential height and temperature at 850 hPa during flight B547.

The model simulation accurately predicted O_3 concentrations throughout flight B547 a shown in figure 2; which is integral to accurately predicting formic and nitric acid mixing ratios (figure 2). Although only a small range of O_3 concentrations were observed on this day, the diurnal structure is seen within the model and measurements, with the maxima seen at midday and the lowest levels in the morning. In general nitric acid concentrations were reasonably well predicted by the model but some elevated events were not reproduced (see later discussion). Model formic acid concentrations were under predicted throughout in comparison with the measurements, on inclusion of a primary source (correlated with direct NO_x emissions (Bannan *et al.*, 2013)) of formic acid better agreement was observed for part of the morning measurements. Evaluations of the model outputs for formic and nitric acid are assessed in the following sections. The overall comparison between modelled and measured NO_x is good in terms of temporal variation, but the model tends to underestimate NO_x levels somewhat, typical of trajectory models (e.g. Evans *et al.*, 2000).

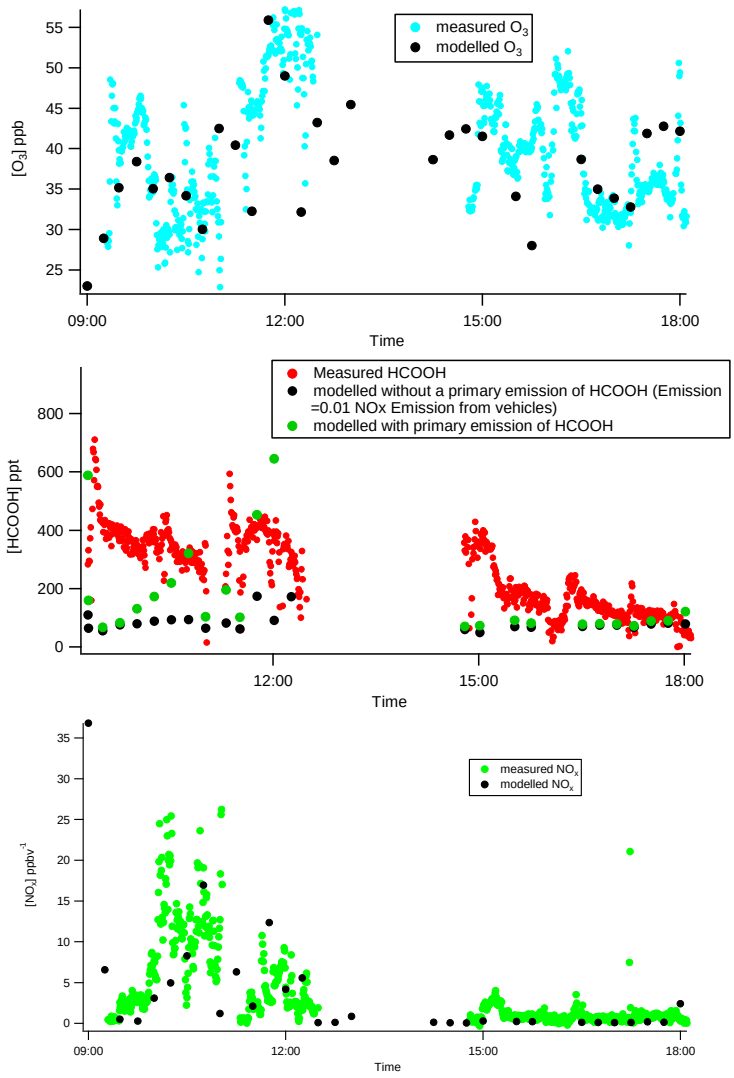

Figure 2. Time series of modelled and measured O_3, NO_x and formic acid data from flight B547. The green markers for formic are modelled concentrations of formic acid with primary emissions (emitting HCOOH (E_{HCOOH}) using a factor of $0.01E_{NOx}$) and the black markers are without primary emissions.

Plumes

During flight B547, 4 distinct nitric acid plumes were intersected (A, B, C and D) as shown in figure 3. The peak concentrations for the plumes were 4365, 2417, 2546 and 1501 pptv respectively. The background concentrations before and after these plumes were 1786, 1473, 112 and 168 pptv respectively (defined as a 3 sigma reduction in noise for a 5 minute mean). Although the peak concentrations are quite similar (a factor of 2-3

at most), the background concentrations decrease significantly on the North and North East side of the United Kingdom, particularly Scotland (a factor of 10 lower); since nitric acid production is directly related to NO_2 levels, lower NO_x emissions in these regions are consistent with these observations. The median concentrations for the plumes are 3080, 4292, 4384, 2475 pptv respectively.

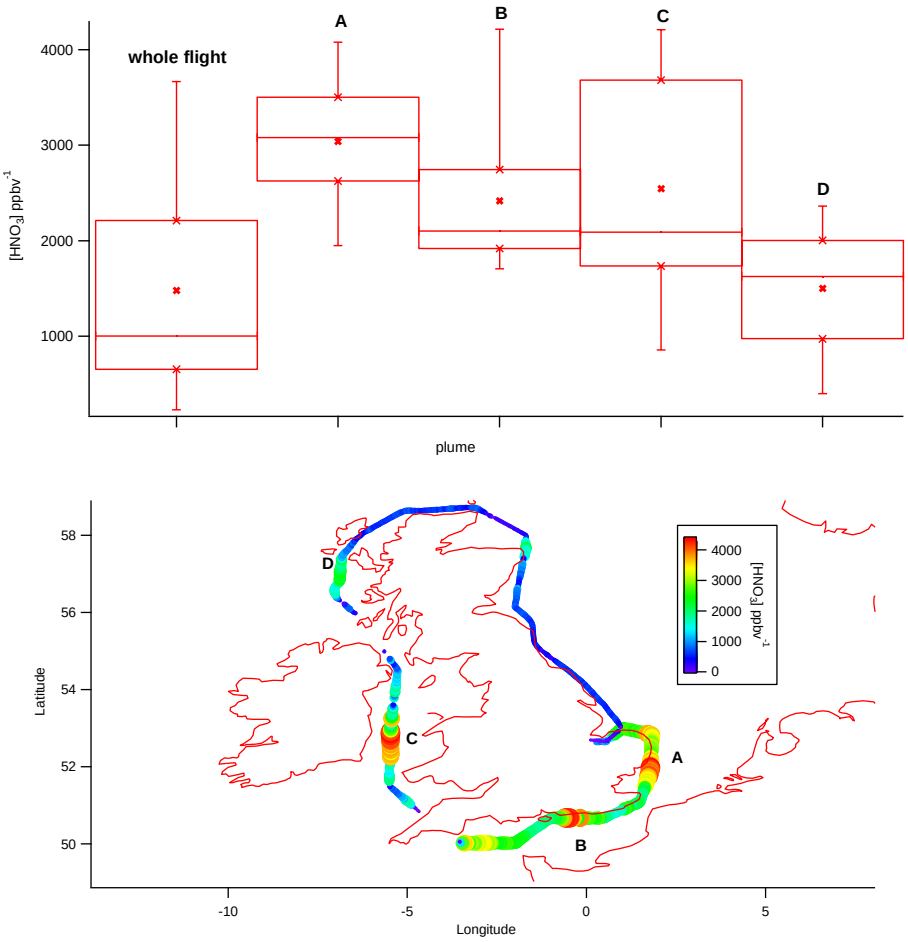

Figure 3. Flight path of the aircraft over the UK during flight B547 with the track colour and size coded to nitric acid concentration. The box plot shows the minimum, maximum, mean, median, 5th, 25th, 75th and 95th percentile.

Two formic acid plumes were measured during flight B547 (A and B) as shown in figure 4. Plume A was encountered at 11 00 feet and had a maximum concentration of 710 pptv. It should be noted that instrumental calibration have been validated to be constant up to 10 00 feet. Although this plume is measured above this altitude, it is

highly unlikely that the sensitivity changes further than 3 sigma of error at this altitude. The peak concentration within plume B was 596 ppt, with an average background concentration of 290 ppt. The median concentrations in plumes A and B are 612 and 458 ppt respectively. The plumes identified for formic acid are not coincident with those for nitric acid and this will be discussed later.

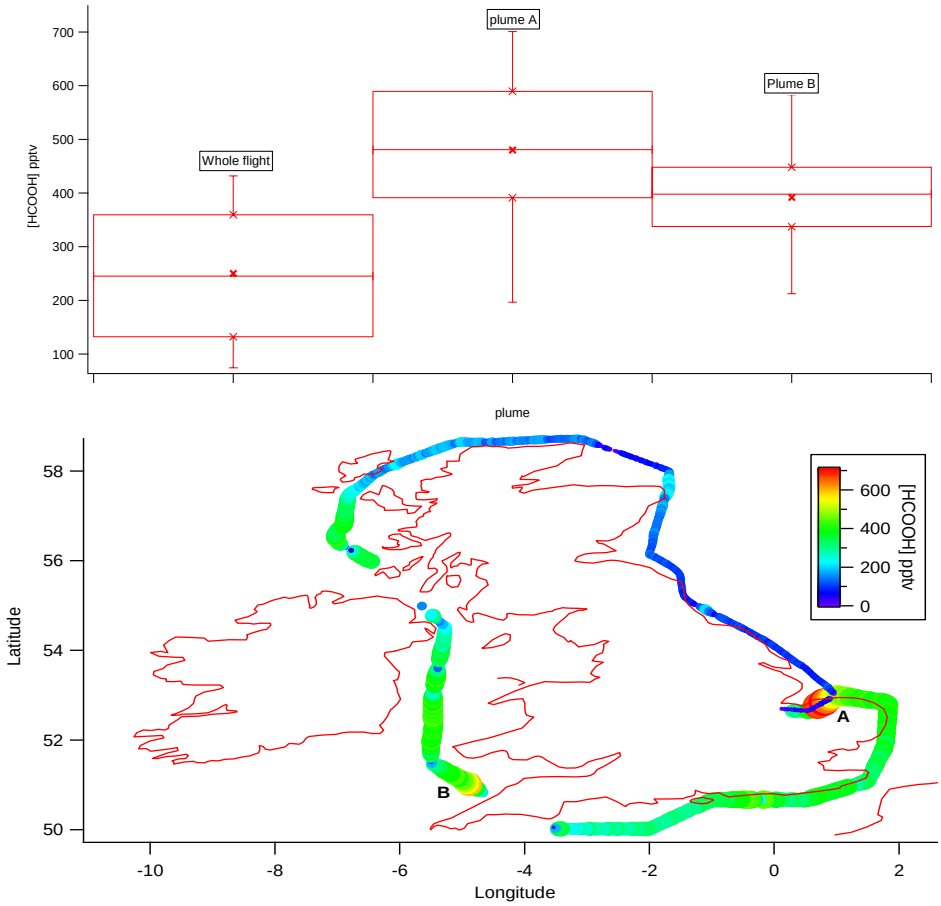

Figure 4. Flight path of the aircraft over the UK during flight B547 with the track colour and size coded to formic acid concentration. The box plot shows the minimum, maximum, mean, median, 5th, 25th, 75th and 95th percentile.

O_3-NO_x relationship

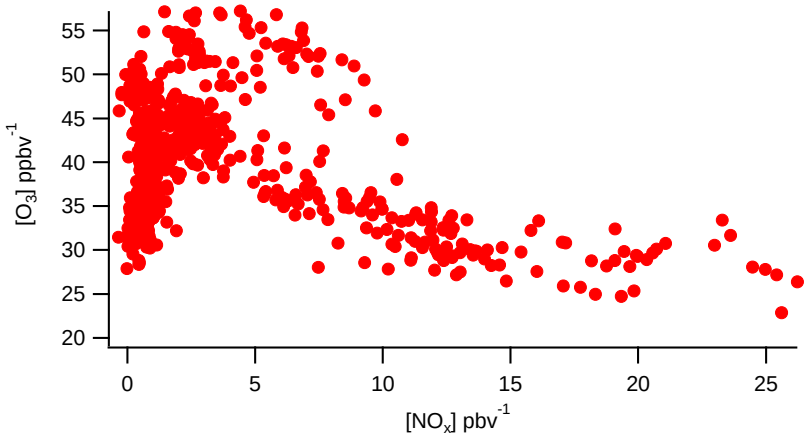

Figure 5. Plot of O_3 v NO_x for the entire flight.

Figure 5 shows a plot of O_3 vs. NO_x for the entire of flight B547. The curve shows the classic photochemical relationship between NO_x and O_x (e.g. Jenkin and Clemitshaw (2000)), where high NO_x levels leads to suppression of O_3 production as a result of reaction (2) but also the formation of PAN (peroxyacetyl nitrate) and PAN type species.

$$OH + NO_2 + M \rightarrow HNO_3 + M \qquad (2)$$

A maximum in O_3 (55 ppb) is observed at 5 ppb of NO_x and occurs at *ca.* midday off the West coast of Wales during nitric acid plume C. Given typical urban levels of NO_x in the UK in September it is safe to assume that concentrations exceeding 15 ppbv during the flight would be determined as an urban ('polluted') air mass. Figure 5 also illustrates that during the flight we encounter fresh plumes as well as somewhat aged air. We will use this O_3-NOx relationship to guide discussions that follow.

Nitric acid

Figure 6 shows the first ever nitric acid measurements around the UK on an aircraft. The main sources of nitric acid in the atmosphere are the reactions;

$$OH + NO_2 + M \rightarrow HNO_3 + M \quad (2)$$

$$N_2O_5 + H_2O \rightarrow 2HNO_3 \quad (3)$$

Where reaction (2) dominates, hence to a first approximation $d[HNO_3]/dt = k_2[NO_2][OH][M]$. So NO_x and nitric acid should be anti-correlated in a polluted plume, as the plume develops so NO_x decreases and OH goes up and so does nitric acid (thick black line), illustrated in figure 7. As the level of NOx decreases and nitric acid increases one assumes that increasingly clean or aged air is encountered. As air becomes lower in NOx concentrations, the production of nitric acid drops off and as either very clean or very aged air is encountered; depositional processes will remove nitric acid leading to the low levels observed. If one extrapolates the correlation observed at high $[NO_x]$ back to $[NO_x] = 0$, a value of ~ 3200 pptv for $[HNO_3]$ is returned. However, the actual observed $[HNO_3]$ levels at such near zero NO_x are 50 pptv for nitric acid. If we imagine that this difference is due to physical loss, it represents some 6 half-lives, if we speculate that this loss occurs over a day it gives a half-life of 4 hours or an e-folding time of ca. 6 hours for physical loss. Although such analysis is speculative, the estimated half-life is in keeping with other studies where nitric acid physical removal has been estimated (e.g. Nunnermacker *et al*., 1998), where a half-life of ca. 5 hours was proposed.

The formation of nitric acid through the heterogeneous reaction between H_2O and dinitrogen pentoxide is assumed to be negligible in the model due to the extremely low daytime N_2O_5 concentrations (sub 5 ppt) (Osthoff *et* al., 2006). There is also a small possibility (0.8% according to Butkovskaya *et al.* (2007) of the reaction between the hydroperoxy radical and nitrogen oxide forming nitric acid rather than the hydroxyl

radical and nitrogen dioxide. Another minor pathway of nitric acid production is via H-abstraction reactions of nitrate radicals, although this reaction is relatively slow under atmospheric conditions (Monks, 2004). The trajectory model therefore only utilises the dominant nitric acid formation pathway, R2. In doing so it is able to accurately predict the minimum and maximum concentrations of nitric acid on the flight, with the midday maxima observed in the model and measurement. Low concentrations were also observed in the morning and evening. In the model, reaction (2) dominates the production of nitric acid, hence it is reasonable to expect peaks in nitric acid to occur where the product [OH][NO_2] is large. Although OH was not measured during this flight, an increase in NO_2 levels is correlated with nitric acid concentrations up to 7 ppb. Figure 6 shows that the elevated morning levels of nitric acid at the start of the measurement period is underestimated by the model as is NO_x, suggesting that the trajectory model either misses surface emissions along the trajectory or that the surface emissions are underestimated.

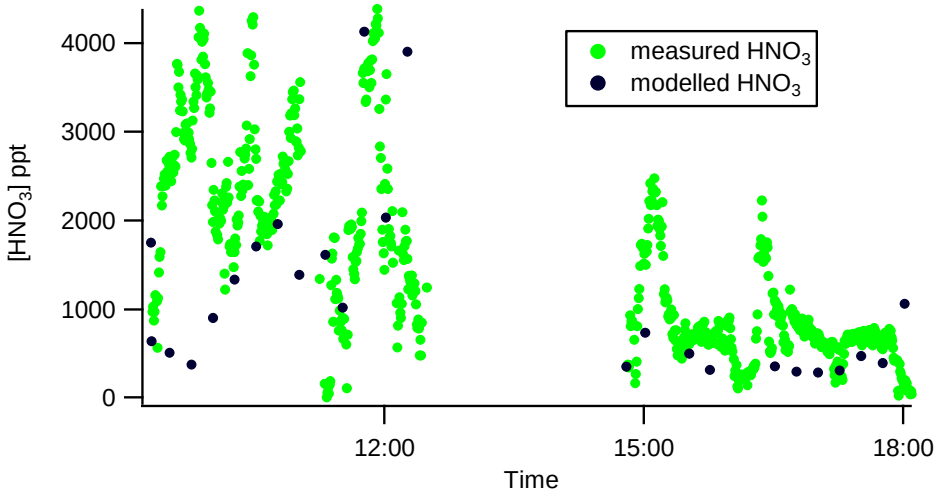

Figure 6. Time series of measured and modelled nitric acid concentrations.

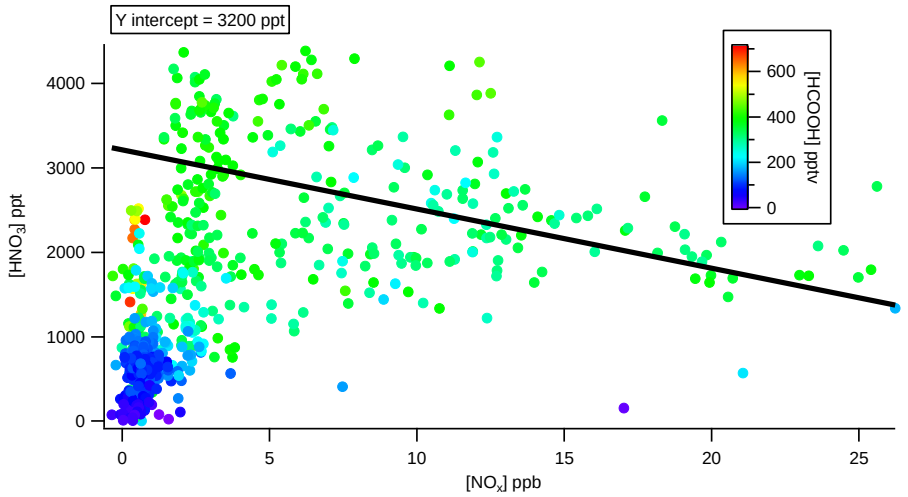

Figure 7. Nitric acid measurements plotted against NO_x and colour coded to formic acid concentrations. The Y intercept is 3200 ppt of HNO_3.

Estimated OH concentrations

Measurements of nitric acid should provide an indication of OH levels along the flight path. In keeping with the work of Veres *et al*. (2010) we see a strong positive correlation between nitric acid and formic acid (figure 11). If we assume that they are both made photochemically in a plume we may estimate that the production terms for each compound are

$$OH + NO_2 + M \rightarrow HNO_3 + M \quad (2)$$

$$O_3 + \text{1-alkene} \rightarrow \text{carbonyl} + CH_2OO \quad (4)$$

$$CH_2OO + H_2O \rightarrow HCOOH + H_2O \quad (5a)$$

$$CH_2OO \rightarrow \text{products} \quad (5b)$$

leading to production rates

$$d[HNO_3]/dt = k_2[NO_2][OH][M] \quad \text{I}$$

$$d[HCOOH]/dt = k_4[O_3][\text{1-alkene}]f(H_2O) \quad \text{II}$$

noting that $f(H_2O) = \Gamma_{SCI(CH2OO)}\, k_{5a}[H_2O] /(k_{5a}[H_2O] + k_{5b})$

where $\Gamma_{SCI(CH2OO)}$ is the fraction of the 1-alkene forms 'stabilised' CH_2OO on ozonolysis and that this 'stabilised' Criegee intermediate reacts with H_2O to form formic acid. For simplicity we assume that 50% of the reaction between O_3 and 1-alkene forms CH_2OO, 50% of these CH_2OO intermediates so formed are stabilised and that 50% of these react with H_2O to form formic acid, i.e. $\Gamma_{SCI(CH2OO)} = 0.25$ and $k_{5a}[H_2O] /(k_{5a}[H_2O] + k_{5b}) = 0.5$. Assuming that the formation of formic acid and nitric acid occurs in the same plume we assume that the transport time is the same. Inspection of the ratio of I:II and rearranging leads to

$$[OH] = \frac{[HNO_3]k_4[O_3][1-alkene]f(H_2O)}{[HCOOH]k_2[NO_2][M]} \qquad \text{III}$$

The OH field generated using a constant source of 1-alkene is shown in figure 8. We have assumed a constant level of 1-alkene (here 2 ppb of propene) and used the rate coefficient for the reaction of O_3 with propene as k_4. There are several caveats with such an analysis, but the OH field returned is reasonable in terms of absolute level, although the distribution is skewed towards the afternoon. It is well known that OH levels can be very high in urban plumes and so elevated levels returned could be real. Further refinement of the method is of course required but may provide an alternative way to estimate OH and increase the information that can be retrieved from co-measurements of nitric acid and organic acids. 1-alkene data is a necessity in providing much more confidence in this method, as they will not have a homogenous distribution as assumed here and will be depleted as the plume ages. Inclusion of a direct emission of formic acid (related to NOx) will modify the expression III to (where E(HCOOH) = 0.01NOx). The average concentration calculated for OH along the flight path using this estimation is 3.5×10^5 molecules cm^{-3}. Although the structure observed in the time series cannot be assessed, the average concentration retrieved lies within range of that observed by Smith *et al*. (2006).

$$[OH] = \frac{[HNO_3]\{k_4[O_3][1-alkene]f(H_2O) + E(HCOOH)\}}{[HCOOH]k_2[NO_2][M]} \qquad \text{IIIb}$$

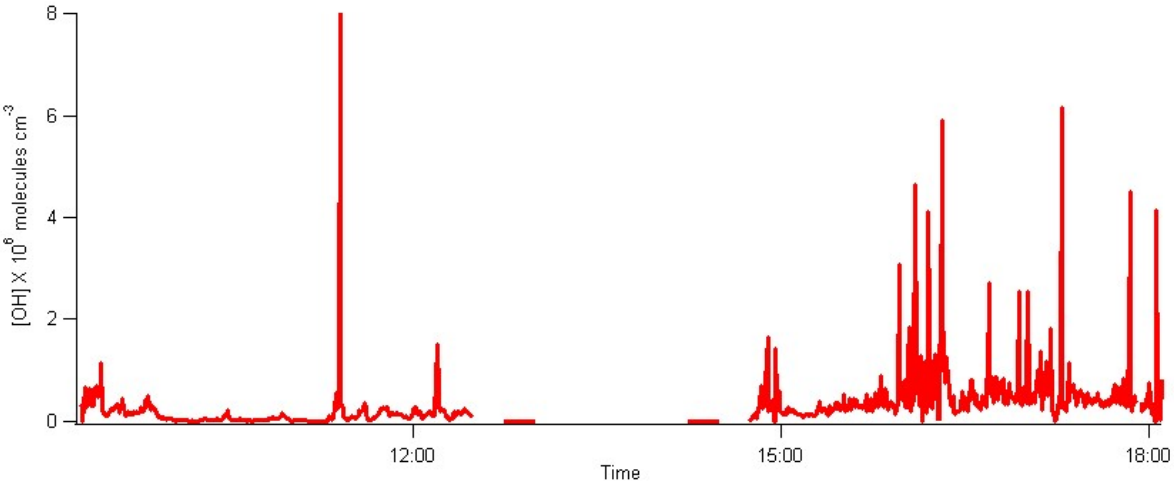

Figure 8. Estimated OH concentrations using the measured formic and nitric acid during flight B547.

Formic acid

The average concentration for the modelled run without primary emissions of formic acid and with primary emissions (E_{HCOOH} = $0.01E_{NOx}$) was 79.6 and 184.4 pptv respectively. This indicates that the model is under predicting the emissions by a factor of 2-3. However, it should be noted that the agreement between the model and measured formic acid is improved on inclusion of a direct emission, which is in agreement with Archibald *et al*. (2007) who postulated that direct emission of organic acids, as a result of incomplete combustion, can be a significant source in the urban environment. Furthermore, recent fieldwork from Le Breton *et al*. (2012) has identified direct emission of formic acid in urban plumes. During flight B547 two formic acid plumes were observed. At 09:22 the maximum concentration of 710 pptv was detected north of Norwich, plume A, which the model is able to reproduce with the inclusion of primary emissions, although the concentration is below that of the measured. An anti-correlation

exists between formic acid and nitric acid during this period of the flight; shown in figure 9, indicating this enhancement of formic acid to be from primary production. Apart from this episode, maximum formic acid concentrations are located in regions where low NO_x (0.5 ppbv) and high O_3 (47 ppbv) occurs, these peaks are not coincident with high nitric acid. One suggestion for this observation is that a secondary source is responsible for the maximum formic acid, e.g. the reaction of CH_2OO, formed from the ozonolysis of alkenes, with water (Leather *et al.*, 2012; Vereecken *et al.*, 2012; Welz *et al.*, 2012)

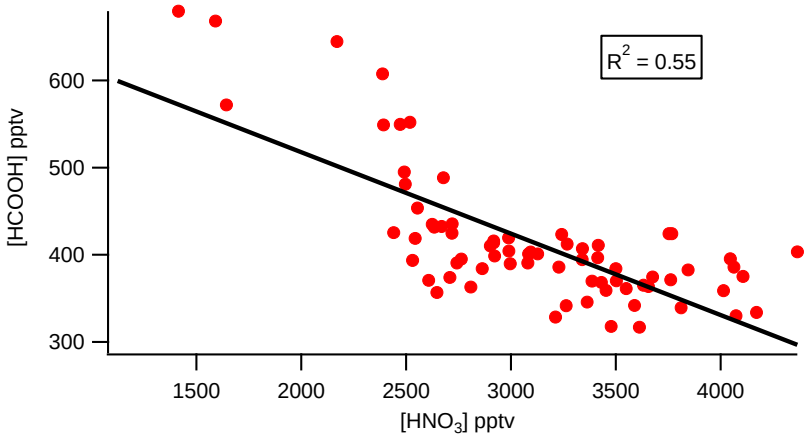

Figure 9. Formic acid vs nitric acid in the plume at 09:22.

Secondary formation of formic acid is thought to be under predicted in current models and is evident in these data during increased regions which are not predicted by the model during this flight e.g. at 15:05 elevated concentrations of formic acid are observed north west of Glasgow by the CIMS but the model is unable to generate such elevated levels. Comparisons with the nitric acid measurements suggest this increase of formic acid concentration is due to photochemical processing (Veres *et al.*, 2011). This secondary formation pathway is noticed also when this measurement is compared with figure 7 as it is situated where nitric acid and NO_x correlated, therefore exhibiting signatures of an aged air mass. An increase in O_3 and formic acid imply secondary production via oxidation of alkenes. A small plume at 16:20 also exhibits a correlation with O_3, formic and nitric acid which again suggests a secondary source that is not

represented in the model. Although the model contains some alkenes, e.g. ethene and propene, there are many potential 1-alkenes that can yield CH_2OO on ozonolysis.

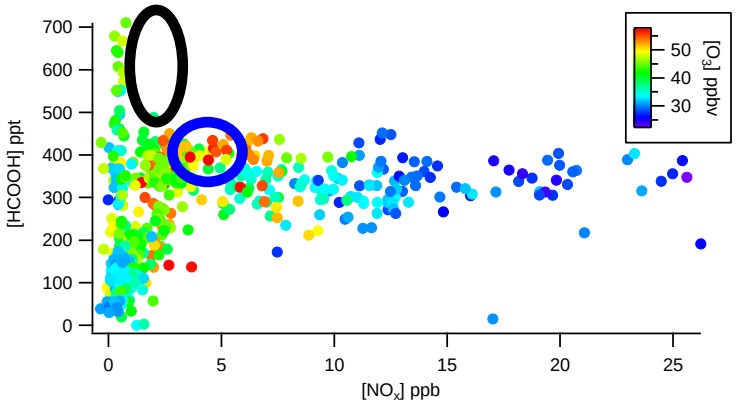

Figure 10. Formic acid vs NO_x measurements throughout the whole of flight B547 colour coded to O_3 concentrations.

The area within the black ellipse on figure 10 shows formic acid concentrations elevated to 700 pptv where NO_x concentrations do not exceed 1 ppbv. This area of high formic acid and ozone and low NO_x are likely to be regions where secondary photochemical production from ozonolysis of alkenes is elevated. The blue circle indicates the maximum oxidation point where secondary production of formic is the dominant pathway. Areas of higher NO_x and formic acid corresponding with lower O_3 levels and suppressed levels of OH, indicate primary production.

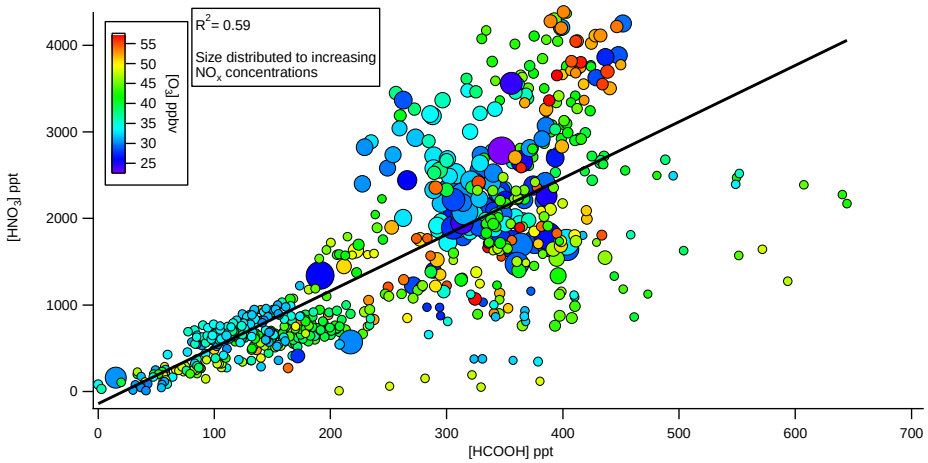

Figure 11. Nitric acid vs formic acid measurements colour coded to O_3 concentrations and size coded to NO_x concentrations.

As NO_x controls the production of nitric acid and O_3 which in part makes formic acid through ozonolysis of alkenes, a correlation with nitric acid is observed, as shown in figure 11; with the same R^2 as Veres *et al.* (2011). This graph enables regions of primary and secondary production to be clustered. There are regions of high O_3, low NO_x and high formic and nitric acid indicating secondary production of formic acid. Regions of high formic and nitric acid with low O_3 and relatively high NO_x are characteristic of a high oxidation rate region. There is also a cluster of high formic acid and NO_x with relatively low concentrations of O_3 and nitric acid, implying a primary production pathway.

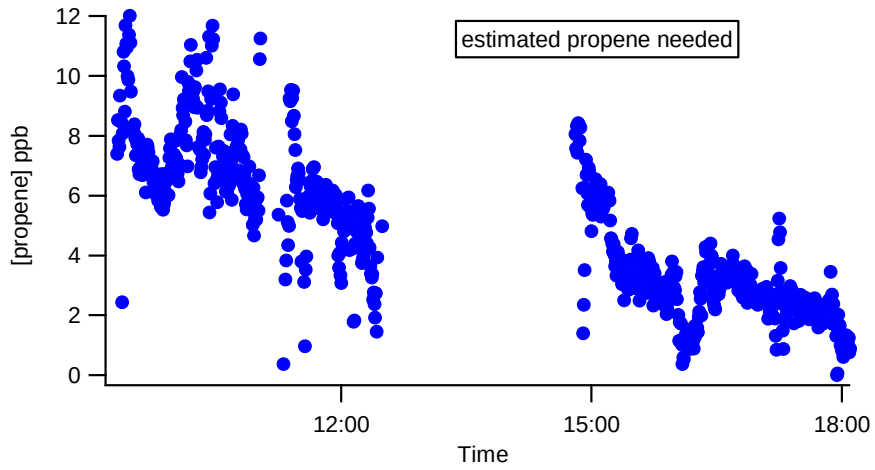

Figure 12. Time series of propene concentrations needed to be implemented into the model for formic acid predicted concentrations to match the measured levels via oxidation.

This under prediction of secondary sources of formic acid can be accounted for in the model by increasing the concentrations of alkenes which will form formic acid via oxidation. Figure 12 shows a time series of the propene concentration needed to produce the measured levels of formic acid. A similar structure to that of formic acid is observed,

indicating that in order to model formic acid levels, model chemistry needs to consider 1-alkene emissions more precisely.

In order to test this hypothesis we mined the UK air quality archive for data on 1-alkenes that could act as precursors to the formic acid. Data were collected for the month of September from up to 14 sites around the UK incorporating the years 1995-2011. First, it is clear that levels of 1-alkenes have decreased over this period of time. Second, the levels of propene measured in 2010 in urban locations during the time of the flight are around 0.5 – 1.5 ppbv on average, which would account for some of the 1-alkene required but not enough to account for all (see figure 12). However, inspection of 1-butene levels suggest that around 0.5 ppbv. is a reasonable average level. In all (ethene, propene, 1-butene, isoprene, 1, 3, butadiene and 1-pentene) about 2-3 ppbv. of 1-alkene (propene equivalent) can be accounted for. Therefore, either another source of formic acid is in operation or other 1-alkenes that are not measured by the network are present. It is perfectly possible for a number of fast reacting 1-alkenes that are present at low levels to make up this difference (AQIRP, 1995). Therefore, there is corroborating evidence that some of the formic acid could arise from ozonolysis of appropriate alkenes. Although the high 'propene' levels required early on in the flight (great than 6 ppb) are hard to account for in total.

Conclusions

The simultaneous measurements of nitric and formic acid for the first time on a 'Round Britain' flight have provided data that are rich in information. It is clear that nitric acid is a good indicator of plume activity, where peaks indicate a plume that has undergone a degree of ageing. Analysis of the whole dataset shows that nitric acid and formic acid are correlated as illustrated by other studies (e.g. Veres *et al*., 2010). However, more detailed analysis reveals, first, evidence for a direct source (primary emission) of formic acid and second high formic acid when O_3 levels are high suggesting that ozonolysis of 1-alkenes could be a significant source of formic acid. A trajectory model fails to reproduce observed formic acid levels, underestimating them, some improvement is

made by assuming a primary 'vehicular' source but inclusion of a non-negligible level of 'propene' equivalent 1-alkene is required to generate sufficient formic acid. Inspection of data archives suggest that these levels of 1-alkene are possible post ca. 11 am, but early flight data for both formic and nitric acid are too high for the model to simulate. Therefore, in these data, the relationship between nitric acid and formic acid cannot be attributed to related photochemical production solely.

References

AQIRP., 1995. Effects of gasoline T50, T90 and sulfur on exhaust emissions of current and future technology vehicles. Auto/Oil Air Quality Improvement Research Program, Technical Bulletin No. 18.

Archibald, A.T., McGillen, M.R., Taatjes, C.A., Percival C. J., and Shallcross, D.E.,2007. The importance of ethenol in urban atmospheres. Geophysical Research Letters 34, L21801, doi:10.1029/2007GL031032.

Archibald, A.T., Cooke, M.C., Utembe, S.R., Shallcross, D.E., Derwent, R.G., and Jenkin, M.E.,2010. Impacts of mechanistic changes on HOx formation and recycling in the oxidation of isoprene. Atmospheric Chemistry Physics 10, 8097–8118, doi:10.5194/acp-10-8097-2010.

Arlander, D.W., Cronn, D.R., Farmer, J.C., Menzia, F.A., and Westberg, H. H., 1990. Gaseous oxygenated hydrocarbons in the remote marine troposphere. Journal of Geophysical Research - Atmospheres 95, 16391–16403.

Baboukas, E.D., Kanakidou, M., and Mihalopoulos, N., 2000. Carboxylic acids in gas and particulate phase above the Atlantic Ocean. Journal of Geophysical Research - Atmospheres 105, 14459–14471.

Bannan, T.J. Bacak, A., Muller, J.B.A., Booth, A.M., Bacak, A., Jones,B., Le Breton, M., Leather, K.E., Xiao, P., Shallcross, D.E., Percival, C.J., 2012, Importance of Direct Anthropogenic Emissions of Formic Acid measured by a Chemical Ionisation Mass Spectrometer (CIMS) during the Winter ClearfLo Campaign in London, January 2012, submitted to Atmospheric Environment.

Bertram, T.H., Kimmel, J.R., Crisp, T.A., Ryder, O.S., Yatavelli, R.L.N., Thornton, J.A., Cubison, M.J., Gonin, M., and Worsnop, D.R., 2011. A field-deployable, chemical ionization time-of-flight mass spectrometer. Atmospheric Measurement Techniques 4, 1471–1479, doi:10.5194/amt-4-1471-2011.

Broadgate, W.J., Liss, P.S., and Penkett, S.A., 1997. Seasonal emissions of isoprene and other reactive hydrocarbon gases from the ocean. Geophyical Research Letters 24, 2675–2678.

Burling, I.R., Yokelson, R.J., Grifith, D.W.T., Johnson, T. J., Veres, P., Roberts, J.M., Warneke, C., Urbanski, S.P., Reardon, J., Weise, D.R., Hao, W.M., and de Gouw, J., 2010. Laboratory measurements of trace gas emissions from biomass burning of fuel types from the southeastern and southwestern United States. Atmospheric Chemistry and Physics 10, 11115–11130, doi:10.5194/acp-10-11115-2010.

Chebbi, A. and Carlier, P., 1996. Carboxylic acids in the troposphere, occurrence, sources, and sinks: A review. Atmospheric Environment 30, 4233–4249.

Draxler, R.R. and Rolph, G.D., 2003. HYSPLIT (HYbrid Single-Particle Lagrangian Integrated Trajectory) Model access via NOAA ARL READY Website (http://www.arl.noaa.gov/ready/hysplit4.html). NOAA Air Resources Laboratory, Silver Spring, MD, 2003.

Evans, M.J., Shallcross, D.E., Law, K.S., Wild, J.O.S., Simmonds, P.G., Spain, T.G., Berrisford, P., Methven, J., Lewis, A.C., McQuaid, J.B., Pilling, M.J., Bandy, B.J., Penkett, S.A., and Pyle, J., 2000. Evaluation of a Lagrangian box model using field measurements from EASE (Eastern Atlantic Summer Experiment) 1996. Atmospheric Environment 34, 3843–3863.

Granby, K., Christensen, C., and Lohse, C., 1997. Urban and semi-rural observations of carboxylic acids and carbonyls. Atmospheric Environment., 31, 1403–1415.

Grosjean, D. and Seinfeld, J.H., 1989. Parameterization of the formation potential of secondary organic aerosols. Atmospheric Environment 23, 1733–1747.

Grosjean, D., 1992. Formic acid and acetic acid emissions, atmopsheric formication and dry seposition at 2 southern California locations. Atmospheric Environment 26, 3279–3286.

Hartmann, W.R., Santana, M., Hermoso, M.,Andreae, M.O., and Sanhueza, E., 1991. Diurnal cycles of formic and acetic acids in the northern part of the Guayana shield, Venezuela. Journal Atmospheric Chemistry 13, 63–72.

Ito, A., Sillman, S., Penner, J.E., 2007. Effects of additional nonmethane volatile organic compounds, organic nitrates, and direct emissions of oxygenated organic species on global tropospheric chemistry. Journal of Geophysical Research - Atmospheres 112, D6, D06309, 10.1029/2005JD006556.

Jenkin, M.E., Saunders, S.M., Derwent, R.G., and Pilling, M.J., 1997. Construction and application of a master chemical mechanism (MCM) for modelling tropospheric chemistry. Abstract Paper in American Chemistry Society 214, 116-COLL.

Jenkin M.E. and Clemitshaw K.C.,2000. Ozone and other secondary photochemical pollutants: chemical processes governing their formation in the planetary boundary layer. *Atmospheric Environment* 34, 2499-2527.

Jenkin, M.E., Watson, L.A., Utembe, S.R., and Shallcross, D.E., 2008. A Common Representative Intermediates (CRI) mechanism for VOC degradation. Part 1: Gas phase mechanism development. Atmospheric Environment 42, 7185–7195.

Johnson, B.J. and Dawson, G.A., 1993. A preliminary study of the carbon isotopic content of ambient formic acid and 2 selected sources – automobile exhaust and formicine ants. Journal of Atmospheric Chemistry 17, 123–140.

Johnson, D., Utembe, S.R., Jenkin, M.E., Derwent, R.G., Hayman, G.D., Alfarra, M.R., Coe, H., and McFiggans, G., 2000. Simulating regional scale secondary organic aerosol formation during the TORCH 2003 campaign in the southern UK. Atmospheric Chemistry and Physics 6, 403 – 418, doi:10.5194/acp-6-403-2006.

Keene, W.C. and Galloway, J.N., 1986. Considerations regarding sources of formic and acetic acids in the troposphere. Journal of Geophysical Research - Atmospheres 91, 14466–14474.

Keene, W.C., Galloway, J.N., and Holden, J.D., 1986. Measurement of weak organic acidity in precipitation from remote areas of the world, J. Geophys. Res.-Atmos., 88, 5122–5130, 1983.Jacob, D. J.: Chemistry of OH in remote clouds and its role in the production of formic acid and peroxymonosulfate. Journal of Geophysical Research 91, 9807–9826.

Le Breton, M., Mcgillen, M.R., Muller, J.B.A., Bacak, A., Shallcross, D.E., Xiao, P., Huey, L.G., Tanner, D., Coe, H., Percival, C.J., 2012. Airborne observations of formic acid using a chemical ionisation mass spectrometer. Atmospheric Measurement Techniques 4, 5807-5835.

Leather, K.E., McGillen, M.R., Cooke, M.C., Utembe, S.R., Archibald, A.T., Jenkin, M.E., Derwent, R.G., Shallcross, D.E., and Percival, C.J., 2012. Acid-yield measurements of the gas-phase ozonolysis of ethene as a function of humidity using Chemical Ionisation MassSpectrometry (CIMS). Atmospheric Chemistry and Physics 12, 469 – 479, doi:10.5194/acp-12-469-2012.

Taatjes, C.A., Meloni, G., Selby, T.M., Trevitt, A.J., Osborn, D.L., Percival, C.J., and Shallcross, D.E., 2008. Direct observation of the gas-phase Criegee intermediate (CH2OO). Journal of American Chemistry Society 130, 11883–11885.

Nowak, J.B., Neuman, J.A., Kozai, K., Huey, L.G., Tanner, D.J., Holloway, J.S., Ryerson, T.B., Frost, G.J., McKeen, S.A., and Fehsenfeld, F.C., 2007. A chemical ionization mass spectrometry technique for airborne measurements of ammonia. Journal of Geophysical Research -Atmospheres 112, D10S02, doi:10.1029/2006JD007589.

Nunnennacker, L.J., Imre, D., Dau, P.H., Kleinman, L., Lee, Y-H., Lee, J. H., Springston, S.R., Newman, K., Weinstein-Lloyd, J., Luke, W.T., Banta, R., Alvarez, R., Senff, C., Sillman, S., Holdren, M., Keigley, G.W., and Zhou, X., 1998. Characterization of the Nashville urban plume on July 3 and July 18, 1995. Journal of Geophysical Research 103, D21, 28, 1298-28, 148.

Paulot, F., Wunch, D., Crounse, J.D., Toon, G.C., Millet, D.B., DeCarlo, P.F., Vigouroux, C., Deutscher, N.M., Abad, G.G., Notholt, J.,Warneke, T., Hannigan, J.W.,Warneke, C., de Gouw, J.A., Dunlea, E.J., De Maziere, M., Griffith, D.W.T., Bernath, P., Jimenez, J.L., andWennberg, P.O., 2011. Importance of secondary sources in the atmospheric budgets of formic and acetic acids. Atmospheric Chemistry and Physics 11, 1989–2013, doi:10.5194/acp-11-1989- 2011.

Paulot, F., Wunch, D., Crounse, J.D., Toon, G.C., Millet, D.B., DeCarlo, P.F., Vigouroux, C., Deutscher, N.M., Gonzalez abad, G., Notholt, J., Warneke, T., Hannigan, J.W., Warneke, C., de Gouw, J.A., Dunlea, E.J., De Maziere, M., Griffith, D.W.T., Bernath, P., Jiminez, J.L., and Wennberg, P.O., 2011. Importance of secondary sources in the atmospheric budgets of formic and acetic acids. Atmospheric Chemistry and Physics 11, 1989-2013, doi:10.5194/acp-11-1989-2011.

Poisson, N., Kanakidou, M., Crutzen, P.J., 2000. Impact of non-methane hydrocarbons on tropospheric chemistry and the oxidizing power of the global troposphere: 3-dimensional modelling results. Journal of Atmospheric Chemistry 36, 2, 157-230.

Polson, D., Fowler, D., Nemitz, E., Skiba, U., McDonald, A., Famulari, D., Di Marco, C., Simmons, I., Weston, K., Purvis, R., Coe, H., Manning, A.J., Webster, H., Harrison, M., O'Sullivan, D., Reeves, C., Oram, D., 2011. Estimation of spatial apportionment of greenhouse gas emissions for the UK using boundary layer measurements and inverse modelling technique. *Atmospheric Environment* 45. 1042-1049. 10.1016.

Preunkert, S., Legrand, M., Jourdain, B., and Dombrowski-Etchevers, I., 2007. Acidic gases (HCOOH, CH_3COOH, HNO_3, HCl, and SO_2) and related aerosol species at a high mountain Alpine site (4360 m elevation) in Europe. Journal of Geophysical Research - Atmospheres 112, D23S12, doi:10.1029/2006JD008225.

Real, E., Law, K.S., Weinzierl, B., Fiebig, M., Petzold, A., Wild, O., Methven, J., Arnold, S., Stohl, A., Huntrieser, H., Roiger, A., Schlager, H., Stewart, D., Avery, M., Sachse, G.,Browell, E., Ferrare, R., and Blake, D., 2007. Processes influencing ozone levels in Alaskan forest fire plumes during long-range transport over the North Atlantic. Journal of Geophysical Research - Atmospheres 112, D10S41, doi:10.1029/2006JD007576.

Rinsland, C.P., Mahieu, E., Zander, R., Goldman, A., Wood, S., and Chiou, L., 2004. Free tropospheric measurements of formic acid (HCOOH) from infrared ground-based solar absorp-tion spectra: Retrieval approach, evidence for a seasonal cycle, and comparison with model calculations. Journal of Geophysical Research - Atmospheres 109, D18308, doi:10.1029/2004JD004917.

Roberts, J.M., Veres, P.R., Warneke, C., Neuman, J.A., Washenfelder, R.A., Brown, S.S., Baasandori, M., Burkholder, J.B., Burling, I.R., Johnson, T.J., Yokelson, R.J., and de Gouw, J., 2010. Measurement of HONO, HNCO, and other inorganic acids by negative-ion proton-transfer chemical-ionization mass spectrometry (NI-PT-CIMS): application to biomass burning emissions. Atmospheric Measurement Techniques 3, 4, 981-990, DOI: 10.5194/amt-3-981-2010.

Roberts, J.M., Veres, P.R., Cochran, A.K., Warneke, C., Burling, I.R., Yokelson, R.J., Lerner, B., Gilman, J.B., Kuster, W.C., Fall, R., and de Gouw, J., 2011. Isocyanic acid in the atmosphere and its possible link to smoke-related health effects. Proceedings of the National Academy of Sciences 108, 41, 17234-17234, DOI: 10.1073/pnas.1113250108.

Sanhueza, E. and Andreae, M.O., 1991. Emissions of formic and acetic acids from tropical Savanna soils. Geophysical Research Letters 18, 1707–1710.

Sanhueza, E., Figueroa, L., and Santana, M., 1996. Atmospheric formic and acetic acids in Venezuela. Atmospheric Environment 30, 1861–1873.

Slusher, D.L., Huey, L.G., Tanner, D.J., Flocke, F.M., and Roberts, J.M., 2004. A thermal dissociation-chemical ionization mass spectrometry (td-cims) technique for the simultaneous measurement of peroxyacyl nitrates and dinitrogen pentoxide. Journal of Geophysical Research 109(13), D19315, doi:10.1029/2004JD004670.

Stavrakou, T., Muller, J.F., Peeters, J., Razavi, A., Clarisse, L., Clerbaux, C., Coheur, P.F., Hurtmans, D., De Maziere, M., Vigouroux, C., Deutscher, N.M., Griffith, D.W.T., Jones, N., and Paton-Walsh, C., 2012. Satellite evidence for a large source of formic acid from boreal and tropical forests. Nature Geoscience 5, 1, 26-30, doi 10.1038/NGEO1354.

Stewart, D.J., Taylor, C.M., Reeves, C.E., and McQuaid, J.B., 2008. Biogenic nitrogen oxide emissions from soils: impact on NOx and ozone over west Africa during AMMA (African Monsoon Multidisciplinary Analysis): observational study. Atmospheric Chemistry and Physics 8, 2285– 2297, doi:10.5194/acp-8-2285-2008.

Talbot, R.W., Beecher, K.M., Harris, R.C., and Cofer, III, W.R., 1988. Atmospheric geochemistry of formic and acetic acids at a midlatitude temperate site. Journal of Geophysical Research 93, 1638–1652.

Talbot, R.W., Dibb, J.E., Scheuer, E.M., Blake, D.R., Blake, N.J., Gregory, G.L., Sachse, G.W., Bradshaw, J.D., Sandholm, S.T., and Singh, H.B., 1999. Influence of biomass combustion emissions on the distribution of acidic trace gases over the southern Pacific basin during austral springtime. Journal of Geophysical Research - Atmospheres 104, 5623–5634.

Utembe, S.R., Watson, L.A., Shallcross, D.E., and Jenkin, M.E., 2009. A Common RepresentativeIntermediates (CRI) mechanism for VOC degradation. Part 3: Development of a secondary organic aerosol module. Atmospheric Environment 43, 1982–1990.

Utembe, S.R., Cooke, M.C., Archibald, A.T., Jenkin, M.E., Derwent, R.J., and Shallcross, D.E., 2010. Using a reduced Common Representative Intermediates (CRIv2-R5) mechanism to simulate tropospheric ozone in a 3-D Lagrangian chemistry transport model. Atmospheric Environment 44, 1609–1622.

Utembe, S.R., Cooke, M.C., Archibald, A.T., Shallcross, D.E., Derwent, R.G., and Jenkin, M.E., 2011. Simulating Secondary Organic Aerosol in a 3-D Lagrangian Chemistry Transport Model using the reduced Common Representative Intermediates Mechanism (CRIv2-R5). Atmospheric Environment 45, 1604–1614.

Veres, P., Roberts, J.M., Warneke, C., Welsh-Bon, D., Zahniser, M., Herndon, S., Fall, R., and de Gouw, J., 2008. Development of negative ion proton-transfer chemical-ionization mass spectrometry (NI-PT-CIMS) for the measurement of gas-phase organic acids in the atmosphere. International Journal of Mass Spectrometer 274, 48–55.

Veres, P.R., Roberts, J.M., Cochran, A.K., Gilman, J.B., Kuster, W.C., Holloway, J.S., Graus, M., Flynn, J., Lefer, B., Warneke, C., and de Gouw, J., 2011. Evidence of rapid production of organic acids in an urban air mass. Geophysical Research Letters Vol. 38, L17807, 5 PP.

Vereecken, L., Hartwig, H., and Novelli, A., 2012. The reaction of Criegee intermediates with NO, RO2, and SO2, and their fate in the atmosphere. Physical Chemistry Chemical Physics, DOI: 10.1039/C2CP42300F.

von Kuhlmann, R., Lawrence, M.G., Crutzen, P.J., and Rasch, P.J., 2003. A model for studies of tropospheric ozone and nonmethane hydrocarbons: Model evaluation of ozone-related species. Journal of Geophysical Research - Atmospheres 108, 4294, doi:10.1029/2002JD002893,2003.

Watson, L.A., Shallcross, D.E., Utembe, S.R., and Jenkin, M.E., 2008. A Common Representative Intermediates (CRI) mechanism for VOC degradation. Part 2: Gas phase mechanism reduction Atmospheric Environment 42, 7196–7204.

Welz, O., Savee, J.D, Osborn, D.L, Vasu, S.S, Percival, C. J.,Shallcross, D.E., and Taatjes, C.A., 2012. Direct Kinetic Measurements of Criegee Intermediate (CH_2OO) Formed by Reaction of CH_2I with O_2. Science 335, 6065.

Yu, S.C., 2000. Role of organic acids (formic, acetic, pyruvic and oxalic) in the formation of cloud condensation nuclei (CCN): a review. Atmospheric Research 53, 185–217.

4. Paper C

"Airborne Hydrogen cyanide measurements using a chemical ionisation mass spectrometer for the plume identification of biomass burning forest fires"

Atmospheric Chemistry and Physics Discussion., 13, 5649–5685, 2013

Authors: M. Le Breton, A. Bacak, J. B. A. Muller, S. J. O`Shea, P. Xiao, M. N. R. Ashfold, B. M. A. Shallcross, R. Batt, M. C. Cooke, D. J. Lary, D. E. Shallcross, D. E. Oram, S. J-B. Bauguitte and C. J. Percival.

The CIMS was developed in the laboratory before the BORTAS campaign with help from J. Muller and A Bacak. J. Muller performed inlet tests at low pressures. Carl Percival directed me to the 10 sigma "in plume" data approach which I then developed to 6 sigma using the data I collected during the campaign. The paper was written by myself with inputs from co-authors. S-J. Bauguitte supplied the NO_x data from the core chemistry instrument on the aircraft. D. E. Shallcross performed atmospheric modelling and produced the global HCN budgets with help from P. Xiao and his group in Bristol. M. N. R. Ashfold helped produced a HCN vessel for the first CIMS calibration. All work was carried out under the supervision of C. J. Percival.

Atmos. Chem. Phys. Discuss., 13, 5649–5685, 2013
www.atmos-chem-phys-discuss.net/13/5649/2013/
doi:10.5194/acpd-13-5649-2013

Atmospheric Chemistry and Physics Discussions

Airborne hydrogen cyanide measurements using a chemical ionisation mass spectrometer for the plume identification of biomass burning forest fires

M. Le Breton[1], A. Bacak[1], J. B. A. Muller[1], S. J. O'Shea[1], P. Xiao[2], M. N. R. Ashfold[2], M. C. Cooke[2], R. Batt[2], D. E. Shallcross[2], D. E. Oram[3], G. Forster[4], S. J.-B. Bauguitte[5], and C. J. Percival[1]

[1]The Centre for Atmospheric Science, The School of Earth, Atmospheric and Environmental Sciences, The University of Manchester, Simon Building, Brunswick Street, Manchester, M13 9PL, UK
[2]School of Chemistry, University of Bristol, Cantock's Close, Bristol, BS8 1TS, UK
[3]National Centre for Atmospheric Science, School of Environmental Sciences, University of East Anglia, Norwich, NR4 7TJ, UK
[4]School of Environmental Sciences, University of East Anglia, Norwich, NR4 7TJ, UK
[5]Facility for Airborne Atmospheric Measurements (FAAM), Building 125, Cranfield University, Cranfield, Bedford, MK43 0AL, UK

Received: 31 January 2013 – Accepted: 9 February 2013 – Published: 27 February 2013

Correspondence to: C. J. Percival (carl.percival@manchester.ac.uk)

Published by Copernicus Publications on behalf of the European Geosciences Union.

Abstract

A Chemical Ionisation Mass Spectrometer (CIMS) was developed for measuring hydrogen cyanide (HCN) from biomass burning events in Canada using I^- reagent ions on board the FAAM BAe-146 research aircraft during the BORTAS campaign in 2011. The ionisation scheme enabled highly sensitive measurements at 1 Hz frequency through biomass burning plumes in the troposphere.

A strong correlation between the HCN, carbon monoxide (CO) and acetonitrile (CH_3CN) was observed, indicating the potential of HCN as a biomass burning (BB) marker. A plume was defined as being 6 standard deviations above background for the flights. This method was compared with a number of alternative plume defining techniques employing CO and CH_3CN measurements. The 6 sigma technique produced the highest R^2 values for correlations with CO. A Normalised Excess Mixing Ratio (NEMR) of 3.76 ± 0.022 pptv ppbv^{-1} was calculated which is within the range quoted in previous research (Hornbrook et al., 2011). The global tropospheric model STOCHEM-CRI incorporated both the observed ratio and extreme ratios derived from other studies to generate global emission totals of HCN via biomass burning. Using the ratio derived from this work the emission total for HCN from BB was 0.92 Tg(N) yr^{-1}.

1 Introduction

Biomass burning (BB) is considered to be a major source of trace gases in the atmosphere (Li et al., 2000, 2003, 2009; Shim et al., 2007) and at levels significant enough to perturb regional and global atmospheric chemistry and composition (Levine, 2000). For example, large boreal forest fires in Russia from 2002–2003 were responsible for global growth rates of many trace gases including carbon dioxide and methane (Kasischke et al., 2005; Yurganov et al., 2005; Simpson et al., 2006). Fires in boreal regions are estimated to account for 9 % of global fire carbon emissions (Van derWerf et al., 2010) and their occurrences are predicted to increase by 30 % by 2030, with

a 74–118 % increase in area burned by 2100 (Flannigan et al., 2005). The area burned in Canada has increased since 1970 as a result of rising surface temperatures (Gillett et al., 2004; Kasischke and Turtesky, 2006) resulting in an expected doubling of CO_2 equivalent greenhouse gas emissions from Canadian fires (Amiro et al., 2009). Long-range transport of the emissions is enabled in the troposphere and lower stratosphere via convection and pyroconvection (Fromm et al., 2000; Jost et al., 2004; Val Martin et al., 2010). This enables fires to not only impact local and regional air quality (Colarco et al., 2004; Morris et al., 2006), but also contribute to climate change (Damoah et al., 2004; Vivchar et al., 2010; Tilmes et al., 2011).

BB is considered to be the major source of HCN in the atmosphere (Li et al., 2000, 2003, 2009; Liang et al., 2007; Shim et al., 2007) via the pyrolysis of N-containing species within the fuel (Johnson and Kang, 1971; Glarborg et al., 2003). HCN has previously been observed from field biomass fires (Hurst et al., 1994a,b; Goode et al., 2000; Yokelson et al., 2007b; Crounse et al., 2009) and using laboratory biomass combustion systems (Lobert et al., 1991; Holzinger et al., 1999; Christian et al., 2004; Becidan et al., 2007). Column measurements of HCN were measured from the International Scientific Station of the Jungfraujoch (ISSJ) by solar infrared (IR) spectroscopy in 1998 during an intense period of biomass burning in the tropics (Rinsland et al., 2000). Singh et al. (2003) observed a HCN contribution from automobiles and from aircraft over the United States, although sources from automobile exhaust and industrial processes are thought to be negligible in comparison with BB (Lobert et al., 1991; Bange and Williams., 2000; Holzinger et al., 2001). A field experiment also indicated no detectable emissions of HCN from domestic biofuels (Bertschi et al., 2003). Thermodynamic calculations carried out by Boldi (1993) predict that an air parcel associated with lightning strikes could have a chemical composition such that the HCN/CO ratio would be around 10^{-4}. Stribling and Miller (1987) showed that simulated lightning in a laboratory could produce HCN on planets such as Jupiter, strengthening the case that lightning-produced HCN has been observed on this planet (e.g. Podolak and Barnum, 1988). There have been examples where HCN has been observed in lightning

perturbed air in the Earth's troposphere (Singh et al., 2007; Liang et al., 2007), making lightning a possible additional source of HCN, although how much is still to be determined.

HCN is lost in the troposphere via the reaction with the hydroxyl radical (OH), creating a lifetime of a few years, although the reaction with singlet oxygen (O^1D) is suggested to be important in the lower stratosphere. Uptake into the ocean is currently thought to be the dominant sink with an inferred global HCN biomass burning source of 1.4–2.9 Tg(N) yr^{-1} and an oceanic saturation ratio of 0.83 (Li et al., 2000). This oceanic loss produces a lifetime of 2–5 months (Li et al., 2000, 2003; Singh et al., 2003). Although HCN may play an insignificant role in atmospheric chemistry (Cicerone and Zellner, 1983), it is thought to be an important source of nitrogen in remote oceanic environments (Li et al., 2000). HCN is currently thought to be a useful tracer of BB as a consequence of its limited sources and sufficiently long atmospheric lifetime (Lobert et al., 1990; Holzinger et al., 1999).

Carbon monoxide (CO), acetonitrile (CH_3CN) and HCN are all currently used as a BB tracer, but a standard approach has not been well defined. Thresholds of CO are used, but CO has many other strong sources (e.g. industrial activity), there can be difficulties in filtering out plumes which do not originate from BB. Recent studies implementing these various methods of identifying a BB plume have resulted in an uncertainty in the ratio of HCN to CO (Simpson et al., 2011; Vay et al., 2011; Hornbrook et al., 2011; Yokelson et al., 2009; Sinha et al., 2003; Andreae and Merlet., 2001). Using measurements of HCN and CO, BB plumes can be uniquely identified and emission factors can be calculated.

Previous atmospheric measurements of HCN have been made using IR spectroscopy (Coffey et al., 1981; Zhao et al., 2002; Kleinböhl et al., 2006; Rinsland et al., 2007; Li et al., 2000). In situ measurements were first made in the stratosphere using NI-CIMS (Negative Ion-Chemical Ionisation Mass Sepctrometry) (Schneider et al., 1997). Tropospheric measurements were then made by long-path Fourier transform IR (FTIR) spectroscopy within BB plumes (Goode et al., 2000; Yokelson et al., 2007), with

a GC system, using a reduction gas detector (RGD) (Singh et al., 2003), by NI-CIMS using CF_3O^- as the reagent ion (Crounse et al., 2006, 2009; Yokelson et al., 2007), and by PTR-MS (Proton Transfer-Mass Spectrometry) (Knighton et al., 2009). Crounse et al. (2006) have shown that CIMS can be used to detect HCN selectively in the lower atmosphere, with a low detection limit and at a high frequency. Hornbrook et al. (2011) recently reported HCN to CO ratios from BB plumes using HCN measurements from a chemical ionisation mass spectrometer.

The overall goal of the "quantifying the impact of BOReal forest fires on Tropospheric oxidants using Aircraft and Satellites (BORTAS)" campaign was to investigate the connection between the composition and the distribution of biomass burning outflow, ozone production and loss within the outflow, and the resulting perturbation to oxidant chemistry in the troposphere (Palmer et al., 2013). Airborne measurements were taken onboard the BAe-146 large Atmospheric Research Aircraft (ARA) over Eastern Canada between the 12 July and 3 August 2011. The evolution and composition of these BB plumes were studied using the airborne instruments, ground instruments and satellite. In order to study the characteristics of these plumes, an accurate method of plume identification is required. The rapid time response of CIMS utilizing the I^- ionisation scheme (Le Breton et al., 2012) is deployed here for HCN measurements. The main aim of this work is to develop a statistical methodology to define BB plumes using HCN measurements and chemical enhancements within the plume which can then determine their emission factors with respect to CO and VOC's.

2 Experimental

2.1 CIMS

A Chemical Ionisation Mass Spectrometer (CIMS) was used for real-time detection of HCN. The CIMS instrument employed here was built by the Georgia Institute of Technology as previously described by Nowak et al. (2007) and has been previously

described for formic acid measurements (Le Breton et al., 2012). Subsequently various adjustments have been made to the inlet and these are described in the following section. The schematic in Fig. 1 shows the set up used and operating conditions of the CIMS on board the airborne platform FAAM BAe-146 research aircraft.

The inlet consisted of 3/8″ OD diameter PFA tubing of length 580 mm which was heated to 40 °C to reduce surface losses. An orifice of diameter 0.9 mm was positioned at the front of the inlet to restrict the flow to 5.8 SLM. The pressure in the ionisation region was maintained at 19 Torr (133.322 Pa) throughout the flight by controlling the flow of nitrogen into the ionisation region using a mass flow meter.

2.2 Ionisation scheme

The ion-molecule chemistry using iodide ions (I^-) for trace gas detection has been described by Slusher et al. (2004) and was utilised here to detect HCN. A gas mixture of methyl iodide, CH_3I, and H_2O in N_2 is used to obtain reagent ions I^- and water clusters $I^- \cdot (H_2O)_n$, of which the latter is important for the ionisation of HCN, forming the adduct observed in the mass spectrum (Fig. 2). HCN was ionised by I^- via an adduct reaction,

$$I^- \cdot (H_2O)_n + HCN \rightarrow HCN \cdot I^- \cdot (H_2O)_n \quad (1)$$

which enabled HCN to be detected selectively at $m/z = 154$.

2.3 HCN calibrations, sensitivity and LOD

HCN was calibrated relative to that of formic acid which was measured and calibrated in-flight throughout the campaign. The response of HCN relative to formic acid was determined from laboratory calibrations performed with lab air with an RH ~ 55 % and dry air by passing the lab air through a drierite dryer. Known concentrations of HCN and HCOOH were flowed into the CIMS under these conditions and sensitivities for both gases were calculated. An average sensitivity ratio of 33 : 1 was observed. The

HCN sensitivity was found to be independent of water cluster counts. The ion count signal throughout the flights were normalised to the formic acid sensitivity to altitude The average sensitivity ($\pm 1\sigma$) for each flight was determined by taking the normalized sensitivity and multiplying by the reagent ion count rate to account for reagent ion variability from flight to flight. The average sensitivity for HCN was 4 ± 0.9 Hz pptv^{-1} for 1 MHz of reagent ion signal. The 0.8 Hz data were then averaged over 3 s for the analysis here.

2.4 STOCHEM-CRI modelling

The STOCHEM-CRI global chemistry-transport model has been described in detail in several recent papers (Archibald et al., 2010; Cooke et al., 2010a,b; Utembe et al., 2009, 2011) and will only be briefly described here. STOCHEM-CRI is a global three-dimensional model, which uses a Lagrangian approach to advect 50 000 air parcels using a fourth-order Runge-Kutta scheme with advection time steps of 3 h (Collins et al., 1997). The transport and radiation models are driven by archived meteorological data, generated by the Met. Office numerical weather prediction models as analysis fields with a resolution of 1.25° longitude and 0.83° latitude and on 12 vertical levels extending to 100 hPa (Derwent et al., 2008). The CRI (Common Representative Intermediates) chemical mechanism (CRIv2-R5; Jenkin et al., 2008; Watson et al., 2008; Utembe et al., 2009) has been incorporated into STOCHEM. CRIv2-R5 emits methane and 22 non-methane hydrocarbons. Each air parcel contains the concentrations of 219 species involved in 618 photolytic, gas-phase and heterogeneous chemical reactions, using a 5-min time step. Formation of secondary organic aerosol (SOA) was derived from the oxidation of aromatic hydrocarbons, monoterpenes and isoprene (Utembe et al., 2009, 2011). Surface emissions for CO, NO_x and non methane hydrocarbons (NMHC), distributed over five emission types (anthropogenic, biomass burning, vegetation, ocean and soil) are taken from the POET (Precursors of Ozone and their Effects in the Troposphere) inventory (Granier et al., 2005). The distributions for lightning emissions are parameterized based on the work of Price and Rind (1992) with the emissions

being distributed evenly between the convective cloud top height and the surface. The emissions are scaled so that the global total NO_x emission from lightning is 5 Tg (N) yr^{-1}. The NO_x emissions from civil and military aircraft are taken from NASA inventories for 1992 (Penner et al., 1999). The implementation of the emissions from aircraft is the same as for lightning with an annual total of 0.85 Tg(N) yr^{-1}.

2.5 HCN

Using the biomass burning emission ratios derived in this work for HCN : CO (3.76×10^{-3}) the total emission of HCN via biomass burning introduced into the model was 0.92 Tg(N) yr^{-1} HCN is removed by reaction with OH ($k = 1.2x10^{-13} \exp(-400/T)$ cm^3 $molecule^{-1}$ s^{-1}) and deposited to the ocean at a rate of 3.4×10^{-15} g(N) cm^{-2} s^{-1}. The model derived lifetime for HCN is then ca. 3 months, consistent with other studies. Further simulations were carried out using more extreme ratios derived from other studies, e.g. 0.43×10^{-3} which yields a total emission of 0.11 Tg(N) yr^{-1} and 12.6×10^{-3} which yields a total emission of 3.13 Tg(N) yr^{-1}. In addition to these three integrations, a second set of three, using the three HCN BB emission ratios relative to CO were performed with a lower deposition velocity (halved) leading to an overall lifetime of ca. 6 months.

2.6 Aircraft measurements

In addition to HCN data, observations of CO and CH_3CN are also used in the analysis. CO data are reported at 1 Hz using a fast fluorescence CO analyser with an uncertainty of ± 5 % (Gerbig et al., 1999). CH_3CN was measured by proton-transfer-reaction mass spectrometry (PTR–MS) (see Murphy et al., 2010 for experimental details). During the BORTAS flights the PTR-MS measured selected VOCs (volatile organic compounds) with a cycle time of around 15 s. CH_3CN, was measured at a *m/z* value of 42, which corresponds to the CH_3CNH^+ ion.

2.7 Biomass burning plume identification

HCN is a known BB tracer (Lobert et al., 1990) and CH_3CN is also an indicator of BB emissions which is not significantly enhanced in areas of anthropogenic activity (de Gouw et al., 2003, 2006). These tracers and CO are regularly used to identify BB plumes but a consistent method has not yet been established. Variation in background levels can make it difficult to define exactly when a plume is encountered without the aid of trace gas measurements which are not characteristic of BB fires. Hornbrook et al. (2011) defined a BB plume as having a CO mixing ratio above 175 ppbv, a CH_3CN mixing ratio of > 200 pptv and an HCN mixing ratio of > 400 pptv. Detection of BB plumes occurred when background levels of these species were low. When the background concentrations are low, the plumes selected are generally picked by enhancement above background, but this is an inaccurate method. Vay et al. (2011) limited the HCN mixing ratio to above 500 pptv, CO to above 160 ppbv and CH_3CN to above 225 pptv, but again will experience similar issues with background concentrations. Simpson et al. (2011) states that the plume locations are defined by maximum CO concentrations. Holzinger et al. (2005) define a plume as CH_3CN concentrations increasing three standard deviations above neighbouring points.

Here we evaluate a statistical approach to plume identification by assuming that the limit of quantification of a plume is ten times that of the standard deviation above the variation in the background (ICH-Q2B, 2009). The lifetime of HCN is long enough to allow plumes to be identified weeks away from the date of the fire. Dilution during this period will lower the concentrations but there will still be a strong characteristic enhancement above the background levels. The long range transport and evolution of BB plumes can be evaluated using this method as the plume is not identified by a general enhancement for any air mass.

In order to define the plume, the median background concentration for each flight was calculated and the 6th and 10th standard deviation above this value were set as the two alternative lower limits of the plume. This was utilised to create a HCN to CO

Normalized Excess Mixing Ratio (NEMR) as shown in Table 1. The difference between the slopes produced by the 6 and 10 sigma approach are within 2 sigma error and have similar R^2 values 0.72 and 0.67, respectively. The 6 sigma method reports a higher R^2 and utilises more data points in the calculation; therefore the 6 sigma approach is used for the analysis of flights B621, B622, B624, B626 and B628 as shown in Fig. 3. The HCN to CO ratios derived from the BORTAS flights are similar to those reported in the literature (Table 2). In order to assess the accuracy of this method, other possible approaches to BB plume identification were implemented using this data set. HCN, CO and CH_3CN have all been used in previous work (Vay et al., 2011; Hornbrook et al., 2011) to indentify BB plumes. We have used 7 methods to define a plume; (1) 6 sigma above the HCN background (2) 6 sigma above the CO background (3) 6 sigma above the CH_3CN background (4) above 100 ppb of CO (5) above 300 ppt of HCN (6) above 175 ppt of CH_3CN and 100 of ppb CO (7) above 200 ppb of CO. The HCN to CO NEMRs for each of the methods with the corresponding errors and R^2 value are shown in Table 3 and the percentage of data calculated to be in a plume is shown in Table 4.

The 6 sigma HCN method produced the highest average R^2 of 0.76. The methods using CO as a threshold exhibited low correlations on flight B628, as a result of a peak in CO during low level sections of the flight, as shown in Fig. 4. This can be attributed to non-BB sources of CO enhancing the CO levels where no HCN sources were present, as CO is known to have other natural and anthropogenic sources (Logan et al., 1981). This highlights a potential problem when using CO as a marker, as other measurements are required in order to determine the source. B622 had low CO concentrations but did show structure which was reciprocated by the HCN measurements. The CH_3CN data was too close to the detection limit during flight B628 to be able to determine a 6 sigma above background. The 200 ppb CO threshold approach removed all of these data from this flight, which would suggest that none of the flight encountered a BB plume. The method previously used by Hornbrook et al. (2011) produced an R^2 of 0.30 for this flight as a result of the low CO and CH_3CN concentrations, whereas the 6 sigma HCN approach produced an R^2 of 0.69. Using CO as a BB marker is limited

due to the variability in sources of CO. This method can be used for relatively fresh and unmixed plumes, whereas aged plumes may suffer from enhancements of CO from other sources.

The methods using CH_3CN data did produce a high R^2 on many flights, as shown in Table 3. However, the Limit of Detection (LOD) of the PTRMS to CH_3CN during BORTAS was a factor of 2.5 worse than the LOD of the CIMS towards HCN. As a result when sampling aged, hence dilute, plumes the *S/N* ratio is not significant enough to identify a plume, as exemplified by flight B628. Furthermore, as the PTRMS was used to detect a range of compounds during each flight, the time response was slower than that of the CIMS system. As a result, the CH_3CN data has a time average from 9 to 20 s, depending on the number of target gases that were being measured. With this particular sampling protocol it is difficult to measure accurately plumes close to the source as the lower measurement frequency may struggle to pickup small plumes as a result of the speed of the aircraft. Nevertheless, CH_3CN can be used to accurately detect a BB plume, under most conditions, as exemplified by flight B626.

2.8 Emission ratios

The 6 sigma technique is used here to calculate the emission ratio of HCN from 4 flights during the BORTAS campaign 2011. Figure 5 shows all the data points which are used to calculate the mean NEMR; 3.76 ± 0.02 pptv ppbv^{-1}. The NEMR was calculated using the equation

$$\mathrm{NEMR} = \frac{\Delta[X]_{\mathrm{plume}} - [X]_{\mathrm{background}}}{[\mathrm{CO}]_{\mathrm{plume}} - [\mathrm{CO}]_{\mathrm{background}}} \quad (2)$$

The data from flight B622 were omitted from this calculation due to the possible ageing and mixing of the plume. The NEMRs calculated during BORTAS are similar to those found in previous work, as seen in Table 2. The previously reported in previous work vary from 0.43–12.8 pptv ppb^{-1}. The NEMRs calculated here for HCN from Canadian

BB plumes is lower than that found by Simpson et al. (2011), 8.2 $\mathrm{pptv^{-1}\,ppb^{-1}}$. Hornbrook does highlight the observed variation in the ratios, and offers a possible explanation for the difference between these NEMRs, but this variation is not seen from flight to flight during the BORTAS campaign, which measured both fresh plumes and aged plumes. Californian fire emission ratios during ARCTAS-CARB were significantly lower than the Canadian and Asian fires (Hornbrook et al., 2011), ranging from 2.4 ± 0.9 to 8.8 ± 3.8 $\mathrm{pptv\,ppbv^{-1}}$, respectively. Andreae and Merlet (2001) reported very low ratios (0.43 to 1.5 $\mathrm{pptv\,ppbv^{-1}}$) in densely forested regions while Yokelson et al. (2007b) reported a ratio in the Mexico City region of 12 ± 7 $\mathrm{pptv\,ppbv^{-1}}$. The increase in these ratios may be attributed to the high NO_x levels found around Mexico City. Although emissions of HCN from motor vehicles are not believed to be important on a global scale, localised emissions may become significant (Crounse et al., 2009). Boreal forests are the primary source of fires in Canada, whereas Californian fires may be as a result of varying fuels, such as coniferous forests and grass and shrubs (Hornbrook et al., 2011).

The 6 sigma HCN method of identifying BB plumes has shown the veracity of HCN as a BB marker. In addition, this method performed better than the others over the BORTAS campaign, as indicated by the statistics presented. Also, the 6 sigma HCN method showed the ability to define BB plumes accurately in air masses which had a low HCN background, enabling the identification of BB plumes in air masses distant from sources that were not constrained by a set threshold concentration. For example, a plume may have dispersed over large distances, lowering the concentration below the limit that defines a plume using previous methods. Nonetheless, this 6 sigma technique is still able to identify these plumes, as they are defined relative to the background. This 6 sigma method also has the same ability to determine VOC to CO ratios with the percentage of data at a high time resolution (3 s). This method is therefore used to determine a HCN to CO ratio for models to calculate a global HCN budget.

3 Model results

The purpose of the model integrations were to inspect the global HCN levels generated using the extreme HCN biomass ratios (relative to CO) reported in the literature and the value determined in this study, using two ocean deposition velocities that lead to HCN lifetimes of ca. 3 months and ca. 6 months. The model results are in line with basic expectations, i.e. as the emission ratio increases the global HCN level increases and when the deposition velocity is decreased the global HCN for all three integrations also increases. Model results are presented in Fig. 6, which shows yearly averaged latitude-altitude profiles. If we assume the lower deposition velocity leading to a lifetime of about 6 months we observe that an emission ratio of 0.4×10^{-3} leads to a global yearly averaged HCN level of 10–20 ppt, an emission ratio of 12.6×10^{-3} leads to a global yearly averaged HCN level of 300–600 ppt and an emission ratio of 3.7×10^{-3} leads to a global yearly averaged HCN level of 80–180 ppt. In each case the highest levels are observed over the tropical regions, obviously driven by high biomass burning, with little variation in vertical structure, reflecting the surface deposition process dominating loss and leading to a sink in the Southern Hemisphere in the model.

There is no attempt here to reproduce field measurements, but it is instructive to compare field data with the model. We have concentrated on lower and mid tropospheric measurements and note that there are measurements in the upper troposphere and lower stratosphere. Liang et al. (2007) observed HCN using aircraft during INTEX-A (July–August 2004). This field campaign ranged across the USA and Canada and took in measurements in both the Pacific and Atlantic Oceans. Although very high levels were detected in biomass burning plumes (1090 ± 850 ppt), the background levels observed were 290 ± 70 ppt. In their comparison, Liang et al. (2007) reported levels in Asian plumes of 420 ± 60 ppt compared with 270 ± 80 ppt returned by Jacob et al. (2003) during Trace-P. Notholt et al. (2000), conducted vertical column measurements of HCN and other gases between 57° N to 45° S across the central Atlantic. HCN was detectable between 30° N and 30° S, with column amounts retrieved between

0–12 km. The HCN column amounts ranged from 100–220 ppt, with the maximum occurring just south of the equator (10–15° S). Singh et al. (2003) report HCN levels of around 250 ± 150 pptv for HCN in February to April and Ambrose et al. (2012) and Rinsland et al. (2007) report mean mixing ratios of 360 ppt and 220 ppt respectively, while Knighton et al. (2009) report a concentration ranging from 100–600 ppt and a mean background of 200 ppt. Therefore, based on the available measurements discussed thus far we would conclude that yearly averaged levels of HCN vary between approximately 100–450 ppt in the lower to mid troposphere. In the upper troposphere lightning may well contribute an additional non-negligible source and this region will be impacted by continental scale plumes, evidenced by a variety of measurements (e.g. Liang et al., 2007; Singh et al., 2007; Park et al., 2008; Randel et al., 2010; Wiegele et al., 2012). These plumes will contain a mixture of potential sources of HCN, of which biomass burning may well be the most predominant. It is also recognised that emission ratios will vary for different types of biomass burning, depending on vegetation type, temperature of burn etc. and no one ratio will be representative of the global emission. However, inspection of the model integrations suggests that the extreme ratios returned from field measurements are indeed extreme values: a ratio of 0.4×10^{-3} returns a globally averaged HCN that is far too low, irrespective of whether the lifetime is 3 or 6 months. Similarly, a ratio of 12.6×10^{-3} produces HCN levels that have been observed but are somewhat higher than expected for a yearly average, given the background measurements made. There is no suggestion that the ratio derived in this study is the one that should be used for global model studies, but it does produce HCN levels that are reasonable, compared with available field measurements, if a little on the low side. The satellite derived measurements of Wiegle et al. (2012), although restricted in altitude to above 5 km, suggest strongly that biomass burning (particularly that located in the Southern Hemisphere) is a dominant source and lends confidence to the present broad brush model comparisons with measurements. Vegetation has also been suggested as a non-negligible source of HCN (e.g. Fall et al., 2001) and vertical profile data from the Jungfraujoch station in Switzerland (Rinsland et al., 2000) suggests that in addition

to biomass burning there may well be a significant direct emission from vegetation. Therefore, the tendency to underpredict lower and mid tropospheric HCN levels using the ratio derived in this study may also point to a strong vegetation source. In summary, model integrations suggest that the extreme ratios reported in the literature generate too little or too much HCN and really are extreme values. The values reported in this study produce HCN levels that are consistent with field measurements but are on the low side.

4 Conclusions

A CIMS instrument was developed for the airborne measurement of HCN in the lower atmosphere using methyl iodide as the ionisation reagent gas. HCN measurements were successfully attained over Canada in July and August 2011, during the BORTAS-B 2012 campaign onboard the FAAM BAe-146 aircraft. The high sensitivity (4 ± 0.9 ion counts s^{-1} $pptv^{-1}$), low limit of detection (5 pptv) and selectivity of the data acquired and presented here with a time resolution of 3 s illustrates the ability of this instrument to measure HCN accurately; it is, therefore, a highly sophisticated instrument for detecting burning plumes. The mixing ratios measured through the biomass burning plumes ranged from sub 0.1–3.7 ppb covering the range of previously reported atmospheric levels (Singh et al., 2003, 2012; Knighton et al., 2009) and were strongly correlated with CO and CH_3CN, strengthening the ability of HCN to be a unique marker for biomass burning.

The 6 sigma methodology implemented and tested here for plume definition has been shown to produce the strongest correlation with CO, indicating that it is potentially an excellent method for defining biomass burning plumes. The NEMR (relative to CO) calculated using this plume identification method was 3.76 ± 0.02 pptv $ppbv^{-1}$ which is in the range of previously reported values (Andrea et al., 2001; Sinha et al., 2003; Yokelson et al., 2009; Hornbrook et al., 2011) indicating the accuracy of the HCN

measurements. The accurate NEMR was then used to estimate the total emission of HCN via biomass burning, which was calculated to be 0.91 $Tg(N)yr^{-1}$.

These first results from CIMS for HCN measurements using I^- chemistry suggest that the instrument is capable to measure HCN in the lower atmosphere with a high sensitivity, low limit of detection and high time resolution. The data produced also shows the accuracy at which HCN measurements can define biomass burning plumes and the reliability of this method.

Acknowledgements. The authors would like to thank everyone involved with the BORTAS project. CJP and DES thank NERC under whose auspices various elements of this work were carried out.

References

Ambrose, J. L., Zhou, Y., Haase, K., Mayne, H. R., Talbot, R., and Sive, B. C.: A gas chromatographic instrument for measurement of hydrogen cyanide in the lower atmosphere, Atmos. Meas. Tech., 5, 1229–1240, doi:10.5194/amt-5-1229-2012, 2012.

Amiro, B. D., Cantin, A., Flannigan, M. D., and de Groot, W. J.: Future emissions from Canadian boreal forest fires, Can. J. Forest Res., 39, 383–395, 2009.

Andreae, M. O. and Merlet, P.: Emission of trace gases and aerosols from biomass burning, Global Biogeochem. Cy., 15, 955–966, doi:10.1029/2000GB001382, 2001.

Burton, S. P., Thomason, L. W., and Zawodny, J. M.: Technical Note: Time-dependent limb-darkening calibration for solar occultation instruments, Atmos. Chem. Phys., 10, 1–8, doi:10.5194/acp-10-1-2010, 2010.

Bange, H. W. and Williams, J.: New directions: acetonitrile in atmospheric and biogeochemical cycles, Atmos. Environ., 34, 4959–4960, 2000.

Becidan, M., Skreiberg, Ø., and Hustad, J. E.: NO_x and N_2O precursors (NH_3 and HCN) in pyrolysis of biomass residues, Energ. Fuels, 21, 1173–1180, 2007.

Bertschi, I. T., Yokelson, R. J., Ward, D. E., Christian, T. J., and Hao, W. M.: Trace gas emissions from the production and use of domestic biofuels in Zambia measured by open-path Fourier transform infrared spectroscopy, J. Geophys. Res., 8, 8469, doi:10.1029/2003JD004402, 2003.

Boldi, R. A.: A Model of the Ion Chemistry of Electrified Convection, Ph. D. Thesis MIT, USA, available at: http://dspace.mit.edu/handle/1721.1/51502,1993, last access: September 2012.

Christian, T. J., Kleiss, B., Yokelson, R. J., Holzinger, R., Crutzen, P. J., Hao, W. M., Shirai, T., and Blake, D. R.: Comprehensive laboratory measurements of biomass-burning emissions: 2. first intercomparison of open-path FTIR, PTR-MS, and GC-MS/FID/ECD, J. Geophys. Res., 109, D02311, doi:10.1029/2003JD003874, 2004.

Cicerone, R. J. and Zellner, R.: The atmospheric chemistry of hydrogen cyanide (HCN), J. Geophys. Res., 88, 10689–10696, 1983.

Coffey, M. T., Mankin, W. G., and Cicerone, R. J.: Spectroscopic detection of stratospheric hydrogen cyanide, Science, 214, 333–335, 1981.

Colarco, P. R., Schoeberl, M. R., Doddridge, B. G., Marufu, L. T., Torres, O., and Welton, E. J.: Transport of smoke from Canadian forest fires to the surface near Washington, DC: injection height, entrainment, and optical properties, J. Geophys. Res., 109, D06203, doi:10.1029/2003JD004248, 2004.

Collins, W., Stevenson, D., Johnson, C., and Derwent, R.: Tropospheric ozone in a global-scale three-dimensional Lagrangian model and its response to NO_x emission controls, J. Atmos. Chem., 26, 223–274. 1997.

Cooke, M. C., Utembe, S. R., Archibald, A. T., Jenkin, M. E., Derwent, R. G., and Shallcross, D. E.: Using a reduced Common Representative Intermediates (CRIv2-R5) mechanism to simulate tropospheric ozone in a 3-D Lagrangian chemistry transport model, Atmos. Environ., 44, 1609–1622, 2010a.

Cooke, M. C., Utembe, S. R., Carbajo, P. G., Archibald, A. T., Orr-Ewing, A. J., Derwent, R. G., Jenkin, M. E., and Shallcross, D. E.: Impacts of formaldehyde photolysis rates on tropospheric chemistry, Atmos. Sci. Lett., 11, 33–38, 2010b.

Cooke, M. C., Marven, A. R., Utembe, S. R., Archibald, A. R., Ensor, G. W. R., Jenkin, M. E., Derwent, R. G., O'Doherty, S. J., and Shallcross, D. E.: On the effect of a global adoption of various fractions of biodiesel on key species in the troposphere, Int. J. Oil Gas Coal Tech., 3, 88–103. 2010c.

Crounse, J. D., McKinney, K. A., Kwan, A. J., and Wennberg, P. O.: Measurement of gas-phase hydroperoxides by chemical ionization mass spectrometry, Anal. Chem., 78, 6726–6732, doi:10.1021/ac0604235, 2006.

Crounse, J. D., DeCarlo, P. F., Blake, D. R., Emmons, L. K., Campos, T. L., Apel, E. C., Clarke, A. D., Weinheimer, A. J., McCabe, D. C., Yokelson, R. J., Jimenez, J. L., and Wennberg, P. O.: Biomass burning and urban air pollution over the Central Mexican Plateau, Atmos. Chem. Phys., 9, 4929–4944, doi:10.5194/acp-9-4929-2009, 2009.

Damoah, R., Spichtinger, N., Forster, C., James, P., Mattis, I., Wandinger, U., Beirle, S., Wagner, T., and Stohl, A.: Around the world in 17 days – hemispheric-scale transport of forest fire smoke from Russia in May 2003, Atmos. Chem. Phys., 4, 1311–1321, doi:10.5194/acp-4-1311-2004, 2004.

de Gouw, J. A., Warneke, C., Parrish, D. D., Holloway, J. S., Trainer, M., and Fehsenfeld, F. C.: Emission sources and ocean uptake of acetonitrile (CH_3CN) in the atmosphere, J. Geophys. Res., 108, 4329, doi:10.1029/2002JD002897, 2003.

de Gouw, J. A., Warneke, C., Stohl, A., Wollny, A. G., Brock, C. A., Cooper, O. R., Holloway, J. S., Trainer, M., Fehsenfeld, F. C., Atlas, E. L., Donnelly, S. G., Stroud, V., and Lueb, A.: Volatile organic compounds composition of merged and aged forest fire plumes from Alaska and western Canada, J. Geophys. Res., 111, D10303, doi:10.1029/2005JD006175, 2006.

Derwent, R. G., Stevenson, D. S., Doherty, R. M., Collins, W. J., Sanderson, M. G., and Johnson, C. E.: Radiative forcing from surface NO_x emissions: spatial and seasonal variations, Climatic Change, 88, 385–401, 2008.

Fall, R., Custer, T. G., Kato, S., and Bierbaum, V. M.: The biogenic acetne-HCN connection, Atmos. Environ., 35, 1713–1714, 2001.

Flannigan, M. D., Logan, K. A., Amiro, B. D., Skinner, W. R., and Stocks, B. J.: Future area burned in Canada, Climatic Change, 72, 1–16, 2005

Fromm, M., Alfred, J., Hoppel, K., Hornstein, J., Bevilacqua, R., Shettle, E., Servranckx, R., Li, Z. Q., and Stocks, B.: Observations of boreal forest fire smoke in the stratosphere by POAM III, SAGE II, and lidar in 1998, Geophys. Res. Lett., 27, 1407–1410, doi:10.1029/1999GL011200, 2000.

Gerbig, C., Schmitgen, S., Kley, D., and Volz-Thomas, A.: An improved fast-response vacuum UV resonance fluorescence CO instrument, J. Geophys. Res., 104, 1699–1704, 1999.

Gillett, N. P., Weaver, A. J., Zwiers, F. W., and Flannigan, M. D.: Detecting the effect of climate change on Canadian forest fires, Geophys. Res. Lett., 31, L18211, doi:10.1029/2004GL020876, 2004.

Glarborg, P., Jensen, A. D., and Johnsson, J. E.: Fuel nitrogen conversion in solid fuel fired systems, Prog. Energy Combust. Sci., 29, 89–113, 2003.

Goode, J. G., Yokelson, R. J., Ward, D. E., Susott, R. A., Babbitt, R. E., Davies, M. A., and Hao, W. M.: Measurements of excess O_3, CO_2, CO, CH_4, C_2H_4, C_2H_2, HCN, NO, NH_3, HCOOH,CH_3OOH, HCHO, and CH_3OH in 1997 Alaskan biomass burning plumes by airborn Fourier transform infrared spectroscopy (AFTIR), J. Geophys. Res., 105, 22147–22166, 2000.

Goode, J. G., Yokelson, R. J., Susott, R. A., and Ward, D. E.: Trace gas emissions from laboratory biomass fires measured by openpath FTIR: fires in grass and surface fuels, J. Geophys. Res., 104, 21237–21245, 2000.

Granier, C., Lamarque, J., Mieville, A., Muller, J., Olivier, J., Orlando, J., Peters, J., Petron, G., Tyndall, S., and Wallens, S.: A Database of Surface Emissions of Ozone Precursors, available at: http://www.aero.jussieu.fr/projet/ACCENT/POET.php, last access: 20 November 2012.

Holzinger, R., Warneke, C., Hansel, A., Jordan, A., and Lindinger, W.: Biomass burning as a source of formaldehyde, acetaldehyde, methanol, acetone, acetonitrile, and hydrogen cyanide, Geophys. Res. Lett., 26, 1161–1164, 1999.

Holzinger, R., Jordan, A., Hansel, A., and Lindinger, W.: Automobile emissions of acetonitrile: assessments of its contribution to the global source, Atmos. Environ., 38, 187–193, 2001.

Holzinger, R., Williams, J., Salisbury, G., Klüpfel, T., de Reus, M., Traub, M., Crutzen, P. J., and Lelieveld, J.: Oxygenated compounds in aged biomass burning plumes over the Eastern Mediterranean: evidence for strong secondary production of methanol and acetone, Atmos. Chem. Phys., 5, 39–46, doi:10.5194/acp-5-39-2005, 2005.

Hornbrook, R. S., Blake, D., Diskin, G. S., Fried, A., Fuelberg, H. E., Meinardi, S., Mikoviny, T., Richter, D., Sachse, G. W., Vay, S. A., Walega, J., Weibring, P., Weinheimer, A. J., Wiedinmyer, C., Wisthaler, A., Hills, A., Riemer, D. D., Apel, E. C.: Observations of nonmethane organic compounds during ARCTAS – Part 1: Biomass burning emissions and plume enhancements, Atmos. Chem. Phys., 11, 11103–11130, doi:10.5194/acp-11-11103-2011, 2011.

Hurst, D. F., Griffith, D. W. T., and Cook, G. D.: Trace gas emissions from biomass burning in tropical Australian savannas, J. Geophys. Res., 99, 16441–16456, 1994b.

ICH-Q2B Validation of Analytical Procedure: Methodology, International Conference on Harmonisation of Technical Requirements for Registration of Pharmaceuticals for HUman Use, Geneva, Switzerland, November 1996, 9 pp., 1996.

Jacob, D. J., Crawford, J. H., Kleb, M. M., Connors, V. S., Bendura, R. J., Raper, J. L., Sachse, G. W., Gille, J. C., Emmons, L., and Heald, C. L.: Transport and Chemical Evolution

over the Pacific (TRACE-P) aircraft mission: design, execution, and first results, J. Geophys. Res., 108, 9000, doi:10.1029/2002JD003276, 2003.
Jenkin, M. E., Watson, L. A., Utembe, S. R., and Shallcross, D. E.: A Common Representative Intermediates (CRI) mechanism for VOC degradation. Part 1: Gas phase mechanism development, Atmos. Environ., 42, 7185–7195. 2008.
Johnson, W. R. and Kang, J. C.: Mechanisms of hydrogen cyanide formation from the pyrolysis of amino acids and related compounds, J. Org. Chem., 36, 189–192, 1971.
Jost, H. J., Drdla, K., Stohl, A., Pfister, L., Loewenstein, M., Lopez, J. P., Hudson, P. K., Murphy, D. M., Cziczo, D. J., Fromm, M., Bui, T. P., Dean-Day, J., Gerbig, C., Mahoney, M. J., Richard, E. C., Spichtinger, N., Pittman, J. V., Weinstock, E. M., Wilson, J. C., and Xueref, I.: In-situ observations of mid-latitude forest fire plumes deep in the stratosphere, Geophys. Res. Lett., 31, 11101, doi:10.1029/2003GL019253, 2004.
Kasischke, E. S. and Turetsky, M. R.: Recent changes in the fire regime across the North American boreal region – spatial and temporal patterns of burning across Canada and Alaska, Geophys. Res. Lett., 33, L09703, doi:10.1029/2006GL025677, 2006.
Kasischke, E. S., Hyer, E. J., Novelli, P. C., Bruhwiler, L. P., French, N. H. F., Sukhinin, A. I., Hewson, J. H., and Stocks, B. J.: Influences of boreal fire emissions on Northern Hemisphere atmospheric carbon and carbon monoxide, Global Biogeochem. Cy., 19, GB1012, doi:10.1029/2004GB002300, 2005.
Kleinböhl, A., Toon, G. C., Sen, B., Blavier, J.-F. L., Weisenstein, D. K., Strekowski, R. S., Nicovich, J. M., Wine, P. H., and Wennberg, P. O.: On the stratospheric chemistry of ydrogen cyanide, Geophys. Res. Lett., 33, L11806, doi:10.1029/2006GL026015, 2006.
Knighton, W. B., Fortner, E. C., Midey, A. J., Viggiano, A. A., Herndon, S. C., Wood, E. C., and Kolb, C. E.: HCN detection with a proton transfer reaction mass spectrometer, Int. J. Mass. Sp., 283, 112–121, 2009.
Le Breton, M., McGillen, M. R., Muller, J. B. A., Bacak, A., Shallcross, D. E., Xiao, P., Huey, L. G., Tanner, D., Coe, H., and Percival, C. J.: Airborne observations of formic acid using a chemical ionization mass spectrometer, Atmos. Meas. Tech., 5, 3029–3039, doi:10.5194/amt-5-3029-2012, 2012.
Levine, J. S.: Global biomass burning: a case study of the gaseous and particulate emissions released to the atmosphere during the 1997 fires in Kalimantan and Sumatra, Indonesia, in: Biomass Burning and its Inter-Relationships with the Climate System, edited by: Innes, J. L., Beniston, M., and Verstraete, M. M., Kluwar Academic Publishers, Boston, 15–31, 2000.

Li, Q. B., Jacob, D. J., Bey, I., Yantosca, R. M., Zhao, Y. J., Kondo, Y., and Notholt, J.: Atmospheric hydrogen cyanide (HCN): biomass burning source, ocean sink?, Geophys. Res. Lett., 27, 357–360, doi:10.1029/1999GL010935, 2000.
Li, Q., Jacob, D. J., Yantosca, R. M., Heald, C. L., Singh, H. B., Koike, M., Zhao, Y., Sachse, G. W., and Streets, D. G.: A global three-dimensional model analysis of the atmospheric budget of HCN and CH_3CN: constraints from aircraft and ground measurements, J. Geophys. Res., 108, 8827, doi:10.1029/2002JD003075, 2003.
Li, Q., Palmer, P. I., Pumphrey, H. C., Bernath, P., and Mahieu, E.: What drives the observed variability of HCN in the troposphere and lower stratosphere?, Atmos. Chem. Phys., 9, 8531–8543, doi:10.5194/acp-9-8531-2009, 2009.
Liang, Q., Jaegle, L., Hudman, R. C., Turquety, S., Jacob, D. J., Avery, M. A., Browell, E. V., Sachse, G. W., Blake, D. R., Brune, W., Ren, X., Cohen, R. C., Dibb, J. E., Fired, A., Fuelberg, H., Porter, M., Heikes, B. G., Huey, G., Singh, H. B., and Wennberg, P. O.: Summertime influence of Asian pollution in the free troposphere over North America, J. Geophys. Res., 112, D12S11, doi:10.1029/2006JD007919, 2007.
Lobert, J. M., Scharffe, D. H., Hao, W. M., and Crutzen, P. J.: Importance of biomass burning in the atmospheric budgets of nitrogen-containing gases, Nature, 346, 552–554, 1990.
Lobert, J. M., Scharffe, D. H., Kuhlbusch, T. A., Seuwen, R., and Crutzen, P. J.: Experimental evaluation of biomass burning emissions: nitrogen and carbon containing compounds, in: Global Biomass Burning: Atmospheric, Climatic, and Biospheric Implications, edited by: Levine, J. S., MIT Press, Cambridge, Massachusetts, USA, 289–304, 1991.
Logan, J. A., Prather, M. J., Wofsy, S. C., and McElroy, M. B.: Tropospheric chemistry: a global perspective, J. Geophys. Res., 86, 7210–7254, 1981.
Morris, G. A., Hersey, S., Thompson, A. M., Pawson, S., Nielsen, J. E., Colarco, P. R., McMillan, W. W., Stohl, A., Turquety, S., Warner, J., Johnson, B. J., Kucsera, T. L., Larko, D. E., Oltmans, S. J., and Witte, J. C.: Alaskan and Canadian forest fires exacerbate ozone 20 pollution over Houston, Texas, on 19 and 20 July 2004, J. Geophy. Res., 111, D24S03, doi:10.1029/2006JD007090, 2006.
Murphy, J. G., Oram, D. E., and Reeves, C. E.: Measurements of volatile organic compounds over West Africa, Atmos. Chem. Phys., 10, 5281–5294, doi:10.5194/acp-10-5281-2010, 2010.
Nowak, J. B., Neuman, J. A., Kozai, K., Huey, L. G., Tanner, D. J., Holloway, J. S., Ryerson, T. B., Frost, G. J., McKeen, S. A., and Fehsenfeld, F. C.: A chemical ionization mass spectrometry

technique for airborne measurements of ammonia, J. Geophys. Res.-Atmos., 112, D10S02, doi:10.1029/2006JD007589, 2007.

Notholt, J., Toon, G. C., Rinsland, C. P., Pougatchev, N. S., Jones, N. B., Connor, B. J., Weller, R., Gautrois, M., and Schrems, O.: Latitudinal variations of trace gas concentrations in the free troposphere measured by solar absorption spectroscopy during a ship cruise, J. Geophys. Res., 105, 1337–1349, 2000.

Palmer, P. I., Parrington, M., Lee, J. D., Lewis, A. C., Rickard, A. R., Bernath, P. F., Duck, T. J., Waugh, D. L., Tarasick, D. W., Andrews, S., Aruffo, E., Bailey, L. J., Barrett, E., Bauguitte, S. J.-B., Curry, K. R., Di Carlo, P., Chisholm, L., Dan, L., Forster, G., Franklin, J. E., Gibson, M. D., Griffin, D., Helmig, D., Hopkins, J. R., Hopper, J. T., Jenkin, M. E., Kindred, D., Kliever, J., Le Breton, M., Matthiesen, S., Maurice, M., Moller, S., Moore, D. P., Oram, D. E., O'Shea, S. J., Christopher Owen, R., Pagniello, C. M. L. S., Pawson, S., Percival, C. J., Pierce, J. R., Punjabi, S., Purvis, R. M., Remedios, J. J., Rotermund, K. M., Sakamoto, K. M., da Silva, A. M., Strawbridge, K. B., Strong, K., Taylor, J., Trigwell, R., Tereszchuk, K. A., Walker, K. A., Weaver, D., Whaley, C., and Young, J. C.: Quantifying the impact of BOReal forest fires on Tropospheric oxidants over the Atlantic using Aircraft and Satellites (BORTAS) experiment: design, execution and science overview, Atmos. Chem. Phys. Discuss., 13, 4127–4181, doi:10.5194/acpd-13-4127-2013, 2013.

Park, M., Randel, W. J., Emmons, L. K., Bernath, P. F., Walker, K. A., and Boone, C. D.: Chemical isolation in the Asian monsoon anticyclone observed in Atmospheric Chemistry Experiment (ACE-FTS) data, Atmos. Chem. Phys., 8, 757–764, doi:10.5194/acp-8-757-2008, 2008.

Penner, J. E., Lister, D. H., Griggs, D. J., Dokken, D. J., Mc-Farland, M.: IPCC Special Report on Aviation and the Global Atmosphere, Technical report, tech.rep., IPCC, Cambridge University Press, Cambridge, UK and New York, NY, USA, 365 pp., 1999.

Podolak, M. and Barnum, A.: Moist convection and the abundance of lighning-produced CO, C_2H_2 and HCN on Jupiter, ICARUS 75, 566–570, doi:10.1016/0019-1035(88)90165-0, 1988.

Price, C. and Rind, D.: A simple lightning parameterization for calculating global lightning distributions, J. Geophys. Res., 97, 9919–9933, doi:10.1029/92JD00719, 1992.

Randel, W. J., Park, M., Emmons, L., Kinnison, D., Pernath, P., Walker, K. A., Boone, C., and Pumphrey, H.: Asian monsoon transport of pollution to the stratosphere, Science, 328, 611–613, 2010.

Rinsland, C. P., Mahieu, E., Zander, R., Demoulin, P., Forrer, J., and Buchmann, B.: Free tropospheric CO, C_2H_6, and HCN above central Europe: recent measurements from the Jungfraujoch station including the detection of elevated columns during 1998, J. Geophys. Res., 105, 24235–24249, 2000.

Rinsland, C. P., Goldman, A., Hannigan, J. W., Wood, S. W., Chiou, L. S., and Mahieu, E.: Long-term trends of tropospheric carbon monoxide and hydrogen cyanide from analysis of high resolution infrared solar spectra, J. Quant. Spectros. Ra., 104, 40–51, 2007.

Schneider, J., Burger, V., and Arnold, F.: Methyl cyanide and hydrogen cyanide measurements in the lower stratosphere: implications for methyl cyanide sources and sinks, J. Geophys. Res., 102, 25501–25506, 1997.

Shim, C., Wang, Y., Singh, H. B., Blake, D. R., and Guenther, A. B.: Source characteristics of oxygenated volatile organic compounds and hydrogen cyanide, J. Geophys. Res., 112, D10305, doi:10.1029/2006JD007543, 2007.

Simpson, I. J., Rowland, F. S., Meinardi, S., and Blake, D. R.: Influence of biomass burning during recent fluctuations in the slow growth of global tropospheric methane, Geophys. Res. Lett., 33, L22808, doi:10.1029/2006GL027330, 2006.

Simpson, I. J., Blake, N. J., Barletta, B., Diskin, G. S., Fuelberg, H. E., Gorham, K., Huey, L. G., Meinardi, S., Rowland, F. S., Vay, S. A., Weinheimer, A. J., Yang, M., and Blake, D. R.: Characterization of trace gases measured over Alberta oil sands mining operations: 76 speciated C_2–C_{10} volatile organic compounds (VOCs), CO_2, CH_4, CO, NO, NO_2, NO_y, O_3 and SO_2, Atmos. Chem. Phys., 10, 11931–11954, doi:10.5194/acp-10-11931-2010, 2010.

Simpson, I. J., Akagi, S. K., Barletta, B., Blake, N. J., Choi, Y., Diskin, G. S., Fried, A., Fuelberg, H. E., Meinardi, S., Rowland, F. S., Vay, S. A., Weinheimer, A. J., Wennberg, P. O., Wiebring, P., Wisthaler, A., Yang, M., Yokelson, R. J., and Blake, D. R.: Boreal forest fire emissions in fresh Canadian smoke plumes: C_1–C_{10} volatile organic compounds (VOCs), CO_2, CO, NO_2, NO, HCN and CH_3CN, Atmos. Chem. Phys., 11, 6445–6463, doi:10.5194/acp-11-6445-2011, 2011.

Singh, H. B., Salas, L., Herlth, D., Kolyer, R., Czech, E., Viezee, W., Li, Q., Jacob, D. J., Blake, D., Sachse, G., Harward, C. N., Fuelberg, H., Kiley, C. M., Zhao, Y., and Kondo, Y.: In situ measurements of HCN and CH_3CN over the Pacific Ocean: sources, sinks, and budgets, J. Geophys. Res., 108, 8795, doi:10.1029/2002JD003006, 2003.

Singh, H. B., Salas, L., Herlth, D., Kolyer, R., Czech, E., Avery, E., Crawford, J. H., Pierce, R. B., Sachse, G., Blake, D. R., Cohen, R. C., Bertram, T. H., Perring, A., Wooldridge, P. J.,

Dibb, J., Huey, G., Hudman, R. C., Turquety, S., Emmons, L. K., Flocke, F., Tang, Y., Carmichael, G. R., and Horowitz, L. W.: Reactive nitrogen distribution and partitioning in the North American troposphere and lowermost stratosphere, J. Geophys. Res., 112, D12S04, doi:10.1029/2006JD007664, 2007.

Sinha, P., Hobbs, P. V., Yokelson, R. J., Bertschi, I. T., Blake, D. R., Simpson, I. J., Gao, S., Kirchstetter, T. W., and Novakov, T.: Emissions of trace gases and particles from savanna fires in Southern Africa, J. Geophys. Res., 108, 8487, doi:10.1029/2002JD002325, 2003.

Slusher, D. L., Huey, L. G., Tanner, D. J., Flocke, F. M., and Roberts, J. M.: A thermal dissociation-chemical ionization mass spectrometry (td-cims) technique for the simultaneous measurement of peroxyacyl nitrates and dinitrogen pentoxide, J. Geophys. Res., 109, D19315, doi:10.1029/2004JD004670, 2004.

Stribling, R. and Miller, S. L.: Electron-discharge synthesis of HCN in simulated jovian atmospheres, ICARUS 72, 48–52, doi:10.1016/0019-1035(87)90117-5, 1987.

Tilmes, S., Emmons, L. K., Law, K. S., Ancellet, G., Schlager, H., Paris, J.-D., Fuelberg, H. E., Streets, D. G., Wiedinmyer, C., Diskin, G. S., Kondo, Y., Holloway, J., Schwarz, J. P., Spackman, J. R., Campos, T., Nédélec, P., and Panchenko, M. V.: Source contributions to Northern Hemisphere CO and black carbon during spring and summer 2008 from POLARCAT and START08/preHIPPO observations and MOZART-4, Atmos. Chem. Phys. Discuss., 11, 5935–5983, doi:10.5194/acpd-11-5935-2011, 2011.

Utembe, S. R., Watson, L. A., Shallcross, D. E., and Jenkin, M. E.: A Common Representative Intermediates (CRI) mechanism for VOC degradation. Part 3: Development of a secondary organic aerosol module, Atmos. Environ., 43, 1982–1990. 2009.

Utembe, S. R., Cooke, M. C., Archibald, A. T., Shallcross, D. E., Derwent, R. G., and Jenkin, M. E.: Simulating secondary organic aerosol in a 3-D Lagrangian chemistry transport model using the reduced Common Representative Intermediates Mechanism (CRIv2-R5), Atmos. Environ., 45, 1604–1614, 2011.

Val Martin, M., Logan, J. A., Kahn, R. A., Leung, F.-Y., Nelson, D. L., and Diner, D. J.: Smoke injection heights from fires in North America: analysis of 5 years of satellite observations, Atmos. Chem. Phys., 10, 1491–1510, doi:10.5194/acp-10-1491-2010, 2010.

van der Werf, G. R., Randerson, J. T., Giglio, L., Collatz, G. J., Mu, M., Kasibhatla, P. S., Morton, D. C., DeFries, R. S., Jin, Y., and van Leeuwen, T. T.: Global fire emissions and the contribution of deforestation, savanna, forest, agricultural, and peat fires (1997–2009), Atmos. Chem. Phys., 10, 11707–11735, doi:10.5194/acp-10-11707-2010, 2010.

Vay, S. A., Choi, Y., Vadrevu, K. P., Blake, D. R., Tyler, S. C., Wisthaler, A., Hecobian, A., Kondo, Y., Diskin, G. S., Sachse, G. W., Woo, J.-H., Weinheimer, A. J., Burkhart, J. F., tohl, A., and Wennberg, P. O.: Patterns of CO_2 and radiocarbon across high northern latitudes during International Polar Year 2008, J. Geophys. Res.-Atmos., 116, D14301, doi:10.1029/2011JD015643, 2011.

Vivchar, A. V., Moiseenko, K. B., and Pankratova, N. V.: Estimates of carbon monoxide emissions from wildfires in Northern Eurasia for airquality assessment and climate modeling, Atmos. Ocean. Phys., 46, 281–293, doi:10.1134/S0001433810030023, 2010.

Watson, L. A., Utembe, S. R., Shallcross, D. E., and Jenkin, M. E.: A Common Representative Intermediates (CRI) mechanism for VOC degradation. Part 2: Gas phase mechanism reduction, Atmos. Environ., 42, 7196–7204. 2008.

Wiegele, A., Glatthor, N., Höpfner, M., Grabowski, U., Kellmann, S., Linden, A., Stiller, G., and von Clarmann, T.: Global distributions of C_2H_6, C_2H_2, HCN, and PAN retrieved from MIPAS reduced spectral resolution measurements, Atmos. Meas. Tech., 5, 723–734, doi:10.5194/amt-5-723-2012, 2012.

Yokelson, R. J., Karl, T., Artaxo, P., Blake, D. R., Christian, T. J., Griffith, D. W. T., Guenther, A., and Hao, W. M.: The Tropical Forest and Fire Emissions Experiment: overview and airborne fire emission factor measurements, Atmos. Chem. Phys., 7, 5175–5196, doi:10.5194/acp-7-5175-2007, 2007a.

Yokelson, R. J., Urbanski, S. P., Atlas, E. L., Toohey, D. W., Alvarado, E. C., Crounse, J. D., Wennberg, P. O., Fisher, M. E., Wold, C. E., Campos, T. L., Adachi, K., Buseck, P. R., and Hao, W. M.: Emissions from forest fires near Mexico City, Atmos. Chem. Phys., 7, 5569–5584, doi:10.5194/acp-7-5569-2007, 2007b.

Yokelson, R. J., Crounse, J. D., DeCarlo, P. F., Karl, T., Urbanski, S., Atlas, E., Campos, T., Shinozuka, Y., Kapustin, V., Clarke, A. D., Weinheimer, A., Knapp, D. J., Montzka, D. D., Holloway, J., Weibring, P., Flocke, F., Zheng, W., Toohey, D., Wennberg, P. O., Wiedinmyer, C., Mauldin, L., Fried, A., Richter, D., Walega, J., Jimenez, J. L., Adachi, K., Buseck, P. R., Hall, S. R., and Shetter, R.: Emissions from biomass burning in the Yucatan, Atmos. Chem. Phys., 9, 5785–5812, doi:10.5194/acp-9-5785-2009, 2009.

Yurganov, L. N., Duchatelet, P., Dzhola, A. V., Edwards, D. P., Hase, F., Kramer, I., Mahieu, E., Mellqvist, J., Notholt, J., Novelli, P. C., Rockmann, A., Scheel, H. E., Schneider, M., Schulz, A., Strandberg, A., Sussmann, R., Tanimoto, H., Velazco, V., Drummond, J. R., and Gille, J. C.: Increased Northern Hemispheric carbon monoxide burden in the troposphere in

2002 and 2003 detected from the ground and from space, Atmos. Chem. Phys., 5, 563–573, doi:10.5194/acp-5-563-2005, 2005.

Zhao, Y., Strong, K., Kondo, Y., Koike, M., Matsumi, Y., Irie, H., Rinsland, C. P., Jones, N. B., Suzuki, K., Nakajima, H., Nakane, H., and Murata, I.: Spectroscopic measurements of tropospheric CO, C_2H_6, C_2H_2, and HCN in northern Japan, J. Geophys. Res., 107, 4343, doi:10.1029/2001JD000748, 2002.

Table 1. HCN : CO NEMRs (in pptv ppbv^{-1}) for 5 flights during BORTAS campaign in plumes determined by 6 or 10 sigma above background and R^2 of correlations. NEMR units are ppt ppb^{-1}.

Flight	6 sigma slope	10 sigma slope	6 sigma R^2	10 sigma R^2
B621	4.7 ± 0.05	4.68 ± 0.05	0.83	0.83
B622	0.66 ± 0.02	0.66 ± 0.02	0.46	0.46
B624	2.68 ± 0.03	2.68 ± 0.03	0.82	0.79
B626	2.72 ± 0.09	2.82 ± 0.06	0.81	0.83
B628	3.68 ± 0.05	3.3 ± 0.08	0.69	0.45
average	2.89 ± 0.05	2.83 ± 0.05	0.72	0.67
Average without B622	3.45 ± 0.06	3.37 ± 0.06	0.79	0.73

Table 2. HCN : CO NEMRs as quoted in literature and the calculated NEMR for HCN from data collected throughout the BORTAS campaign, excluding flight B622. NEMR ratio units are ppt ppb^{-1}.

Andrea	Sinha	Yokelson	Simpson	Hornbrook	This work
0.43 ± 0.15 (Sv)	9 ± 3 (Sv)	12.8 ± 9.5 (MC)	8.2 ± 2 (Can)	8.8 ± 3.8 (As)	3.76 ± 0.02 (Can)
1.5 (TF)	6 ± 2 (W)	6.6 ± 4.8 (Yu)		2.4 ± 0.9 (CA)	
1.4(TF)	9 ± 5 (G)	7 ± 5.9 (TF)		7.7 ± 3.2 (Can)	

Sv: African savannas, TF: tropical forests, W: savanna woodland, G: savanna grassland, MC: Mexico city region, Yu: Yucatan, As: Asian, CA: California, Can: Canada

Table 3. The HCN : CO NEMRs (in pptv ppbv^{-1}) with R^2 of slope for 5 flights during BORTAS campaign calculated using varying methods previously described in literature.

	6 sigma HCN		6 sigma CO		6 sigma of CH3CN, HCN : CO		100 ppb CO		300 ppt HCN		175 ppt CH3CN and 100 ppb CO		200 ppb CO	
	Slope	R^2	Slope	R^2	Slope	R^2	Slope	R^2	Slope	R^2	Slope	R^2	Slope	R^2
B621	4.70 ± 0.042	.83	4.92 ± 0.038	0.83	4.75 ± 0.11	0.83	4.81 ± 0.035	0.85	5.03 ± 0.06	0.82	5.11 ± 0.049	0.84	5.81 ± 0.087	0.83
B622	0.46 ± 0.016	0.66	0.74 ± 0.010	0.62	0.85 ± 0.021	0.74	0.73 ± 0.011	0.59	0.40 ± 0.030	0.25	0.78 ± 0.013	0.61	0.69 ± 0.017	0.45
B624	2.68 ± 0.029	0.82	2.91 ± 0.037	0.76	3.24 ± 0.072	0.85	2.93 ± 0.418	0.72	2.72 ± 0.035	0.76	2.98 ± 0.047	0.70	3.13 ± 0.064	0.64
B626	2.72 ± 0.094	0.81	2.85 ± 0.074	0.83	2.83 ± 0.109	0.96	2.94 ± 0.050	0.83	2.97 ± 0.069	0.83	3.00 ± 0.134	0.81	2.64 ± 0.254	0.74
B628	3.68 ± 0.050	0.69	6.77 ± 0.10	0.60	0	0	6.21 ± 0.17	0.42	0.74 ± 0.11	0.24	4.66 ± 0.270	0.30	0	0
average	2.85 ± 0.047	0.76	3.64 ± 0.052	0.73	2.33 ± 0.062	0.68	3.52 ± 0.062	0.68	2.37 ± 0.061	0.58	3.31 ± 0.103	0.65	2.45 ± 0.084	0.53

Table 4. Percentage of data determined to be within a plume from the BORTAS flights using varying possible plume identification methods.

% data in plume flight	6 sigma HCN	6 sigma CO	6 sigma CH_3CN	100 ppb CO	300 ppt HCN	175 ppt CH_3Cn and 100 ppb CO	200 ppb CO
B621	25.05	38.60	22.35	43.28	16.65	39.00	11.00
B622	46.80	83.47	62.51	73.40	12.31	51.00	49.00
B624	58.25	64.92	55.23	61.07	49.42	49.00	37.00
B626	13.71	22.12	13.89	48.23	24.22	8.00	3.00
B626	46.49	63.65	0	48.52	2.52	12.00	0.00
average	38.06	54.44	30.80	54.90	21.02	31.80	20.00

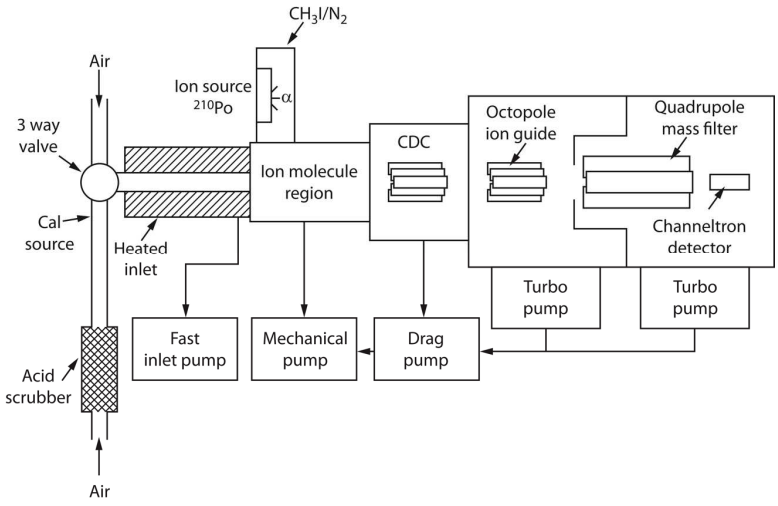

Fig. 1. Schematic of chemical ionisation mass spectrometer (CIMS) used in this study. Arrows indicate direction of gas flow. Dimensions are not to scale.

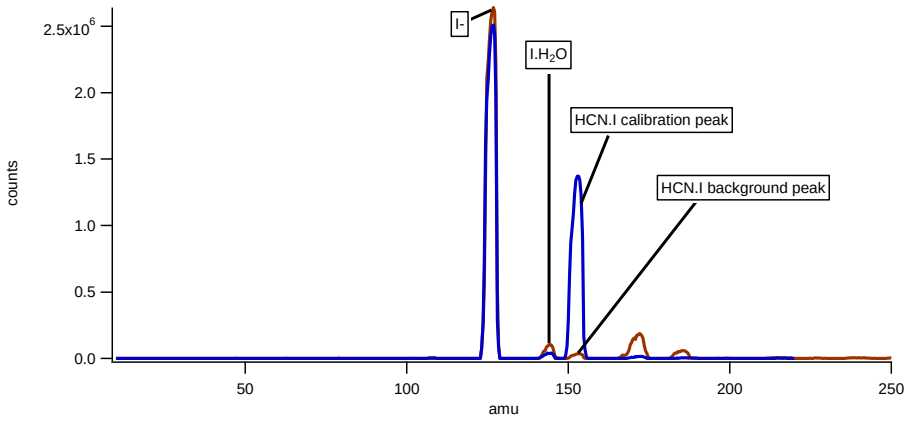

Fig. 2. Mass scan from the CIMS during background (red line) and encountering a HCN calibration peak at mass 154 (blue line).

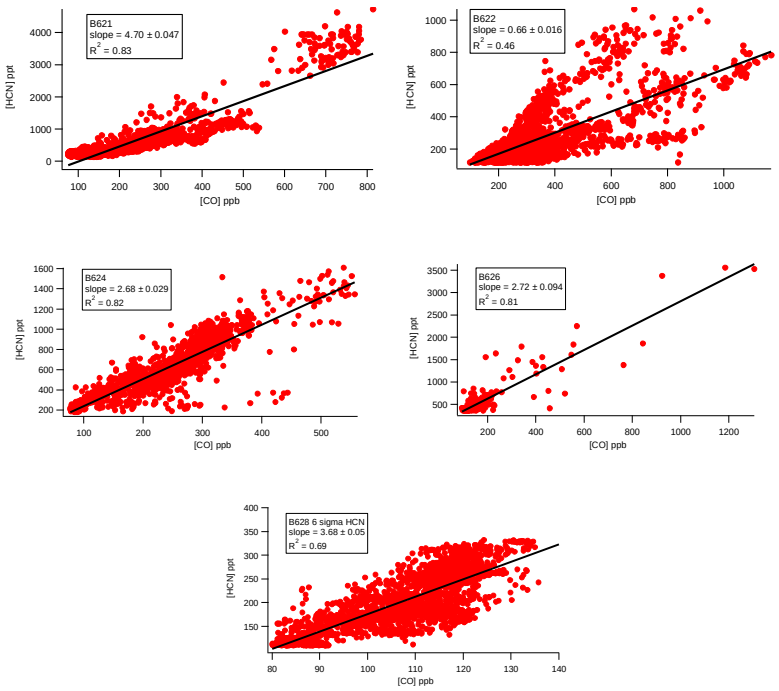

Fig. 3. HCN : CO correlations in plume determined by the 6 sigma HCN approach for 5 flights during the BORTAS campaign.

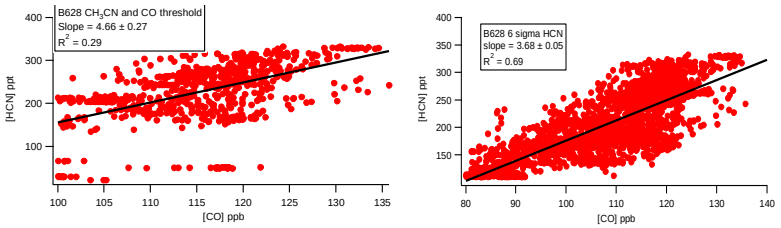

Fig. 4. In plume HCN : CO ratio from flight B628 using the 6 sigma HCN approach and the 175 ppt CH_3CN and 100 ppb CO thresholds.

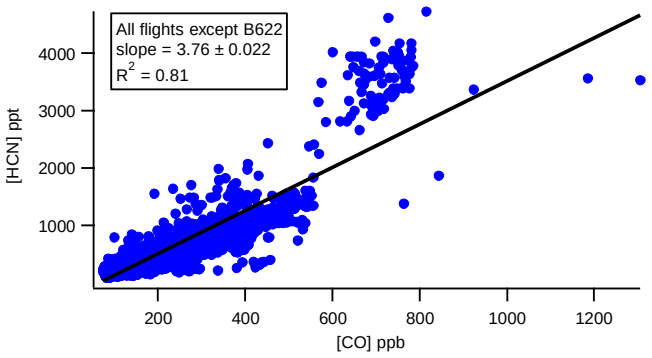

Fig. 5. HCN : CO correlations within BB plumes from the BORTAS campaign as determined using the 6 sigma HCN approach. Flight B622 data has been excluded due to the possible two separate slopes observed.

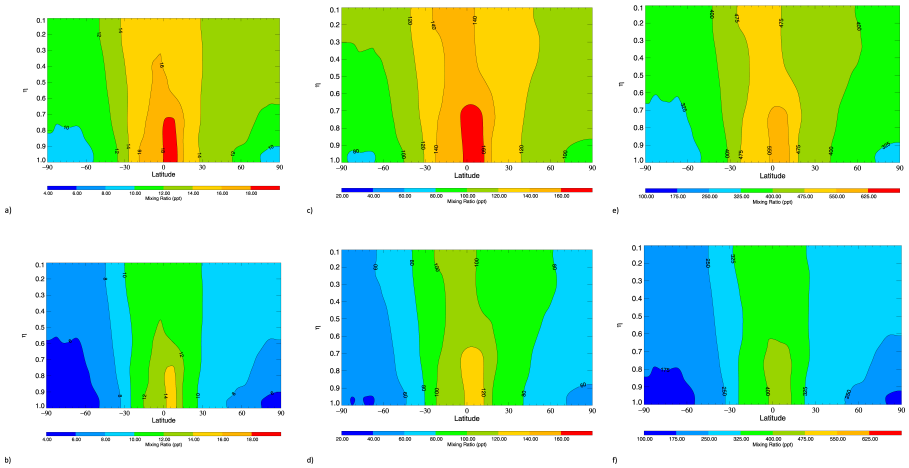

Fig. 6. Year average HCN derived from model integrations with two ocean deposition velocities leading to a lifetime of 3 months and 6 months. **(a)** Emission ratio (HCN : CO) of 4×10^{-4} ppb ppb^{-1} and a lifetime with respect to deposition of 3 months. **(b)** Emission ratio of $4 \times 10^{-4}$and a lifetime with respect to deposition of 6 months. **(c)** Emission ratio of 3.7 x 10^{-3} and a lifetime with respect to deposition of 3 months. **(d)** Emission ratio of $3.7 \times 10^{-3}$and a lifetime with respect to deposition of 6 months. **(e)** Emission ratio of 12×10^{-3} and a lifetime with respect to deposition of 3 months. **(f)** Emission ratio of 12×10^{-3} and a lifetime with respect to deposition of 6 months.

5. Paper D

"The first airborne comparison of N_2O_5 measurements over the UK using chemical ionisation mass spectrometer and broadband cavity enhanced absorption spectrometer during the RONOCO 2010/2011 campaign"

Submitted to Atmospheric Environment

By M. Le Breton, A. Bacak, J. B.A. Muller, T. Bannan, O. Kennedy, B. Ouyang, P. Xiao, S. J.-B. Bauguitte, D. E. Shallcross, R. L. Jones and C. J. Percival.

J. Muller and A. Bacak helped with the initial setup for aircraft measurements and laboratory tests. S-J. Bauguitte supplied the NO_x data from the core chemistry instrument on the aircraft. The operation of the instrument and analysis of the data was performed by myself. The development of the paper and writing was by myself, supported by Carl Percival. D. E. Shallcross developed the idea to use a steady state model on the dataset collected during RONOCO. All work was carried out under the supervision of C. J. Percival.

The first airborne comparison of N_2O_5 measurements over the UK using a Chemical Ionisation Mass Spectrometer (CIMS) and Broadband Cavity Enhanced Absorption Spectrometer (BBCEAS) during the RONOCO 2010/2011 campaign

Michael Le Breton[1], Asan Bacak[1], Jennifer B.A. Muller[1], Tomas. J. Bannan[1], Oliver Kennedy[3], Bin Ouyang[3], Ping Xiao,[2] S. J.-B. Bauguitte[4] Dudley E. Shallcross[2] R. L. Jones[3] and Carl J. Percival[1]*

[1]*The Centre for Atmospheric Science, The School of Earth, Atmospheric and Environmental Sciences, The University of Manchester, Simon Building, Brunswick Street, Manchester, M13 9PL, UK.*

[2]*School of Chemistry, The University of Bristol, Cantock's Close BS8 1TS, UK.*

[3]*Department of Chemistry, University of Cambridge, Cambridgeshire, UK*

[4]*British Antarctic Survey, Natural Environment Research Council, High Cross, Madingley Road, Cambridge, CB3 0ET, UK.*

[*]*Corresponding author Email: carl.percival@manchester.ac.uk*

Abstract

Dinitrogen pentoxide (N_2O_5) plays a central role in nighttime tropospheric chemistry as its formation limits the following days O_3 potential. Hence, accurate measurements of N_2O_5 are critical to examine our understanding of this chemistry, therefore the comparison of measurement techniques are vital to evaluate their capabilities. A chemical ionization mass spectrometer (CIMS) and broadband cavity enhanced absorption spectrometer (BBCEAS) were deployed during the 20010/2011 Role of Nighttime Chemistry in Controlling the Oxidising Capacity of the Atmosphere (RONOCO) campaign onboard the BAe-146 aircraft over the United Kingdom. 1 Hz mixing ratios of N_2O_5 were simultaneously measured during 8 flights throughout this campaign. The CIMS measured N_2O_5 directly

using I^- ionisation chemistry and the BBCEAS indirectly measured N_2O_5 via a heated inlet, thermally dissociating it to measure NO_3.

The sensitivity for the CIMS was 52 ion counts $pptv^{-1}$ with a limit of detection of 7.4 pptv for 1Hz measurements. The limit of detection for the BBCEAS was 2 pptv. The comparison of N_2O_5 mixing ratios show excellent agreement between the instruments for the whole dataset as indicated by the square of the linear correlation coefficient, $R^2 = 0.89$ which increased to as high as 0.98 for flight B568. BBCEAS measurements for flight B534 return higher concentrations in comparison with the CIMS instrument, possibly due to N_2O_5 conversion efficiency in the BBCEAS and also a change in sensitivity for the CIMS due to ionisation molecule concentration reduction below an excess threshold. Altitudinal profiles obtained during the campaign show close agreement, with a correlation coefficient $R^2 = 0.93$. Large positive correlations of the BBCEAS and CIMS N_2O_5 concentrations with NO_2 were observed within plumes, as both instruments present an R^2 of 0.93. The dusk to dawn flight allowed the transition from day to night time chemistry to be observed; each instrument simultaneously detecting increases in N_2O_5 at sunset, supported by a simultaneous rise in NO_2 levels. The CIMS and BBCEAS performance indicate their significant ability to constrain night time N_2O_5 chemistry through the accurate acquirement of high frequency measurements on an aircraft.

1. Introduction

Dinitrogen pentoxide (N_2O_5) is an important reactive nighttime oxide of nitrogen in both the stratosphere and troposphere. Its formation in the stratosphere limits ozone (O_3) production (Johnston *et al*,. 1971) and presence in the troposphere enables halogen activation and the production of inorganic nitrate (Atkinson and Arey, 2003) by reaction with salt aerosols, forming $ClNO_2$ (Osthoff *et al*., 2008). The efficiency of daytime tropospheric ozone production and the formation of secondary aerosols are affected by nitrate (NO_3) and N_2O_5 levels the previous night (Brown *et al*., 2006). NO_3 initiates the processing of anthropogenic and biogenic emissions at nighttime and has been shown to be as dominant as the daytime hydroxyl radical processing, due to its reactivity with unsaturated VOC`s (Atkinson, 1991). To improve the understanding of the processes affecting O_3 formation and air quality, it is necessary to improve the understanding of the

atmospheric cycle of NO_3 through its formation, loss, spatial variability and role in the regulation of NO_x and budgets of VOCs (Atkinson, 2000).

NO_3 is formed through the reaction of O_3 and NO_2, which can then further react with NO_2 to form N_2O_5. N_2O_5 is in thermal equilibrium with NO_3 which is established in a few minutes in the atmosphere (Brown, 2003).

$$NO + O_3 \rightarrow NO_2 + O_2 \qquad \text{R1}$$

$$NO_2 + O_3 \rightarrow NO_3 + O_2 \qquad \text{R2}$$

$$NO_2 + NO_3 + M \rightleftarrows N_2O_5 + M \qquad \text{R3}$$

N_2O_5 is only abundant at night due to the rapid photolysis of NO_3; j (NO_3) is 0.2 s^{-1} according to Stark *et al.* (2007) and undergoes fast reaction with NO during the daytime. N_2O_5 mixing ratios can build up during the nighttime with maximum concentrations of a few ppbv (Brown *et al*., 2007). Nighttime production of N_2O_5 has a significant impact on the lifetime of NO_x, enabling N_2O_5 to act as a nighttime sink of NO_x or a reversible storage of NO_x allowing possible transport (Dentener and Crutzen 1993).

N_2O_5 acts as a sink for NO_x in the troposphere through its reaction with water producing nitric acid (HNO_3), which ultimately has a direct effect on tropopsheric O_3 production (Morris and Niki 1973; Mozurkewich and Calvert 1988).

$$N_2O_5 + H_2O \rightarrow 2HNO_3 \qquad \text{R4}$$

Therefore, the nighttime oxidative capacity of the troposphere and NO_3 availability is partially dependent upon the hydrolysis of N_2O_5, reaction 4. This removal of NO_3 and N_2O_5 at night directly impacts the production of daytime oxidants such as OH and O_3. Due to this complex relationship between NO_x and O_3 production, the hydrolysis of N_2O_5 is thought to decrease O_3 concentrations in low NO_x conditions and increase O_3 in high NO_x regions (Riemer *et al*. 2003).

N_2O_5 also affects the tropospheric aerosol budget as the nitric acid produced, via its hydrolysis, partitions to the aerosol phase at low temperatures or in regions of excess ammonia (Stelson and Seinfeld 1982; Russell and Cass 1986). N_2O_5 can also be directly taken up on particles or fog droplets resulting in a production of dissolved nitrate (Lillis *et al*. 1999). The dynamics of this resulting particle phase NO_3 is an area of uncertainty in aerosol prediction (Yu *et al*. 2005) and its impact on regional air quality and climate is difficult to quantify (Liao and Seinfeld 2005; Feng and Penner 2007; Bauer *et al*. 2007). This uptake rate is not well known as it depends on aerosol composition and meteorological conditions (Brown *et al*. 2006b; Bertram *et al*. 2009). Recent studies have shown heterogeneous chemistry of N_2O_5 on chloride containing aerosols efficiently release chlorine radicals to the atmosphere (Osthoff *et al*. 2008).

The first measurements of NO_3 in the troposphere using DOAS (Platt *et al*., 1980) was followed by a wide range of ground studies investigating the role of NO_3 in polluted and clean tropospheric environments (e.g. Geyer *et al*., 2001; Smith *et al*., 1995). The measurement of N_2O_5 during these studies was not possible as it does not absorb at visible wavelengths. Techniques measuring NO_3 were then developed to infer N_2O_5 concentrations via the thermal equilibrium of NO_3 and N_2O_5. Following experiments used high-finesse cavity techniques (e.g. Brown *et al*., 2007a; Dube *et al*., 2006), ionisation mass spectrometry (Slusher *et al*., 2004) or Laser Induced Fluorescence (LIF) which were able to detect NO_3 produced from the thermal dissociation of N_2O_5 (Matsumoto *et al*., 2005b; Wood *et al*., 2005). Concentrations up to 800 pptv were measured in Tokyo using such techniques. Previous in situ measurements indicate an instrument with a fast time response is necessary to capture its temporal variability (Brown *et al*., 2001, 2003); however there are limited techniques with this capability. Kennedy *et al* (2012) report measurements of N_2O_5 via the thermal dissociation of N_2O_5 on a second channel of a broadband cavity enhanced absorption spectrometer (BBCEAS) onboard the FAAM BAe-146 aircraft during the RONOCO campaign. In this paper, N_2O_5 detection using a chemical ionisation mass spectrometer is compared with the BBCEAS technique during the RONOCO project.

2. Experiment details

2.1. BBCEAS instrument

The BBCEAS has previously been described for NO_3, N_2O_5 and NO_2 measurements in Kennedy *et al.* (2012). Here, a brief decryption for N_2O_5 measurements is given. The BBCEAS has two rear facing inlets situated on the aircraft fuselage. The first inlet is used for sampling ambient air whereas the second inlet is used for sampling ambient air drawn through a sheath surrounding the inlet, measuring ambient NO_3 concentrations. The sheath is used to maintain the inlet temperature to ensure minimal perturbation by the NO_3/N_2O_5 equilibrium. Air is drawn through channel 1 which consists of a thermally insulated 60 cm long 5/32" internal diameter PFA tube at a rate of 50L per minute. This flow is then divided into two separate conduits, one of which heated to 120 degrees Celsius in a 68 cm long ½" outside diameter PFA tube to facilitate the thermal dissociation of N_2O_5 to NO_3 and NO_2, assuming 100% conversion efficiency. The sum of NO_3 via the two heated and ambient temperature inlets are measured. The amount of NO_3 thus produced was determined by monitoring its absorption in the wavelength range between 640 nm and 672 nm in a cavity which was formed of two mirrors both with peak reflectivity's of about 99.99% at 660 nm. The temperature of the cavity was kept at 80 degrees Celsius. During flight operations, the background spectrum, which is acquired by stopping ambient flow and back flowing nitrogen through conduits 1 and 2, is measured on the ground before sampling begins and half-hourly in flight thereafter to accounts for lamp intensity variations.

2.2. CIMS instrument

The CIMS instrument was built by the Georgia Institute of Technology as previously described by Nowak *et al*. (2007) and Le Breton *et al*. (2012). The schematic in figure 1 shows the set up used and operating conditions of the CIMS on board the airborne platform FAAM BAe-146 research aircraft.

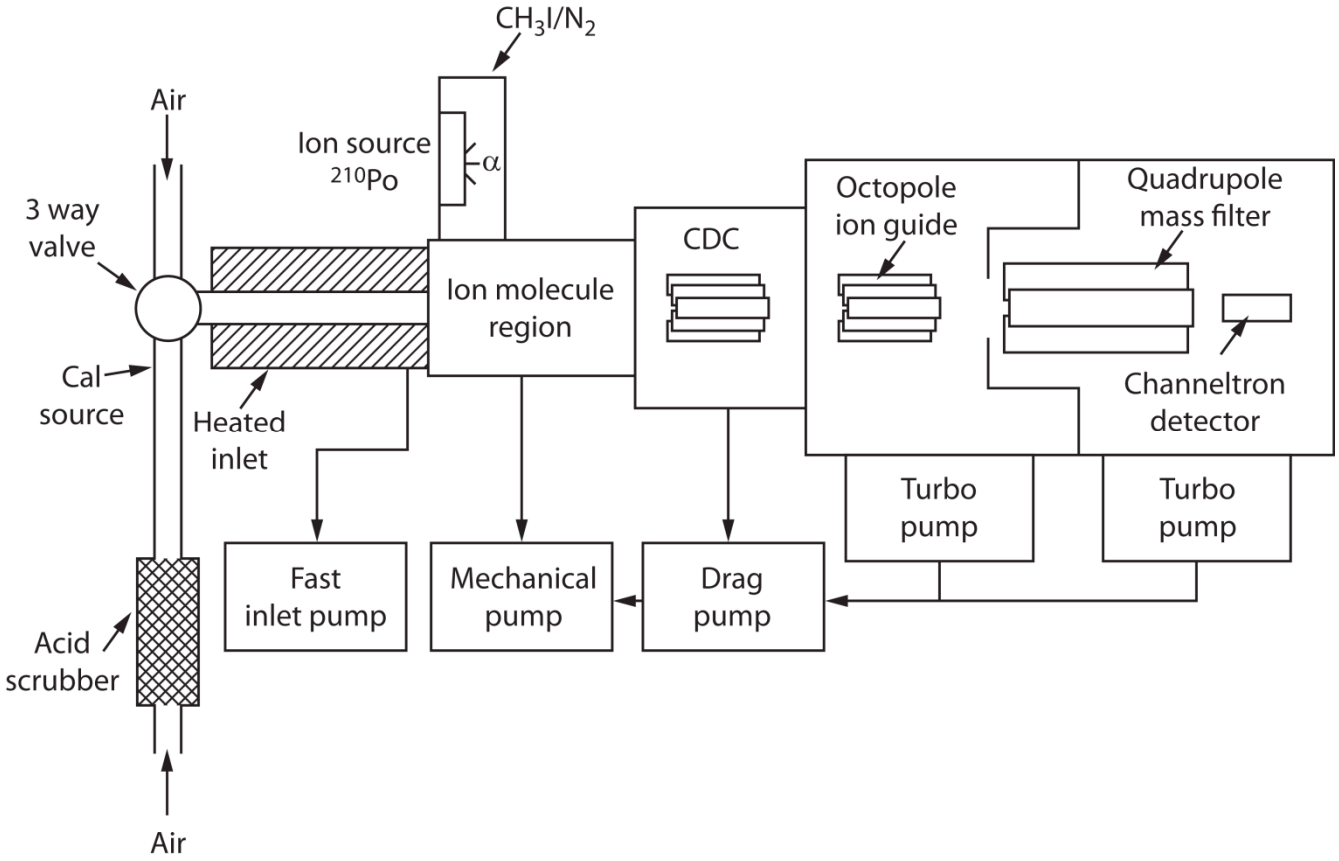

Figure 1. Schematic of chemical ionisation mass spectrometer (CIMS) used in this study. Arrows indicate direction of gas flow. Dimensions are not to scale.

2.2.1. Inlet and ionization

The CIMS is fitted with two identical inlets, one for background measurements and one for sampling. They consist of 6 cm OD diameter PFA tubing of length 580 mm and are heated to 35°C to reduce surface loss. A 3-way PFA valve is used to automate switching between measuring the background scrubbed air or atmospheric sample. An orifice of diameter 0.9 mm was positioned at the front of the inlet to restrict the flow to 5.8 SLM which was brought in using a rotary vane pump (Picolino VTE-3, Gardner Denver Thomas) corresponding to a residence time of 0.28s at standard temperature and pressure) in the total length of inlet tubing.

The pressure in the ionisation region was maintained at 19 Torr throughout the flight and was controlled and measured using a mass flow controller (MKS 1179 and MKS M100

Mass flow controllers, MKS Instruments, UK) and Baratron (1000 Torr range, Pressure Transducer, Model No. 722A, MKS Instruments, UK) and a dry scroll pump (UL-DISL 100, ULVAC Industrial). Here, N_2 and the ionisation gas mixture of $CH_3I/H_2O/N_2$ at a rate of 1 SCCM passed over the ion source (Polonium-210 inline ioniser, NRD inc Static Solutions Limited), producing an excess of I^- and $I^-{\cdot}H_2O$ ions in the IMR, which then ionised the N_2O_5 molecules in the air sample.

2.2.2. Ion filtration and detection

The ions then passed through a pinhole of a charged plate, which entered the mass spectrometer section of the instrument, i.e. the first octopole ion guide chamber which is the collisional dissociation chamber (CDC) at a pressure of 0.25 Torr where the local electric field divided by the gas number density (E/N) was 180 Townsend (Td = 10^{-17} V cm^2). Here, weakly-bound ion-water clusters are broken up to simplify the resultant mass spectrum. The pressure in the CDC of less than 1 Torr was achieved by the use of a molecular drag pump (MDP-5011, Adixen Alcatel Vacuum Technology). After the CDC, the ions passed through the second octopole ion guide, which has the effect of collimating the ions. The octopole chamber was held at a pressure of 10^{-3} Torr which was maintained by a turbomolecular pump (V-81M Navigator, Varian Inc. Vacuum Technologies). Beyond the second octopole chamber, the ions were mass selected by a quadrupole with pre and post filters with entrance and exit lenses (Tri-filter Quadrupole Mass Filter, Extrel CMS).

The quadrupole section was kept at a pressure of 10^{-4} Torr by a second 15 turbomolecular pump (V-81M Navigator, Varian Inc. Vacuum Technologies). The selected ions were then detected and counted by a continuous dynode electron multiplier (7550M detector, ITT Power Solutions, Inc.).

2.2.3 Ionisation scheme

The ion-molecule chemistry using iodide ions (I^-) for trace gas detection has been described by Slusher *et al*. (2004) and was utilised here to detect N_2O_5. A gas mixture of methyl iodide (CH_3I) and H_2O in N_2 is used to obtain reagent ions I^- and water clusters $I^-.H_2O$, of which the latter is important for the ionisation of N_2O_5, forming the adduct as seen in the mass spectrum (Fig. 2). The mix was produced using a manifold by evaporating

the liquid deionised H_2O and CH_3I sequentially into the manifold to reach the following partial pressures of 10 Torr H_2O and 15 Torr CH_3I, before adding 5 bar of N_2 to make a ionization gas mixture of 0.39 % CH_3I and 0.26 % H_2O. CH_3I (≥ 99.5 %) was purchased from Sigma Aldrich and used as provided. N_2O_5 was ionised by I^- via the reaction 5;

$$I^-.H_2O + N_2O_5 \rightarrow NO_3^- + NO_2 + I.H_2O \qquad \text{R5}$$

which enabled N_2O_5 to be detected selectively at *m/z* =62 Typical reagent ion values were I^-= 1.5 ×10^6 Hz, and $I.H_2O$ = 2.5 ×10^6 Hz.

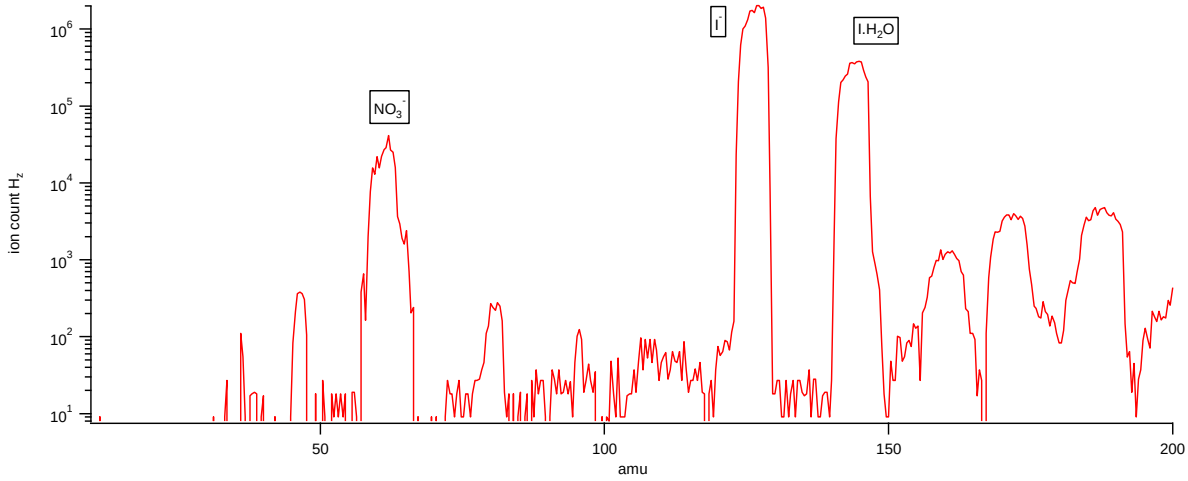

Figure 2. Mass spectrum of CIMS during flight B565, 2011 at 17:22. Ionisation peaks and N_2O_5 detected mass (at mass 62, NO_3) are labelled.

As the ionisation efficiency is dependent on the presence of water vapour through the production of $I^-.H_2O$ (Slusher *et al.*, 2004), water vapour was added to the ionisation gas mixture, so as to produce an excess of $I^-.H_2O$ cluster ions and hence allow operation in the water vapour independent regime. Figure 3 shows a formic acid calibration at a range of RH and therefore $I^-.H_2O$ counts. Mass 145 ($I^-.H_2O$) counts never fell below 150 000 counts during operation onboard the aircraft due to this addition of water vapour. The sensitivity of the CIMS for N_2O_5 is assumed to be independent of water vapour as laboratory tests have shown formic acid and N_2O_5 sensitivities are linear, as explained in detail in section 2.2.4.

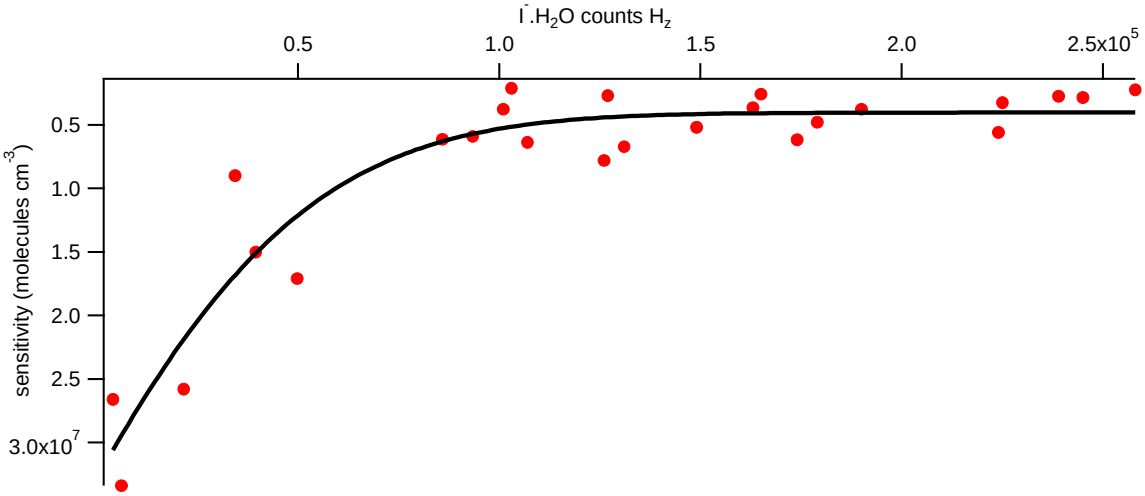

Figure 3. Formic acid calibration at a range of RH values, indicating the stability of sensitivity above 100 000 $I^-.H_2O$ counts.

2.2.4. Calibrations

The CIMS was calibrated relative to the formic acid sensitivity for each flight. Post and in flight formic acid calibrations were taken as described in Le Breton *et al.* (2012). N_2O_5 was calibrated in the laboratory after the campaign by producing a known concentration of N_2O_5 as described later and simultaneously calibrating the instrument for formic acid. A linear relationship was found for formic acid and N_2O_5 sensitivities. Figure 6 shows how the CIMS sensitivity to formic acid and N_2O_5 increase linearly. As the CIMS was unable to calibrate for N_2O_5 during the RONOCO campaign, a single BBCEAS data point was taken to estimate sensitivity for the CIMS for N_2O_5 and ratio to the formic acid in flight calibration. The calculated ratio was then implemented for the whole dataset.

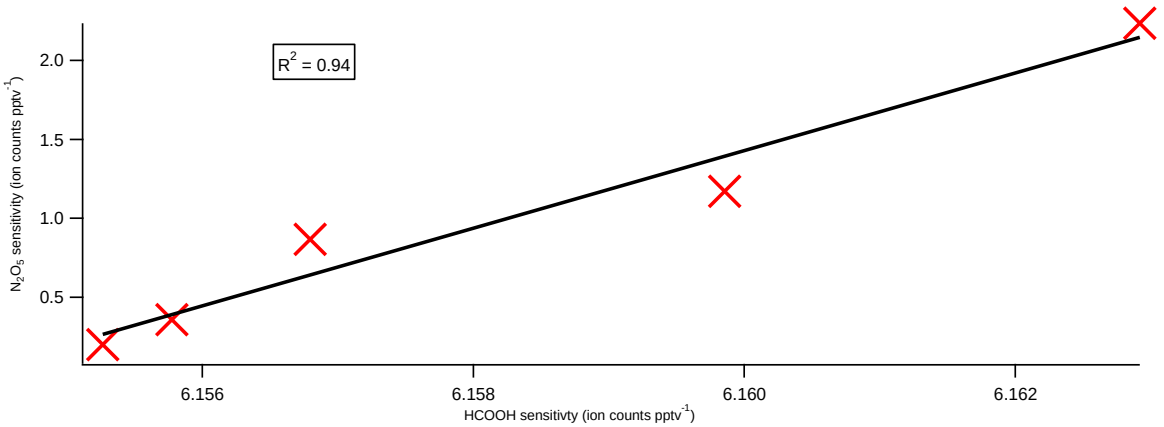

Figure 4. Formic acid and N_2O_5 laboratory calibration correlation at low I.H_2O counts to demonstrate stability at low sensitivities.

N_2O_5 was prepared by the gas phase reaction of nitrogen dioxide (NO_2) and O_3 based on the method described in Davidson *et al*. (1978) and reactions 2 and 3. The glassware consisted of a 5 litre capacity pyrex-glass reaction vessel, of 25 cm diameter, with removable and sealable cold traps at either end, all of which were covered with foil to ensure no photolysis. Youngs taps fitted to the traps in combination with the main synthesis glassware allowed for the periodical reversal of the gas flows. Water vapour was excluded from the glassware by purging the system with O_3 and oxygen for ten minutes before use.

O_3 was generated by passing dry oxygen through a commercial O_3 generator (BMT 802) at a flow rate of 200 $sccm^{-1}$ using a mass flow controller. The NO_2 was then introduced into the gas stream, its colour diminishing in the reaction vessel, an indication of chemical conversion. The product was collected over a methanol/liquid nitrogen trap at 260 K in the trap furthest away from the source. This flow direction was left for 30 minutes for sufficient deposition of N_2O_5. The NO_2 flow was stopped and O_3 flow reversed, moving the cold trap to the other end of the vessel. This was repeated until pine needles were collected in the cold trap, a sign of pure N_2O_5. The ozoniser was then switched off and the system was purged with oxygen for 5 minutes to remove unreacted O_3. The N_2O_5 was then removed and stored at 195 K in the dark to limit decomposition.

The N_2O_5, maintained at 195K, was then introduced to the CIMS and a NO_x analyser with a supporting flow of Nitrogen. The N_2O_5 concentration was then inferred through the stoichiometric ratio of NO_2:N_2O_5 as observed in reaction 7.

2.3 FAAM BAe-146 onboard instruments

In addition to the N_2O_5 data from the BBCEAS and CIMS, NO_2 measurements are used in this analysis. Nitric oxide (NO) and nitrogen dioxide (NO_2) were measured using separate channels of a chemiluminescence detector and were reported every 1 second with an uncertainty of ± 6% ppbv (Stewart *et al*., 2008). Ozone was measured using a UV Photometric Ozone Analyser at 1 Hz with an uncertainty of 15 ±3 ppbv (Real et al., 2007). The FAAM core GPS-aided inertial Navigation system is also used to provide altitude, longitude and latitude.

2.4 RONOCO 2010 campaign

The RONOCO campaign was conducted in the summer and winter 2010/2011 based at East Midlands airport, United Kingdom. The scientific objectives of RONOCO were to determine the morphology of tropospheric NO_3 in different meteorological conditions and seasons, and in a range of gas phase and aerosol environments, in order to quantify the key processes and pathways of oxidized nitrogen chemistry at night in the troposphere. The ultimate aim was to assess the pervasiveness and importance of nighttime chemical processes, and in particular NO_3, for UK regional and Western European air quality, eutrophication, and ultimately to quantify its links to climate change. In this project, NCAS scientists used the FAAM BAe-146 aircraft together with supporting instrument measurements and modelling studies. The CIMS instrument measured formic acid, propanoic acid, butanoic acid, nitric acid and N_2O_5 throughout the RONOCO campaign. The BBCEAS measured NO_3, N_2O_5 water and NO_2. 35 hours of flight data from RONOCO are presented within this paper for comparison; 5 flights at nighttime in summer, 2 in winter and 1dusk to dawn transition in winter to study the transition between daytime and nighttime chemistry. All flights sampled air over the UK, North Sea and English Channel which are impacted by pollution from the UK and occasionally continental Europe.

3. Results

3.1. Overall comparison

The concentrations measured and statistics reported here are at 1Hz for both instruments. The CIMS sensitivity is calculated as the average sensitivity for the 8 flights presented here. The average sensitivity was 52 ± 2 ion counts $pptv^{-1}s^{-1}$, with a limit of detection of 7.8 pptv, calculated as 3 standard deviations above the background counts, and a total measurement error of 15%. The BBCEAS sensitivity is defined by its limit of detection (the smallest change in cavity throughput, I_{Δ} min, that can be detected resulting from molecular absorption inside the cavity), calculated to be 2 pptv for 1Hz data. Good agreement was obtained between the N_2O_5 measurements using both CIMS and BBCEAS for the 8 flights presented here (Figure 4). The linear regression exhibits a line of best fit with a correlation coefficient R^2 = 0.89. The agreement between the CIMS and BBCEAS measurements varies from flight to flight as shown in figure 5. Flight B566 has the highest r^2 value of 0.98, whereas as flight B537 has the lowest R^2 of 0.74. This reduction in R^2 may be a result of the instruments method of concentration retrieval. The BBCEAS depends on the $\sigma(NO_3)$ which is proportional to the temperature, pressure, water vapour, hν and additional absorption causing possible broadening of the peak. Whereas the CIMS sensitivity depends on $I.H_2O$ counts, which may decrease at high N_2O_5 concentrations as shown in figure 3. The mean N_2O_5 mixing ratio was 114 pptv for CIMS and 115 pptv for BBCEAS. Maximum concentrations reported by the CIMS and BBCEAS were 890 ± 133 pptv and 1007 ± 141 pptv respectively, although these peak concentrations do not originate form the same air mass. These maxima were intercepted during measurements of the London plume travelling North East over the North Sea, but the BBCEAS maxima was reported during flight B534, whereas the CIMS report the measurement during flight B565. This discrepancy may arise from the slight curvature in the correlation between the CIMS and BBCEAS for flight B534. A CIMS/BBCEAS [N_2O_5] ratio of 1.73 may indicate a change of sensitivity for the CIMS at high N_2O_5 concentrations. The CIMS sensitivity may have decreased if the $I.H_2O$ counts drop below 150 000, subsequently increase in the calculated concentration. The CIMS was much more sensitive for summer flights, through the efficient production of the $I.H_2O$. This high sensitivity in summer and possible instability of sensitivity at high concentrations possibly explains how this curvature to the correlation is not observed in winter. The BBCEAS conversion efficiency to NO_3 could also decrease at high concentrations.

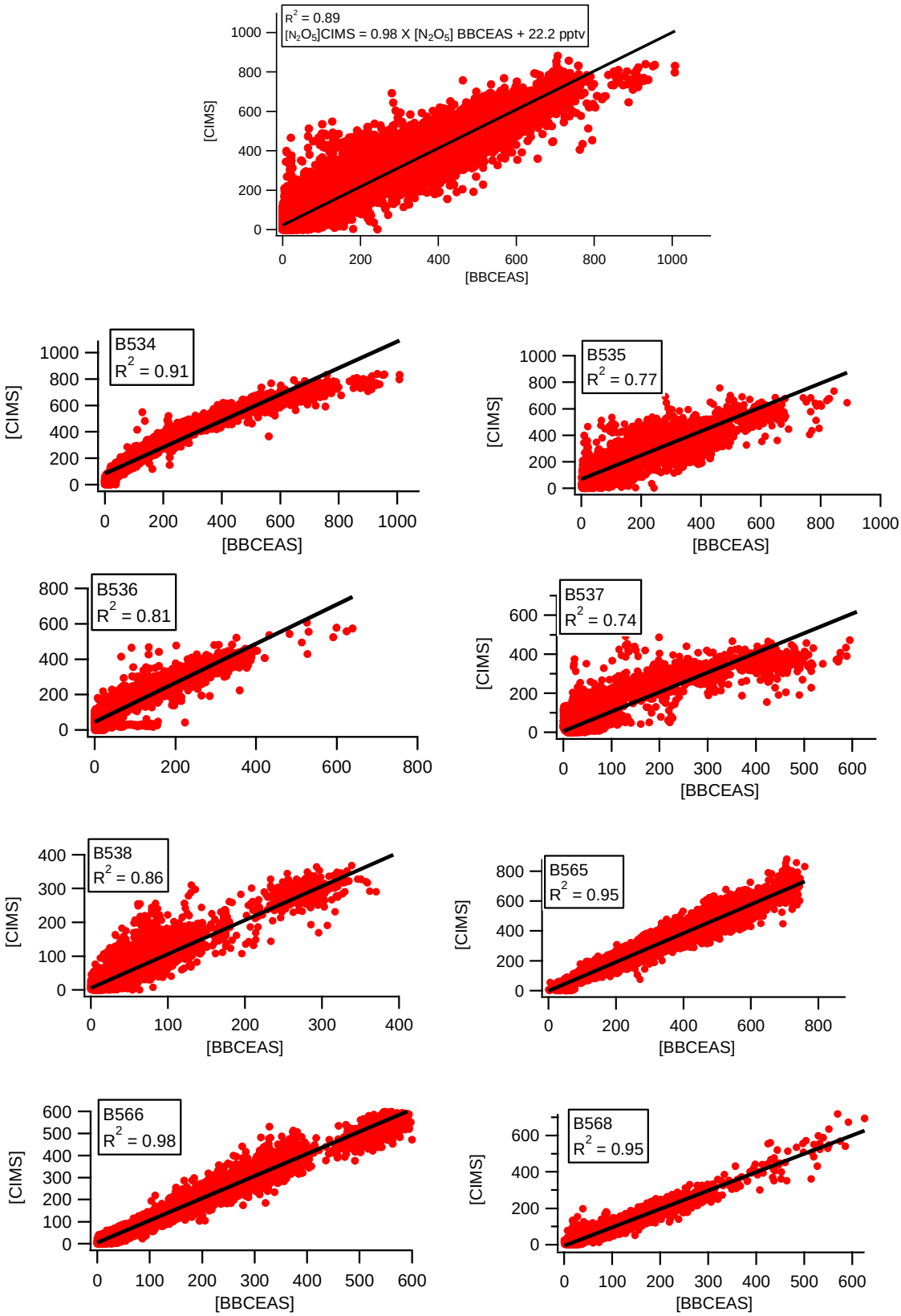

Figure 5: Scatter plots for the entire RONOCO dataset accumulated and for each flight from RONOCO where CIMS and BBCEAS measured [N_2O_5]. The black lines illustrate the linear regression.

3.2. Comparison as a function of altitude

Vertical profiles obtained from aircraft measurements offer the ability to derive profiles from a variety of air masses, locations and meteorological conditions. Previous profiles obtained from aircraft measurements have shown that concentrations are larger and longer lived aloft as compared with the surface (Brown *et al*., 2007), as the sinks for N_2O_5 will generally decrease with altitude due to heterogeneous loss (Fish et al., 1999).

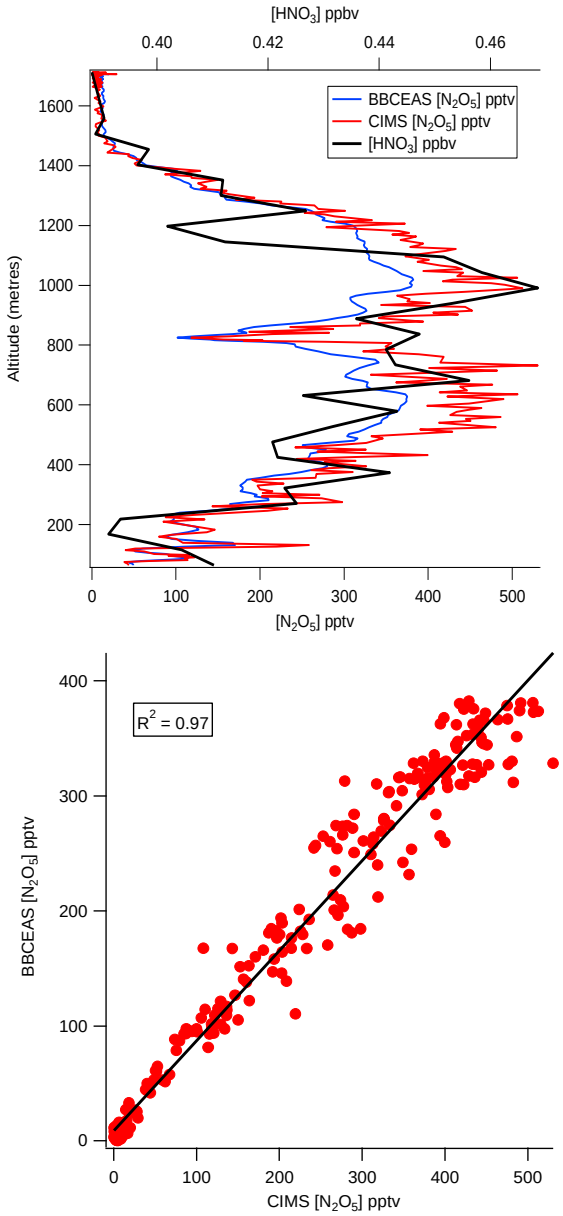

Figure 6: Vertical profiles of N_2O_5 nitric acid (HNO_3) mixing ratios from an altitude of 64 to 1711 metres from the CIMS and BBCEAS. Linear regression line for this data, R^2 = 0.97. HNO_3 measurements are averaged to 15 seconds.

Figure 6 illustrates a concentration profile attained during flight B568, increasing with altitude from 64 metres to 1711 metres. Good agreement between concentrations returned by both instruments, R^2 = 0.97 (as shown in figure 6), confirms the accuracy of the instruments measurements during altitudinal profiles.

At the lowest altitude of 64 metres, both instruments return an average concentration of 45 pptv. A steady increase is observed up to 600 metres where the CIMS records a maximum concentration of 552 pptv and the BBCEAS records a maximum concentration of 353 pptv. Both instruments observe a sharp decrease in concentration to 100 pptv at 820 metres. An increase again is observed steadily to 1000 feet where the CIMS and BBCEAS record concentrations of 512 and 392 pptv respectively. Both instruments observe a very similar drop above this altitude to15 pptv at 1500 metres. The difference in these concentrations during this profile may arise from BBCEAS inlet efficiencies as the heated inlet may not efficiently respond to this sudden change in concentration producing a higher temporary instrumental background.

If it is assumed that nitric acid is produced by the hydrolysis of N_2O_5, correlations to the nitric acid profile can aid a comparison between the instruments. Both instruments profiles show a very similar structure to that of nitric acid, although rapid decreases in nitric acid at 200 metres and 1200 metres are not observed in either N_2O_5 measurements. Further analysis using the steady state approximation is presented in a later section.

3.3. Comparison as a function of NO_2

NO_2 plays a key role in nighttime chemistry as it is a primary reactant to N_2O_5 formation; therefore it is useful to observe NO_2 concentrations at the same time as N_2O_5

measurements to validate the N_2O_5 formation and trends. Figure 7 shows a NO_2 plume detected during flight B566 at 20:44, which increases above ambient concentrations during the flight (1.5 ppbv) to 15.7 ppbv. The CIMS and BBCEAS detect a similar increase in N_2O_5 concentrations at this time with close to identical structure. The correlation of N_2O_5 to NO_2 can be seen in figure 7 for the CIMS and BBCEAS which both show a very similar trend and the same high r^2 value; 0.93. The r^2 for all the data obtained in flight B566 for CIMS and BBCEAS was 0.59 and 0.62 respectively.

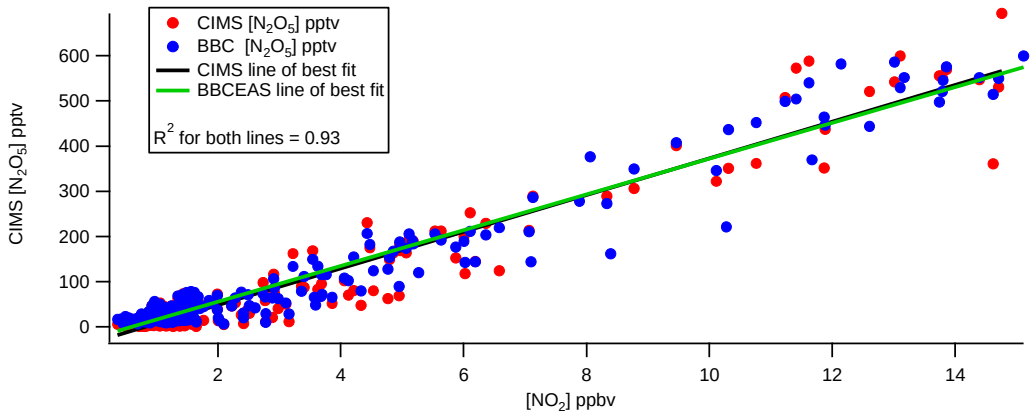

Figure 7: CIMS and BBCEAS N_2O_5 concentration time series during flight B566. NO_2 scatter plot for both N_2O_5 measurements (CIMS in red, BBCEAS in blue) and linear regression line for each (CIMS in black, BBCEAS in green).

3.4. Dusk to dawn transition flight

Flight B568 took off from East Midlands Airport, Leicestershire, UK at 14:53 and flew along the East coast of the UK over the North Sea. The timing of this flight allowed measurements during daylight and nighttime, enabling observation of the transition from day to nighttime chemistry as sunset was at 16:30. The daytime average concentrations measured by the CIMS and BBCEAS were 22 ± 3 pptv and 18 ± 3 pptv respectively. An increase in concentration is then observed from the point of sunset, indicating the transition from daytime chemistry to nighttime chemistry. This transition is confirmed by the increasing NO_2 concentration above the earlier background levels, which is expected due to the reduction in photolysis. The high NO_2 concentrations observed from 17:25 until 17:50 correlate with a decrease in O_3 concentrations. Low O_3 mixing ratios are expected

and observed to reduce NO_3 and N_2O_5 concentrations. Following the recovery to higher O_3 levels, N_2O_5 and NO_3 progress to their maximum concentrations on the flight. The maximum concentration of 867 pptv measured by the BBCEAS was at 18:39 and the CIMS maximum concentration, 704 pptv, was measured at 18:27. The time series in figure 8 shows that these will originate from the same air mass, but CIMS was calibrating during the time when the BBCEAS measured the maxima and therefore no data could be obtained. This flight shows the ability of both instruments, and measurements of N_2O_5, to track accurately the transition from day to nighttime chemistry and the emergence of NO_2, NO_3 and N_2O_5.

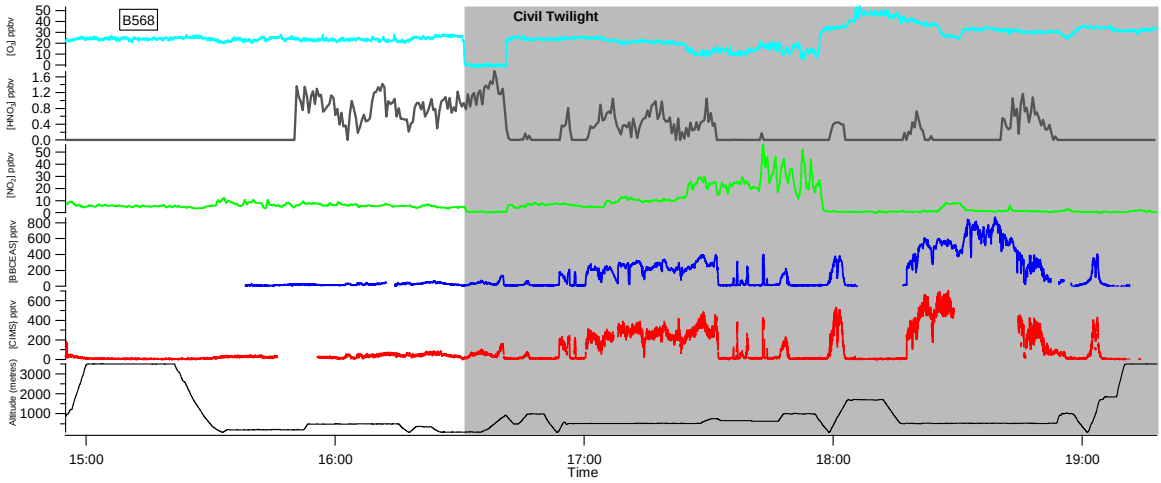

Figure 8: Time series plot from flight B568 for concentrations of N_2O_5 from the CIMS (red line) and BBCEAS (blue line), NO_2 concentrations (green line) and altitude (black line).

4. Steady state analysis

Brown et al., (2003) have described in detail the conditions under which the steady state approximation is valid for the analysis of atmospheric levels of NO_3 and N_2O_5. We have analysed the dataset presented in this paper and conclude that the steady state approximation can be applied to the nighttime datasets. Following the work of Brown et al., (2003) we note that five reactions exist under the conditions encountered that will control both species. These are

$$NO_2 + O_3 \rightarrow NO_3 + O_2 \qquad (1)$$

$NO_3 + NO_2 + M \rightarrow N_2O_5 + M$ (2)

$NO_3 + NO \rightarrow 2NO_2$ (3)

$N_2O_5 + M \rightarrow NO_2 + NO_3 + M$ (4)

$N_2O_5 \rightarrow$ loss (5)

Application of the steady state approximation to NO_3 and N_2O_5 yields the expressions

$$[NO_3] = \frac{k_1[NO_2][O_3]+k_4[N_2O_5[M]]}{k_2[NO_2]M+k_3[NO]} \quad \textbf{I}$$

$$[N_2O_5] = \frac{k_2[NO_3][NO_2]+[M]}{k_4[M]+k_5} \quad \textbf{II}$$

Further analysis using equations I and II then yield an expression for $[N_2O_5]$ involving just NO, NO_2 and O_3.

$$\frac{k_2[NO_2][M]k_1[NO_2][O_3]}{k_4[M]k_3[NO]+k_5k_2[NO_2][M]+k_5k_3[NO]} = [N_2O_5] \quad \textbf{III}$$

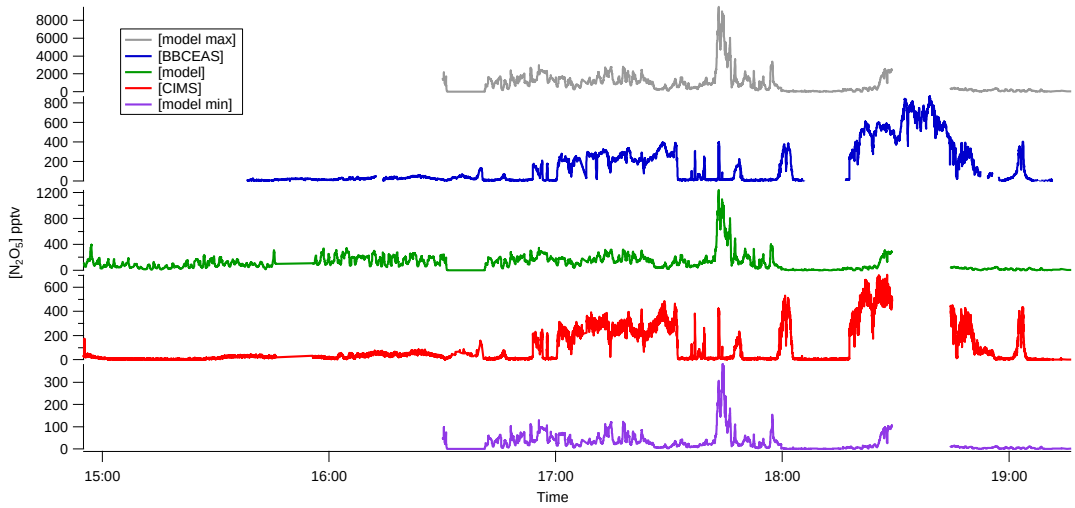

Figure 9: Time series plot from flight B568 of N_2O_5 concentrations from the CIMS (red line) and BBCEAS (blue line) with the results from the model (green line), Model minimum (purple line) and model maximum (grey line).

Comparison of the [N_2O_5] derived using equation III using the measurement data of NO, NO_2 and O_3, together with the rate coefficients taken from laboratory studies, with the measured data produces good agreement in general (figure 9). When one includes the combined uncertainties in rate coefficients and measurements to derive a lower and upper limit for the steady state analysis, these limits easily bracket the measured data. The dataset splits into two regions, one where nighttime NO is large such that NO_3 loss is large via reaction (3). Here, N_2O_5 levels cannot build to high levels and is in keeping with the study by Zheng et al., (2008). These workers studied NO_3 and N_2O_5 vertical profiles during the Milagro campaign over Mexico City and concluded that nighttime NO levels were large and led to a suppression on both species. Alternatively if NO_2 levels dominate, equation III can be simplified to equation IV which further simplifies to equation V (and is in keeping with the linear correlation between N_2O_5 and NO_2).

$$\frac{k_2[NO_2][M]k_1[NO_2[O_3]]}{k_5k_2[NO_2][M]} = N_2O_5 \qquad \textbf{IV}$$

$$\frac{k_1[NO_2][O_3]}{k_5} = [N_2O_5] \qquad \textbf{V}$$

Rearranging equation V yields an expression for k_5 which involves all parameters that are measured in this work. The average value returned is ~ 5 x 10^{-3} s^{-1}, leading to a lifetime for N_2O_5 of *ca.* 3.5 minutes. Assuming that all the N_2O_5 lost produces gas phase HNO_3 (unlikely as one would imagine that a substantial fraction will be incorporated onto aerosol) leads to an upper limit production rate of HNO_3 ~ 30 ppt min^{-1}. Although we note that this is an upper limit, it compares with a typical production rate during daytime through the reaction between OH and NO_2, assuming [NO_2] = 10 ppb, [OH] = 1 x 10^6 molecule cm^{-3}, this produces a production rate of approx. 20 ppt min^{-1}. This result would support the modelling work of Jones et al., (2005) who show that the nighttime production of HNO_3

from N_2O_5 chemistry can be an efficient sink for NOx, comparable to the daytime production of HNO_3 form the hydroxyl radical.

5. Summary and conclusions

The RONOCO campaign 2010/2011 enabled a formal comparison of N_2O_5 concentrations measured by two fundamentally different techniques, CIMS and BBCEAS. The comparison was conducted successfully for the first time on the same aircraft over the UK. The campaign showed how N_2O_5 can be accurately detected at high frequency ($1H_z$), directly with a high sensitivity by the CIMS of 52 ion counts $pptv^{-1}$ and indirectly with limits of detections down to 2 pptv. Good agreement in general was observed. Linear regression results show that $[N_2O_5]$ CIMS = 0.98 X $[N_2O_5]$ BBCEAS + 22.2 pptv with an average correlation coefficient $R^2 = 0.89$. The difference between the CIMS and BBCEAS instruments for N_2O_5 measurements can be explained in general by their combined measurement uncertainties. The high correlation during altitudinal profiles ($R^2 = 0.93$) prove the sensitivity of each instrument remains constant throughout varying flight conditions and allow detailed quick time profiles to be taken in varying environments. Simultaneous NO_2 measurements helped validate the N_2O_5 plumes detected during the campaign and transition from day to night chemistry. These results show that CIMS and BBCEAS techniques can be applied to precise and rapid measurements of N_2O_5 on an aircraft.

Acknowledgments

The authors would like to thank the FAAM staff are also thanked for their assistance in getting the CIMS working onboard the aircraft. CJP and DES thank NERC (NE/F004656/1) under whose auspices various elements of this work were carried out.

References

Atkinson, R. Kinetics and mechanism of the gas-phase reactions of the NO_3 radical with organic compounds, J. Phys. Chem. Ref. Data, 20,459–507, 1991

Atkinson, R.: Atmospheric chemistry of VOCs and NO_x, Atmos. Environ., 34, 2063–2101, 2000.

Atkinson, R., Arey, J. Gas-phase tropospheric chemistry of biogenic volatile organic compounds: a review. Atmospheric Environment, vol. 37, S197–S219, 2003.

Bauer, S. E., Koch, D., Unger, N., Metzger, S. M., Shindell, D. T., and Streets, D. G. Nitrate Aerosols Today and in 2030: Importance Relative to Other Aerosol Species and Tropospheric Ozone. Atmos. Chem. Phys. 7:5043–5059, 2007.

Bertram, T. H. and Thornton, J. A.: Toward a general parameterization of N_2O_5 reactivity on aqueous particles: the competing effects of particle liquid water, nitrate and chloride, Atmos. Chem. Phys., 9, 8351–8363, doi:10.5194/acp-9-8351-2009, 2009.

Brown, S. S., H. Stark, S. J. Ciciora, and A. R. Ravishankara. In-situ measurement of atmospheric NO_3 and N_2O_5 via cavity ring-down spectroscopy, Geophys. Res. Lett., 28, 3227– 3230, 2001.

Brown, S. S.: Absorption spectroscopy in high-finesse cavities for atmospheric studies, Chem. Rev., 103, 5219–5238, doi:10.1021/cr020645c, 2003.

Brown, S. S., Stark, H., and Ravishankara, A. R.: Applicability of the steady state approximation to the interpretation of atmospheric observations of NO_3 and N_2O_5 , J. Geophys. Res.-Atmos., 108(D17), 4539, doi:10.1029/2003JD003407, 2003.

Brown, S. S.: Absorption spectroscopy in high-finesse cavities for atmospheric studies, Chem. Rev., 103, 5219–5238, doi:10.1021/cr020645c, 2003.

Brown, S. S., Neuman, J. A., Ryerson, T. B., Trainer, M., Dub´ e, W. P., Holloway, J. S., Warneke, C., Gouw, J. A. D., Donnelly, S. G., Atlas, E., Matthew, B., Middlebrook, A. M., Peltier, R., Weber, R. J., Stohl, A., Meagher, J. F., Fehsenfeld, F. C., and Ravishankara, A. R.:
20 Nocturnal odd-oxygen budget and its implications for ozone loss in the lower troposphere,
Geophys. Res. Lett., 33, L08801, doi:10.1029/2006GL025900, 2006

Brown, S. S., Dub´ e, W. P., Osthoff, H. D., Stutz, J., Ryerson, T. B., Wollny, A. G., Brock, C. A., Warneke, C., de Gouw, J. A., Atlas, E., Neuman, J. A., Holloway, J. S., Lerner, B. M., Williams, E. J., Kuster, W. C., Goldan, P. D., Angevine, W. M., Trainer, M., Fehsenfeld, F. C., and Ravishankara, A. R.: Vertical profiles in NO_3 and N_2O_5 measured from an aircraft: Results from the NOAA P-3 and surface platforms during NEAQS 2004, J. Geophys. Res., 112, D22304, doi:10.1029/2007JD008883, 2007a

Brown, S. S., Dub´ e, W. P., Osthoff, H. D., Wolfe, D. E., Angevine, W. M., and Ravishankara, A. R.: High resolution vertical distributions of NO3 and N2O5 through the nocturnal boundary layer, Atmos. Chem. Phys., 7, 139–149, doi:10.5194/acp-7-139-2007, 2007b

Davidson, J. A., Viggiano, A. A., Howard, C. J., Dotan, I., Fehsenfeld, F. C., Albritton, D. L., and Ferguson, E. E.: Rate constants for the reactions of O_2^+, NO_2^+, NO^+, H_3O^+ , CO_3^-, NO_2^-, and halide ions with N_2O_5 at 300 K. J. Chem. Phys. 68:2085–2087, 1978.

Dentener, F. J., and P. J. Crutzen (1993), Reaction of N_2O_5 on tropospheric aerosols: Impact on the global distribution of NO_x, O_x, and OH, J. Geophys. Res., 98, 7149–7163.

Dub´ e, W. P., Brown, S. S., Osthoff, H. D., Nunley, M. R., Ciciora, S. J., Paris, M. W., McLaughlin, R. J., and Ravishankara, A. R.: Aircraft instrument for simultaneous, in situ measurement of NO_3 and N_2O_5 via pulsed cavity ring-down spectroscopy, Rev. Sci. Instrum., 77(3), 034101– 034101-11, doi:10.1063/1.2176058, 2006.

Feng, Y., and Penner, J. E. Global Modeling of Nitrate and Ammonium: Interaction of Aerosols and Tropospheric Chemistry. J. Geophys. Res. 112:D01304. doi: 10.1029/2005JD006404, 2007

Fish, D. J., Shallcross, D. E., and Jones, R. L.: The vertical distribution of NO_3 in the atmospheric boundary layer., Atmos. Environ., 33, 687-691,1999

Geyer, A., B. Alicke, S. Konrad, T. Schmitz, J. Stutz, and U. Platt, Chemistry and oxidation capacity of the nitrate radical in the continental boundary layer near Berlin, J. Geophys. Res., 106, 8013–8026, 2001.Johnston *et al*, 1971

Johnston, H. S., Reduction of stratospheric ozone by nitrogen oxide catalysts from supersonic transport exhaust, Science, 173, 517–522, 1971.

Jones, R. L., S. M. Ball, and D. E. Shallcross, Small scale structure in the atmosphere: Implications for chemical composition and observational methods, Faraday Discuss., 130, 165–179, doi:10.1039/b502633b, 2005.

Liao, H., P. J. Adams, S. H. Chung, J. H. Seinfeld, L. J. Mickley, and D. J. Jacob. Interactions between tropospheric chemistry and aerosols in a unified general circulation model, J. Geophys. Res., 108, D1, 4001, doi:10.1029/2001JD001260, 2003.

Le Breton, M., Mcgillen, M.R., Muller, J.B.A., Bacak, A., Shallcross, D.E., Xiao, P., Huey, L.G., Tanner, D., Coe, H., Percival, C.J. Airborne observations of formic acid using a chemical ionisation mass spectrometer, Atmos. Meas. Tec., 4, 5807-5835, 2012.

Lillis, D., Cruz, C. N., Collett, J., Jr., Richards, L. W., and Pandis, P. N. Production and Removal of Aerosol in a Polluted Fog Layer: Model Evaluation and Fog Effect on PM. Atmos. Environ. 33:4797–4816, 1999

Matsumoto, J., Imai, H., Kosugi, N., and Kaji, Y.: In situ measurement of N_2O_5 in the urban atmosphere by thermal decomposition/laser-induced fluorescence technique, Atmos. Environ., 39, 6802–6811, 1995.

Morris, E. D., and Niki, H. Reaction of Dinitrogen Pentoxide with Water. J. Phys. Chem. 77:1929–1932, 1973.

Mozurkewich, M., and Calvert, J. G. Reaction Probability of N_2O_5 on Aqueous Aerosols. J. Geophys. Res. 93:15889–15896, 1988.

Nowak, J. B., Neuman, J. A., Kozai, K., Huey, L. G., Tanner, D. J., Holloway, J.S., Ryerson, T. B., Frost, G. J., McKeen, S. A., and Fehsenfeld, F. C.: A chemical ionization mass spectrometry technique for airborne measurements of ammonia, J. Geophys. Res.-Atmos., 112, D10S02, DOI:10.1029/2006JD007589, 2007.

Osthoff, H., Roberts, J. M., Ravishankara, A. R., Williams, E. J., Lerner, B. M., Sommariva, R., Bates, T. S., Coffman, D., Quinn, P. K., Dibb, J. E., Stark, H., Burkholder, J. B., Talukdar, R. K., Meagher, J., Fehsenfeld, F. C., and Brown, S. S.: High levels of nitryl chloride in the polluted subtropical marine boundary layer, Nat. Geosci., 1, 324–328, doi:10.1038/ngeo177, 2008.

Platt, U., Perner, D., Winer, A. M., Harris, G.W., and Pitts, J. N.: Detection of NO_3 in the polluted troposphere by differential optical-absorption, Geophys. Res. Lett., 7(1), 89–92, 1980.

Phillips, G. J., Tang, M. J., Thieser, J., Brickwedde, B., Schuster, G., Bohn, B., Lelieveld, J., and Crowley, J. N.: Significant concentrations of nitryl chloride observed in rural continental Europe associated with the influence of sea salt chloride and anthropogenic emissions, Geophys. Res. Lett., 39, L10811, doi:10.1029/2012gl051912, 2012.

Riemer, N., Vogel, H., Vogel, B., Schell, B., Ackermann, I., Kessler, C., and Hass, H.: Impact of the heterogeneous hydrolysis of N2O5 on chemistry and nitrate aerosol formation in the lower troposphere under photosmog conditions, J. Geophys. Res., 108, 4144,
doi:10.1029/2002jd002436, 2003.

Slusher, D. L., Huey, L. G., Tanner, D. J., Flocke, F. M., and Roberts, J. M.: A thermal dissociation-chemical ionization mass spectrometry (TD-CIMS) technique for the simultaneous measurement of peroxyacyl nitrates and dinitrogen pentoxide, J. Geophys. Res.-Atmos., 109, D19315, DOI: 10.1029/2004JD004670, 2004.

Smith N, Plane J M C, Nien C F, Solomon P A. Nighttime radical chemistry in the San Joaquin valley. Atmos Environ, 29: 2887– 2897, 1995.

Stark, H., Lerner, B.M., Schmitt, R., Jakoubek, R., Williams, E.J., Ryerson, T.B., Sueper, D.T., Parrish, D.D., Fehsenfeld, F.C.: Atmospheric in situ measurement of nitrate radical (NO3) and other photolysis rates using spectroradiometry and filter radiometry. J. Geophys. Res-Atmos. 112(D10S04), doi:10.1029/2006JD007578, 2007.

Stelson, A.W., Seinfeld, J.H. Relative humidity and temperature dependence of the ammonium nitrate dissociation constant. Atmospheric Environment 16 (5), 983–992, 1982a.

Stewart, D. J., Taylor, C. M., Reeves, C. E., McQuaid, J. B., Biogenic nitrogen oxide emissions from soils: impact on NOx and ozone over west Africa during AMMA (African Monsoon Multidisciplinary Analysis: observational study, Atmos. Chem. Phys., 8, 2285-2297, 2008.

Thornton, J. A., Kercher, J. P., Riedel, T. P.,Wagner, N. L., Cozic, J., Holloway, J. S., Dub´ e,W. P., Wolfe, G. M., Quinn, P. K., Middlebrook, A. M., Alexander, B., and Brown, S. S.: A large atomic chlorine source inferred from mid-continental reactive nitrogen chemistry, Nature, 464, 271– 274, doi:10.1038/nature08905, 2010.

Wood, E. C., Wooldridge, P. J., Freese, J. H., Albrecht, T., and Cohen, R. C.: Prototype for in situ detection of atmospheric NO3 and N2O5 via laser-induced fluorescence, Environ. Sci. 30 Technol., 37, 5732–5738, doi:10.1021/es034507w, 2003.

Yu, S., Dennis, R., Roselle, S., Nenes, A., Walker, J., Eder, B., Schere, K., and Swall, J. An Assessment of the Ability of 3-D Air Quality Models with Current Thermodynamic Equilibrium Models to Predict Aerosol NO3. J. Geophys. Res., 110:D07S13, 2005.

Zheng, J., Zhang, R., Fortner, E. C., Volkamer, R. M., Molina, L., Aiken, A. C., Jiminez, J. L., Gaeggeler, K., Dommen, J., Dusanter, S., Stevens, P. S., and Tie., X.: Measurements of HNO_3 and N_2O_5 using ion drift-chemical ionization mass spectrometerduring the MILAGRO/MCMA-2006 campaign, Atmos. Chem. Phys., 8. 6823-6838, 2008.

6. Conclusions

A CIMS has been implemented for 1 Hz simultaneous measurements of trace gases on the FAAM BAe-146 research aircraft over the UK and Canada using the methyl iodide ionisation scheme. The instrument attained sensitivities up to 35 ion counts ppt^{-1} with limits of detection in the low ppt range (5 ppt for HCN). Simultaneous measurements of HC(O)OH, HNO_3 and N_2O_5 were successfully made during the RONOCO campaign, supporting the research aim to determine the morphology of tropospheric NO_3 in different meteorological conditions and seasons. The CIMS measured HCN and HC(O)OH during the BORTAS 2011 campaign to accurately identify biomass burning plumes, enabling the assessment of how chemicals emitted from forest fires in North America change as they are transported away from the source. The accurate 1 Hz measurements of trace gases in the troposphere have enabled trajectory models to improve their accuracy on the production pathways and subsequently further our understanding of their role in controlling air quality. The simultaneous measurement of important trace species in the daytime and nighttime enabled a lifetime of 3.5 minutes for N_2O_5 and a production rate of 30 ppt min^{-1} for HNO_3 to be calculated. This supports the modelling work of Jones *et al*., (2005) showing how HNO_3 production from N_2O_5 can be an efficient sink for NO_x.

6.1 Instrumental conclusions

An aircraft sampling system was developed consisting of two separate inlets, 580 mm in length, resulting in a low residence time, 0.7 seconds, subsequently reducing the wall surface interaction with sticky molecules such as HNO_3 and optimising the signal to noise ratio. The sample inlet was lined with PFA tubing and heated to 75 degrees Celsius to further reduce loss to the walls. An acid scrubber was implemented on the background inlet to enable in-flight backgrounds and calibrations to be taken, allowing the sensitivity of the CIMS to be calculated at any point during operation.

An in situ calibration system was developed for HC(O)OH and HNO_3 in such a way to enable the HNO_3 and HC(O)OH calibrants to be controlled remotely through the local area network on the aircraft. These calibrations were implemented to test the stability of the CIMS sensitivity under varying operating conditions. An altitudinal dependency experiment was performed during the RONOCO campaign in 2011 where a number of calibrations were made from ground level up to 9200 feet. The results showed no change

of sensitivity for HC(O)OH and HNO_3 across these altitudes, indicating a stable sensitivity throughout flights.

Laboratory experiments investigated the dependency of CIMS sensitivity with varying $I^-.H_2O$ signal counts. The results found that above a threshold level of 1 million counts s^{-1} of $I^-.H_2O$ the CIMS sensitivity is independent of signal counts of that mass. Below this threshold, a linear decay is observed which has been quantified and is successfully accounted for into the data analysis. It must be noted that the instrument can be tuned in such a way that $I.H_2O$ counts do not fall below this threshold. This is achieved by balancing a high sensitivity with high mass resolution. An N_2O_5 calibration has also been developed in the laboratory and it has been shown that the CIMS sensitivity to HC(O)OH is linear to that for N_2O_5. This has enabled accurate, direct measurements of N_2O_5 to be obtained without the use of a N_2O_5 calibration system during the campaigns, on the basis of a relative calibration.

A CIMS data analysis toolkit was developed specifically for aircraft observations. This toolkit allows data to be analysed efficiently post flight. The general user interface takes the raw CIMS signal and allows users to process the data easily by applying corrections for background counts, sensitivities and choosing a data averaging period.

6.2 Observational conclusions

The first ever measurements of HC(O)OH over the UK on the FAAM BAe-146 aircraft enabled the detection of urban and industrial plumes from London, Humberside and Tyneside (Paper A). HC(O)OH observed showed no correlation with known anthropogenic markers such as NO_x, CO and O_3. A trajectory model showed an under-prediction of concentrations by up to a factor of 2, which can be resolved by the addition of 1-alkene surface emissions that oxidise to form HC(O)OH. This flight highlighted how the model cannot reproduce the measured concentrations because of the lack of precursor emissions and direct HC(O)OH emissions from anthropogenic activity.

The first simultaneous measurements of HC(O)OH and HNO_3 around Britain showed how measurements of HNO_3 can be a strong indicator of plume activity as peaks of HC(O)OH and HNO_3 can indicate a degree of ageing, validated by O_3 and NO_x measurements (Paper

B). Although HNO_3 and HC(O)OH correlations suggest photochemical production of the species, as noted by Veres *et al*. (2010), further analysis reveals a direct emission of HC(O)OH and strong secondary production when O_3 concentrations are high, indicating the significance of ozonolysis of 1-alkenes for HC(O)OH production. Trajectory models failed to reproduce the observed HC(O)OH levels, as also observed in paper A. This inaccuracy was improved through the inclusion of vehicular primary sources, but a significant amount of propene equivalent 1-alkene is required to match the measured concentrations. This rich information attained from this flight concludes that the relation between HNO_3 and HC(O)OH cannot be attributed to related photochemical production exclusively.

The first high sensitivity (3±0.6 ion counts s^{-1} $pptv^{-1}$) HCN measurements using I^- chemistry from boreal forest fires over Canada were made during the BORTAS campaign in 2011 (Paper C). In conjunction with high sensitivity, a limit of detection of 5 ppt allowed the use of HCN as a marker for BB plumes, confirmed by a strong correlation with CH_3CN and CO. A successful validation of the 6 sigma methodology for plume definition was implemented by comparison with other available methods through its correlation with CO. A normalised excess mixing ratio (NEMR) ratio to CO obtained via this method was found to be in range of that found in the literature, confirming the accuracy of this method and data obtained by CIMS. The NEMR from this work was then used to calculate a global emission total for HCN of 0.92 Tg (N) yr^{-1} when applied in the STOCHEM CRI model. NEMR`s stated in the literature produced too high or small global emission values when implemented into the model, therefore validating the NEMR obtained in this work.

An airborne comparison between the CIMS and BBCEAS during the RONOCO campaign illustrated how both techniques can precisely and rapidly measure N_2O_5 in the troposphere (Paper D). The CIMS is also the first instrument to directly measure N_2O_5 on an aircraft. An R^2 correlation coefficient value of 0.89 was obtained when comparing 1 Hz data from the CIMS and BBCEAS over 5 flights. The high correlation between the techniques (R^2 = 0.93) and correlation of CIMS HNO_3 with N_2O_5 indicates the significant production of HNO_3 from the hydrolysis of N_2O_5. Simultaneous NO_2 measurement also aided the validation of the N_2O_5 plumes and transition from day to night time chemistry.

The results presented in this thesis have shown the versatility of the CIMS using I^- as the ionisation scheme to measure a number of trace species in the troposphere at low ppt concentrations on board an airborne platform. CIMS is able to take 1 Hz simultaneous measurements of trace gases and can be implemented as a powerful and robust method to further our knowledge of trace gas sources and evolution.

7. Further work

7.1 Instrumental development

An increase in the CIMS sensitivity and precision can be achieved by upgrading the Manchester CIMS to a Chemical Ionisation Time-of-Flight Mass Spectrometer (CI-TOF-MS), such as that described by Bertram *et al*. (2011). Sensitivities of over 300 ion counts ppt^{-1} have been achieved for formic acid measurements with ion duty cycles greater than 20%, lowering the instruments limit of detection to 4 ppt and attain an error of 5% at 1 second averages. This development by Bertram *et al*. (2011) allows full mass spectra to be obtained at 10 Hz. The ability to attain mass spectra and full width half max values of 900 Thomsons (Th) enable the mass spectrometer to resolve peaks at masses which differ by only 0.004 Th. The instrument is then able to provide greater detail on altitude profiles and plume development. Consecutive mass spectra attained at a high frequency also allow the possible detection of compounds which are not already being monitored. Constraining and quantifying the clustering and fragmenting of ions when using different ionisation schemes would also be more accurate.

The raw data that CIMS produces during sampling is processed post flight due to limitations of the software. The CIMS analysis toolkit is to be developed so real time calibrated data is available in flight for future campaigns. Real time data allow the operator not only to be able to gain further understanding of the operational performance of the instrument in flight, but also provides the science team with important information as to plume strength and location. As many flight paths are determined through the information provided by online real time measurements, the CIMS will be able to support these decisions based on its trace gas measurements. Plume intersections, profiles and background concentrations provide the science team with valuable information. Real time data also allow for a more efficient flight planning process for upcoming flights as currently the data analysis takes at least 2 days.

7.2 HC(O)OH uncertainties

Dibb *et al*., (2002) suggested snow photochemistry as a possible source of HC(O)OH in the Arctic region which has not been included in current emission inventories. Anderson *et al*., (2008) offer further support to this claim by identifying HC(O)OH as a large fraction of the water soluble organic carbon in snow over the polar region.

Quantification of the sources based on satellite measurements are very difficult to obtain due to their restrictions in measuring only in the upper troposphere and lower stratosphere (Stavrakou *et al*., 2011). A lack of comprehensive measurements of HC(O)OH over the Northern Hemisphere mid to high latitudes at ground and airborne level also severely limits comparisons with model outputs. Therefore further aircraft and ground-based data are required to investigate the known and unknown sources and their contribution to the global formic acid budget.

7.3 Simultaneous measurements

The hydration of N_2O_5 to yield HNO_3, R6, is considered a relatively important source of HNO_3 at night as this reaction is not photochemically dependent (Finlayson-Pitts & Pitts Jr, 2000). Other sources of HNO_3 include NO_3 free radicals reacting with species with an abstractable hydrogen such as alkanes.

$$NO_3 + RH \rightarrow HNO_3 + R \qquad \textbf{R7}$$

(where R represents any species with an abstractable hydrogen)

Reactions 6 and 7 represent a sink for the strongest nighttime oxidant NO_3, therefore simultaneous measurements of HNO_3 and N_2O_5 on the aircraft will provide further detail and knowledge to the behaviour of these important nighttime species and their oxidising capacity.

The low deposition velocity of NH_4NO_3 to the Earth's surface allows the nitrogen footprint of a source region to change substantially depending on the equilibrium stated in R2, as long range transport is possible. Its formation through reaction between HNO_3 and NH_3 increases the importance of NH_4NO_3 in regional climate by contributing to the cooling effect of aerosol. NH_4NO_3 was found to be the dominant chemical component of the sub-

micron aerosol burden over Northern Europe (Morgan *et al.,* 2010). Constraining NH_4NO_3 concentrations in models has proven to be challenging as it is relatively volatile and its concentration is dependent on the associated gaseous HNO_3 and NH_3. The difficulty in measuring HNO_3 and NH_3 at low ppt concentrations at high frequencies has inhibited our ability to obtain an accurate picture of this nitrogen burden.

The ability for CIMS to measure positive and negative ions provides the possibility for two ionisation gases to be used simultaneously to measure HNO_3 and NH_3. The CIMS would be developed to automatically change between positive ion and negative ion detection mode to implementing the I^- ionisation scheme to detect HNO_3 and an ionisation gas such as protonated ethanol ions to detect NH_3 (Benson *et al*., 2010). This simultaneous measurement of HNO_3 and NH_3 using CIMS with low limits of detection and 1 second time integration will allow the assessment of the co-variability and phase partitioning of NH_3, HNO_3 and NH_4NO_3 in different regions around the UK onboard and aircraft. The co-evolution downwind of plumes can also be studied.

7.4 Detection of new species

Nitryl chloride ($ClNO_2$) is known to be a nighttime reservoir of NO_x and due to its photolysis at sunrise (R8), at a time when oxidants such as O_3 and OH are at a minimum, it can play a major role in affecting the oxidising capacity of the troposphere through halogen activation (Logan *et al*., 1981). $ClNO_2$ is detectable using methyl iodide as the ionisation gas at mass 208 (Osthoff *et al.,* 2008). The development of a $ClNO_2$ permeation source enables the Manchester CIMS to calibrate $ClNO_2$. A sea salt scrubber has been created to produce $ClNO_2$ in the laboratory, as shown by reaction 9, and is currently being tested in a ground based measurement campaign.

$$ClNO_2 + hv \rightarrow Cl + NO_2 \qquad \textbf{R8}$$

$$N_2O_5 + NaCl \rightarrow ClNO_2 + NaNO_3 \qquad \textbf{R9}$$

Simultaneous measurements of N_2O_5, $ClNO_2$ and HNO_3 will further our understanding of the balance of nighttime chemistry through availability of NO_3 and reservoirs of oxidants in nitric acid and $ClNO_2$.

7.5 Criegee intermediate chemistry

There are currently limited data in the world on the impact of CI on tropospheric composition and chemistry. In the UK, Harrison *et al* (2004) have shown that OH production by O_3-alkene initiation was dominated by CI decomposition chemistry and subsequently makes it a significant source of OH in both summer and winter in urban areas. Mauldin *et al.,* (2012) has also shown how 50% of H_2SO_4 in Northern European boreal regions comes from the reaction of SO_2 with an unknown organic oxidant, postulated to be CI. Lu *et al.,* (2011) observed enhancements of OH that were 3 to 5 times higher than expected in China. They hypothesize that the species responsible for this enhancement can form OH independent of NO_x. Further research is required which correlates organic species levels with H_2SO_4 and OH levels with resolved diurnal variations to evaluate the model impact that CI intermediates have on the oxidizing capacity of the troposphere for the first time.

Measurements of HNO_3, NH_3, HC(O)OH and H_2SO_4 by CIMS coupled with simultaneous measurements of OH, alkenes and aerosols will enable the assessment and quantification of:

- The impact of the reaction between CI and SO_2 for the first time
- The link between CI and HO_x formation
- Impact of CI on gas/aerosol partitioning and aerosol nucleation
-

This work will support an overall assessment of the impact of CI chemistry on regional air quality.

8. References

Adams, P. J., Seinfeld, J. H., Koch, D. M, Mickley, L., and Jacob, D.: General circulation model assessment of direct radiative forcing by the sulphate-nitrate-ammonium-water inorganic aerosol system, J. Geophys. Res., 106, 1097–1111, 2001.

Adams, P. J., Seinfeld, J. H., Koch, D., Mickley, L., and Jacob, D.: General circulation model assessment of direct radiative forcing by the sulfate-nitrate-ammonium-water inorganic aerosol system, J. Geophys. Res., 106, 1097–1111, 2011.

Allan, J, D., McFiggans, G., Plane, J. M. C, Coe. H. and McFadyen, G. G.: The nitrate radical in the remote marine boundary layer, J. Geophys. Res., 105, 24,191– 24,204, 2000.

Anderson, J. G., Brune, W. H., and Proffitt, M. H.: Ozone destruction by chlorine radicals within the Antarctic vortex: the spatial and temporal evolution of C1O-O3 anticorrelation based on in situ ER-2 data, J. Geophys. Res., 94(D9), 11465–11479, 1989.

Andreae, M. O. and Merlet, P.: Emission of trace gases and aerosols from biomass burning, Global Biogeochem. Cy., 955–966, doi:10.1029/2000GB001382, 2001.

Appel, B.R., Povard. V., and Kothny, E. L.: Loss of nitric acid within inlet devices intended to exclude coarse particles during atmospheric sampling. Atmos. Environ, 22(11): p. 2535-2540, 1980.

Arijs, E., Brasseur, G.: Acetonitrile in the stratosphere and implications for positive ion composition, J. Geophys. Res. 91:4003–4016, 1986.

Arnold, F., Krankowsky, D., Marien, K. H.: First mass spectrometric measurements of positive ions in the stratosphere, Nature, 267:30, 1977.

Arnold, F., Henschen, G.: First mass analysis of stratospheric negative ions, Nature, 257:521–522, 1978.

Arnold, F., Fabian, R., Henschen, G., Joos, W.: Stratospheric trace gas analysis from ions: H_2O and HNO_3, Planet. Space Sci. 28:681–685, 1980.

Arnold, F., Knop, G., Ziereis, H.: Acetone measurements in the upper troposphere and lower stratosphere - implications for hydroxyl radical abundances. Nature, 321:505–507, 1986.

Arnold, F., and Hauck, G.: Lower Stratospheric Trace gas Detection Using Aircraft-Borne Active Chemical Ionization Mass Spectrometry, Nature, 315, 307-309, 1985.
Arnold, F., and Henschen, G.: First mass analysis of stratospheric negative ions, Nature, 275, 5210-522, 1978.

Aruffo, E., Di Carlo, P., Dari-Salisburgo, C., Biancofiore, F., Giammaria, F., Lee, J., Moller, S., Evans, M. J., Hopkins, J. R., Jones, C., MacKenzie, A. R., and Hewitt, C. N.: Observations of total peroxy nitrates and total alkyl nitrates during the OP3 campaign: isoprene nitrate chemistry above a south-east Asian tropical rainforest, Atmos. Sci. Phys. Disc., 12, 4797-4829, 2012.

Atkinson, R.: Kinetics and mechanisms of the gas-phase reactions of the nitrate (NO_3) radical with organic compounds, J. Phys. Chem. Ref. Data, 20, 459-507, 1991.

Atkinson, R.: Atmospheric chemistry of VOCs and NOx, Atmos. Environ., 34, 2063–2101, 2000.

Atkinson, R., Arey, J. Gas-phase tropospheric chemistry of biogenic volatile organic compounds: a review. Atmospheric Environment, 37, S197–S219, 2003

Bascum, R., Bromberg, P. A., Coast, D. L., Devlin, R., Dockery, D. W., Frampton, M. W., Lambert, W., Samet, J. M., Speizer, F. E., and Utell, M.: Health effects of outdoor air pollution, part 1, Atm. J. Respir. Crit. Care Med., 153, 3-50, 1996a.

Bascum, R., Bromberg, P. A., Coast, D. L., Devlin, R., Dockery, D. W., Frampton, M. W., Lambert, W., Samet, J. M., Speizer, F. E., and Utell, M.: Health effects of outdoor air pollution, part 1, Atm. J. Respir. Crit. Care Med., 153, 477-498, 1996b.

Beaver, M. R., Clair, J. M. St., Paulot, F., Spencer, K. M., Crounse, J. D., LaFranchi, B.W., Min, K. E., Pusede, S. E.,Wooldridge, P. J., Schade, G. W., Park, C., Cohen, R. C., and Wennberg, P. O.: Importance of biogenic precursors to the budget of organic nitrates:observations of multifunctional organic nitrates by CIMS and TD-LIF during BEARPEX 2009, Atmos. Chem. Phys., 12, 5773–5785, doi:10.5194/acp-12-5773-2012, 2012.

Benson, D. R., Markovich, A., Al-Refai, M., and Lee, S. H.: A chemical ionization mass spectrometer for ambient measurements of ammonia. Atmos. Meas. Tech., 3, 1075. doi:10.5194/AMT-3-1075, 2010.

Bertram, T. H., Kimmer. J. R., Crisp. T. A., Ryder. O. S., Yatavelli. R. L. N., Thornton. J. A., Cubison. M. J., Gonin. M., and Worsnop. D. R.: A field-deployable, chemical ionization time-of-flight mass spectrometer: application to the measurement of gas-phase organic and inorganic acids, Atmos. Meas. Tech. Discuss., 4, 1963–1987, 2011.

Bowes, S. M., Franics, M. and Laube, B. L.: Acute exposure to acid fog: Influence of breathing pattern on effective dose. Am. Ind. Hyg. Assoc. J., 56:143-150, 1995.

Brasseur, G., R. Zellner, A. De Rudder, and E. Arjis.: Is hydrogen cyanide a progenitor of acetonitrile in the atmosphere?, Geophys. Res. Lett., 12, 117– 120, 1985.

Brown, S. S.: Absorption spectroscopy in high-finesse cavities for atmospheric studies, Chem. Rev., 103, 5219–5238, doi:10.1021/cr020645c, 2003.

Burling, I. R., Yokelson, R. J., Griffith, D. W. T., Johnson, T. J., Veres, P., Roberts, J. M., Warneke, C., Urbanski, S. P., Reardon, J., Weise, D. R., Hao, W. M., and de Gouw, J.: Laboratory measurements of trace gas emissions from biomass burning of fuel types from the southeastern and southwestern United States, Atmos. Chem. Phys., 10, 11115–11130, doi:10.5194/acp-10-11115-2010, 2010.

Chapman, E. G., Kenny, D. V., Busness, K. M., Thorp, J. M., and Spicer, C. W.: Continuous airborne measurements of gaseous formic and acetic acids over the western North Atlantic, Geophys. Res. Lett., 22, 405–408, doi:10.1029/94GL03023, 1995.

Cicerone, R. J. and Zellner, R.: The atmospheric chemistry of hydrogen cyanide (HCN), J. Geophys. Res., 88, 10689–10696, 1983.
Coffey, M. T., Mankin, W. G., and Cicerone, R. J.: Spectroscopic detection of stratospheric hydrogen cyanide, Science, 214, 333–335, 1981.

Coheur, P.,F., Clarisse, L., Turquety, S., Hurtmans,D., and Clerbaux, C.: IASI measurements of reactive trace species in biomass burning plumes, Atmos. Chem. Phys. Disc., 9, 8757–8789, 2009.

Crosley, D. R.: NO_y Blue Ribbon panel, J. Geophys. Res., 101(D1), 2049–2052, doi:10.1029/95JD02276, 1996.

Crounse, J.D., McKinney, K.A., Kwan, A.J., and Wennberg, P.O.: Measurement of gas-phase hydroperoxides by chemical ionization mass spectrometry, Anal. Chem., 78, 6726-6732, 2006.

Cummings, T.F.: The treatment of cyanide poisoning. Occup. Med. (Lond), 54:82–85, 2004.

Day, D. A., Woolridge, P. J., Dillon, M. B., Thornton, J. A., Cohen, R. C.: A thermal dissociation laser-induced instrument for in situ detection of NO_2, peroxy nitrates, alkyl nitrates, alkyl nitrates, and HNO_3, J. Geophys. Res. Atmos., 107(D5-6): p. 14, 2002.

Dube, W. P., Brown, S. S., Osthoff, H. D., Nunley, M. R., Ciciora, S. J., Paris, M. W., McLaughlin, R. J., and Ravishankara, A. R.: Aircraft instrument for simultaneous, in situ measurement of NO_3 and N_2O_5 via pulsed cavity ring-down spectroscopy, Rev. Sci. Instrum., 77(3), 034101– 034101-11, doi:10.1063/1.2176058, 2006.

Eisele, F. L.: Identification of tropospheric ions, J. Geophys. Res., 91:7897–7906, 1986.

Evans, C. R., McHale, G.: The effect of SU-8 patterned surfaces on the response of the quartz crystal microbalance. Sensors and Actuators A: Physical, 123-24, 73-76, 2005.

Farman, J. C.,Gardiner, B. G., and Shanklin, J. D.: Large Losses of Total Ozone in Antarctica Reveal Seasonal ClO_x/NO_x Interaction, Nature, 315, 6016, 207–210, 1985.

Fehsenfeld, F.C., Huey, L. G., Leibrock, E., Dissly, R., Williams, E., Ryerson, T. B., Norton, R., Sueper, D. T., and Hartsell, B.: Results from an informal intercomparison of ammonia measurement techniques, J. Geophys. Res., 107(D24): p. 15, 2002.

Fehsenfeld, F., Ancellet, G., Bates, T. S., Goldstein, A. H., Hardesty, R. M., Honrath, R., Law, K. S., Lewis, A. C., Leaitch, R., McKeen, S., Meagher, J., Parrish, D. D., Pzzenny, A. A. P., Russel, P. B., Schlager, H., Seinfeld, J., Talbot, R., and Zbinden, R.: International Consortium for Atmospheric Research on Transport and Transformation (ICARTT): North America to Europe. Overview of the 2004 summer field study, J. Geophys. Res., 111, D23S01, doi:10.1029/2006JD007829, 2006

Finlayson-Pitts and B. J. Pitts, J. N.: Tropospheric air pollution: Ozone, airborne toxics, polycyclic aromatic hydrocarbons, and particles, Science, 276, 1045-1052, 1997.

Finlayson-Pitts and B. J. Pitts, J. N.: Chemistry of the Upper and Lower Atmosphere. Academic Press, 969, 2000.

Forster, P., Ramaswamy, V., Artaxo, P., Berntsen, T. K., Betts, R., W. Fahey, D. W., Haywood, J., Lean, J., Lowe, D. C., Myhre, G., Nganga, J., Prinn, R., Raga, G., Schulz, M., and Van Dorland, R.: Changes in atmospheric constituents and in radiative forcing, climate change 2007: The Physical Science Basis. Contribution of Working Group I to the Fourth Assessment Report of the Intergovernmental Panel on Climate Change, Cambridge University Press, Cambridge, United Kingdom and New York, NY, USA, 2007.

Geyer, A., B. Alicke, S. Konrad, T. Schmitz, J. Stutz, and U. Platt, Chemistry and oxidation capacity of the nitrate radical in the continental boundary layer near Berlin, J. Geophys. Res., 106, 8013–8026, 2001.

Goldan, P.D., Kuster, W. C., Albritton, D. L., Fehsenfeld, F. C., Connell, P. S., and Norton, R. B.: calibration and tests of the filter-collection method for measuring clean air, ambient levels for nitric acid, Atmos. Environ., 17(7): p. 1355-1364, 1983

Goldstein, A. H., Mckay, M., Kurpus, M. R., Schade, G. W., Lee, A., Holzinger, R., Rasmussen, R. A.: Forest thinning experiment confirms ozone deposition to forest canopy is dominated by reaction with biogenic VOCs, Geophys. Res. Lett., 31, 2004.

Goldstein, A. H., and Galbally, I. E.: Known and unexplored organic constituents in the earth`s atmosphere, Environmental Science and Technology, 41, 1514-1521, 2007.

Gregory, G. L., Hoell Jr, J. M., Huebert, B. J., Van Bramer, S. E., LeBel, P. J., Vat, S.A., Marinaro, R. M., Schiff, H. I., Hastie, D .R., Mackay, G. I., and Karecki, D. R.: An intercmparison or airborne nitric acid measurements, J. Geophys. Res., 95, NO. D7, P. 10,089, doi:10.1029/JD095iD07p10089, 1990.

González Abad, G., Bernath, P. F., Boone, C. D., McLeod, S. D., Manney, G. L., and Toon, G. C.: Global distribution of upper tropospheric formic acid from the ACE-FTS, Atmos. Chem. Phys., 9(20), 8039–8047, 2009.

Grosjean, D., Tuazon, E. C., and Fujita, E.: Ambient formic acid in southern California air: A comparison of two methods, Fourier transform infrared spectroscopy and alkaline trap-liquid chromatography with UV detection, Env. Sci. and Tech,, 24, 144-146, 1990.

Grosjean, D., Williams, E. L.: Photochemical pollution at two southern California smog receptors, J Air. Waste/ Man. Assoc, 805-809, 42,6, 2001.

Hagg, C., Szabo, I.: New Ion-Optical Devices Utilizing Oscillatory Electric-Fields .3. Stability Of Ion Motion In A two-dimensional octopole field. Int. J. Mass. Spectrom. Ion Proc., 73:277–294, 1986.

Hamm, S. and Warneck, P.: The interhemispheric distribution and the budget of acetonitrile in the troposphere, J. Geophys. Res. Atmos., 95 (D12), 20 593–20 606, 1990.

Hanson, D. R., and Ravishankara, A.R.: The Reaction Probabilities of Clono2 and N2o5 on Polar Stratospheric Cloud Materials. J. Geophys. Res. Atmos., 96:5081–5090, 1991b.

Hausmann, M., Brandenburger, U., Brauers, T., and Dorn, H. P.: Detetcion of tropsopheric OH radicals by long-path differential-optical-absorption spectroscopy: Experimental setup, accuracy, and precision, J. Geophys. Res, 102, D13, 16011-16022, 1997.

Harrison, R. M., Yin, J., Tilling, R. M., Cai, X., Seakins, P. W., Hopkins, J. R., Lansley, D. L., Lewis, A. C., Hunter, M. C., Heard, D. E., Carpenter, L. J., Creasey, D. J., Lee, J. D., Pilling, M. J., Carslaw, N., Emmerson, K. M., Redington, A., Derwent, D. G., Ryall, D., Mills, G., and Penkett, S. A.: Measurement and modelling of air pollution and atmospheric chemistry in the U.K. West Midlands conurbation: overview of the PUMA Consortium project, Sci. Total. Environ., 360, 5-25, 2006.

Herndon, S. C., Zahniser, M. S., Nelson, D. D., Shorter, J., McManus, J. B., Jiménez, R., Warneke, C., and de Gouw, J. A.: Airborne measurements of HCHO and HC(O)OH during the New England Air Quality Study 2004 using a pulsed quantum cascade laser spectrometer, J. Geophys. Res., 112, D10S03, doi:10.1029/2006JD007600l 2007.

Hirokawa, J., Kato, T., and Mafune, F.: In Situ Measurements of Atmospheric Nitrous Acid by Chemical Ionization Mass Spectrometry Using Chloride Ion Transfer Reactions, Anal. Chem., 81, 8380-8386, 2009.

Hoffmann, M. R., and Jacob, D. J.: Kinetics and mechanisms of the catalytic oxidation of dissolved sulfur dioxide in aqueous solution: an application to nighttime fog water chemistry. In Calvert, J. G.,SO_2, NO and NO_2 oxidation mechanisms: atmospheric considerations. Boston, MA Butterworth Publishers; pp. 101-172, 1984.

Horii, C. V.: Tropospheric reactive nitrogen speciation, deposition and chemistry at Harvard forest, Department of Earth and Planetary Sciences. Boston, Harvard University. PhD, 2002.

Hornbrook, R. S., Crawford, J. H., Edwards, G. D., Goyea, O., Mauldin, R. L., Olson, J. S., and C. A. Cantrell.: Measurements of tropospheric HO_2 and RO_2 by oxygen dilution modulation and chemical ionization mass spectrometry, Atmos. Meas. Tech., 4(4), 735-756, 2011.

Huang, G., Zhou, X., Deng, G., Qiao, H., and Civerolo, K.: Measurements of atmospheric nitrous acid, nitric acid and pernitric acid, Atmos. Environ., 36, 2225– 2235, 2002.

Hubler G, Hudson, P. K, Murphy, D. M, Nicks, D. K, Orsini, D., Parrish, D. D, Ryerson, T. B., Sueper, D. T., Sullivan, A., Weber, R.: Variability in ammonium nitrate formation and nitric acid depletion with altitude and location over California, J. Geophys. Res.,108, 2003a.

Huey, L.G., Hanson, D. R., and Howard, C. J.:Reactions of SF_6^- and I^- with Atmospheric Trace Gases, J. Phys. Chem., 99(14): p. 5001-5008, 1995.

Huey, L.G., Tanner, D., Slusher, D., Dibb, J., Arimoto, R., Chen, G., Davis, D., Buhr, M., Nowak, J., Mauldin, R., Eisele, F., and Kosciuch, E.: CIMS measurements of HNO_3 and SO_2 at the South Pole during ISCAT 2000, Atmos. Environ., 38(32): p. 5411-5421, 2004.

Huey, L. G.: Measurement of Trace Atmospheric Species by chemical ionisation mass spectrometry: speciation of reactive nitrogen and future directions, Mass Spectrom. Rev., 26, 166– 184, 2007.

Huey L. G., Dunlea E. J., Lovejoy E., R, Hanson D.,R, Norton R.,B, Fehsenfeld F., C, Howard C, J.: Fast time response measurements of HNO_3 in air with a chemical ionization mass spectrometer, J. Geophys. Res. Atmos., 103:3355–3360, 1998.

IPCC 2007. Summary for Policymakers, in Climate Change 2007: The Physical Science Basis: Contribution of Working Group 1 to the Fourth Assessment Report of the

Intergovernmental Panel on Climate Change. New York: Cambridge University Press, 2007.

Jacob, D.: Chemistry of OH in remote clouds and its role in the production of formic acid and peroxymonosulfate, J. Geophys. Res., 91, 9807–9826, 1986.

Jacobson, M. Z.: Global direct radiative forcing due to multicomponent anthropogenic and natural aerosols, J. Geophys. Res., 106, 1551–1568, 2001.

Jensen N. R., Hanson D. R., Howard C.J.: Temperature-Dependence of the Gas-Phase Reactions of CF_3O with CH_4 and NO, J. Phys. Chem., 98:8574–8579, 1994.

Johnston, H. S., Reduction of stratospheric ozone by nitrogen oxide catalysts from supersonic transport exhaust, Science, 173, 517–522, 1971.

Jones, R. L., S. M. Ball, and D. E. Shallcross, Small scale structure in the atmosphere: Implications for chemical composition and observational methods, Faraday Discuss., 130, 165–179, doi:10.1039/b502633b, 2005.

Keene, W. C., Galloway, J. N. and Holden, J. D.: Measurement of weak organic acidity in precipitation from remote areas of the world, J. Geophys. Res. Atmos., 88, 5122-5130, 1983.
Keene, W. C., & Galloway, J. N.: Considerations Regarding Sources for Formic and Acetic Acids in the Troposphere, J. Geophys. Res., 91, 11466-14474., 1986.

Keene, W. C., Mosher, B. W., Jacob, D. J., Munger, J. W., Talbot, R. W., Artz, R. S.: Carboxylic acids in clouds at high elevation forested site in central Virginia, J. Geophys. Res., 100, 9345-9357, 1995.

Kercher, J. P., Riedel, T. P., and Thornton, J. A.: Chlorine Activation by N_2O_5 : Simultaneous, In-Situ Detection of $ClNO_2$ and N_2 O_5 by chemical ionization mass spectrometry, Atmos. Meas. Tech., 2:193–204, 2009.

Kesselmeier, J., and Staudt, M.: Biogenic volatile organic compounds (VOC): An overview on emission, physiology and ecology, J. Atmos. Chem., 33, 23-88, 1999.

Kim, S., Huey, L. G., Stickel, R. E., Tanner, D. J., Crawford, J. H., Olson, J. R., Chen, G., Brune, W. H., Ren, X., Lesher, R., Wooldridge, P. J., Bertram, T. H., Perring, A., Cohen, R. C., Lefer, B. L., Shetter, R. E., Avery, M., Diskin, G., and Sokolik, I.: Measurement of HO_2NO_2 in the free troposphere during the intercontinental chemical transport experiment, North America 2004, J. Geophys. Res. Atmos., 112, D12s01, doi:10.1029/2006jd007676, 2007.

Kim, S. W., McKeen, S.A., Frost, G. J., Lee, S. H., Trainer, M., Richter, A., Angevine, W. M., Atlas, E., Bianco, L., Boersma, K. F., Brioude, J., Burrows, J. P., de Gouw, J., Fried, A., Gleason, J., Hilboll, A., ellqvist, J., Peischl, J., Richter, D., Rivera, C., Ryerson, T., te Lintel Hekkert, S., Walega, J., Warneke, C., Weibring, P., and Williams, E.: Evaluations of NOx and highly reactive VOC emission inventories in Texas and their implications for ozone plume simulations during the Texas Air Quality Study 2006, Atmos. Chem. Phys., 11, 11361–11386, 2011.

Kita, K., Morino, Y., Kondo, Y., Komazaki, Y., Takegawa, N., Miyazaki, Y., Hirokawa, J., Tanaka, S., Thompson, T. L., Gao, R. S., Fahey, D. W.: A chemical ionization mass spectrometer for ground based measurements of nitric acid, J. Atmos. Ocean, Tech, 23, 1104-1113, 2006.

Kleinbohl, A., Toon, G. C., Sen, B., Blavier, J.-F. L., Weisenstein, D. K., Strekowski, R. S., ¨ Nicovich, J. M., Wine, P. H., and Wennberg, P. O.: On the stratospheric chemistry of ydrogen cyanide, Geophys. Res. Lett., 33, L11806, doi:10.1029/2006GL026015, 2006.

Knighton, W. B., Fortner, E. C., Midey, A. J., Viggiano, A. A., Herndon, S. C., Wood, E. C., and Kolb, C. E.: HCN detection with a proton transfer reaction mass spectrometer, Int. J. Mass. Spectrom., 283, 112–121, 2009.

Knipping, E. M., and Daddub, D.: Impact of chlorine emissions from sea-salt aerosol on coastal urban ozone, Env. Sci.Tech., 37, 2, 275-284, 2003.

Kochian, K. V.: Cellular mechanisms of aluminium toxicity and resistance in plant.
Annu. Rev. Plant Physiol. Mol. Biol., 46, 237-260, 1995.

Komazaki, Y., Hashimoto, S., Inoue, T., and Tanaka, S.: Direct collection of HNO_3 and HCl by a diffusion scrubber without inlet tubes, Atmos. Environ., in press, 2001.

Krug, E. C., Frink, C. R.: Acid rain on acid soil: A new perspective, Science, 221, no. 4610, pp. 520-525, 1983.

Kurten, T., Petaja, T., Smith, J., Ortega, I. K., Sipila, M., Junninen, H., Ehn, M., Vehkamaki, H., Mauldin, L., Worsnop, D. R., Kulmala, M.: The effect of H_2SO_4 - amine clustering on chemical ionization mass spectrometry (CIMS) measurements of gas-phase sulfuric acid, Atmos. Chem. Phys., 11, 6, 3007-3019, 2011.

Landis, M. S., Stevens, R. Rk., Schaedlich, F., and Prestbo, E. M.: Development and Characterization of an Annular Denuder Methodology for the Measurement of Divalent Inorganic Reactive Gaseous Mercury in Ambient Air, Environ. Sci. & Techn., 36(13): p. 3000-3009, 2002.

Le Breton, M., Mcgillen, M.R., Muller, J.B.A., Bacak, A., Shallcross, D.E., Xiao, P., Huey, L.G., Tanner, D., Coe, H., Percival, C.J. Airborne observations of formic acid using a chemical ionisation mass spectrometer, Atmos. Meas. Tech., 4, 5807-5835, 2012.

Le Breton, M., Bacak, A., Muller, J. B. A., O`Shea, S. J., Xiao, P., Ahsfold, M. N. R., Cooke, M. C., Batt, R., Shallcorss, D. E., Oram, D. E., Forster, G., Bauguitte, S. J. B., and Percival, C.: Airborne hydrogen cyanide measurements using a chemical ionisation mass spectrometer for the plume identification of biomass burning forest fires, Atmos. Chem. Phys. Diss, 13, 5649–5685, 2013.

Le Breton, M., Bacak, A., Muller, J. A., Bannan, T. J., Kennedy, O., Ouyang, B., Xiao, P., Ashfold, M. N. R., Bauguitte, S. J. B., Shallcross, D. E., Jones, R. L., and Percival, C.: The first airborne inter-comparison of N_2O_5 measurements over the UK using a Chemical Ionisation Mass Spectrometer (CIMS) and Broadband Cavity Enhanced Absorption Spectrometer (BBCEAS) during the RONOCO 2010/2011 campaign, in preparation for submission, 2013.

Leather, K. E., McGillen, M., Cooke, M. C., Utembe, S. R., Archibald, A. T., Jenkin, M. E.: Acid-yield measurements of the gas-phase ozonolysis of ethene as a function of humidity using Chemical Ionisation Mass Spectrometry (CIMS), Atmos. Chem. Phys., 12, 469-479, 2012.

Li, S., Liu, W., Xie, P., Qin, M., and Yang.: Observation of nitrate radical in the nocturnal boundary layer during a summer field campaign in pearl river delta, China, Terr. Atmos. Ocean. Sci., 23, No. 1, 39-48, 2012

Li, Q. B., Jacob, D. J., Bey, I., Yantosca, R. M., Zhao, Y. J., Kondo, Y., and Notholt, J.: Atmospheric hydrogen cyanide (HCN): biomass burning source, ocean sink?, Geophys. Res. Lett., 27, 357–360, doi:10.1029/1999GL010935, 2000.
Li, Q., Jacob, D. J., Yantosca, R. M., Heald, C. L., Singh, H. B., Koike, M., Zhao, Y., Sachse, G. W., and Streets, D. G.: A global three-dimensional model analysis of the atmospheric budget of HCN and CH3CN: Constraints from aircraft and ground measurements, J. Geophys. Res., 15 108, 8827, doi:10.1029/2002JD003075, 2003.

Li, Q., Palmer, P. I., Pumphrey, H. C., Bernath, P., and Mahieu, E.: What drives the observed variability of HCN in the troposphere and lower stratosphere?, Atmos. Chem. Phys., 9, 8531– 8543, doi:10.5194/acp-9-8531-2009, 2009.

Liao, H., J. H. Seinfeld, P. J. Adams, and L. J. Mickley.: Global radiative forcing of coupled tropospheric ozone and aerosols in a unified general circulation model, J. Geophys. Res., 109, D16207, doi:10.1029/ 2003JD004456, 2004.

Levine, J. S.: Global biomass burning: A case study of the gaseous and particulate matter emissions released to the atmosphere during the 1997 fires in Kalimantan

and Sumatra, Indonesia, in Biomass burning and its inter-relationships with the climate system, edited by J. L. Innes, M. Beniston, and M. M. Verstraete, pp. 1-15, Dordrecht, Kluwer Academic Publishers, 2000

.

Levy, H., 1971: Normal atmosphere: Large radical and formaldehyde concentrations predicted, Science 173, 141–143.

Lobert, J. M., Scharffe, D. H., Hao, W. M., and Crutzen, P. J.: Importance of biomass burning in the atmospheric budgets of nitrogen-containing gases, Nature, 346, 552–554, 1990.

Logan, J. A., Prather, M. J., Wofsy, S. C., and McElroy, M. B.: Tropospheric chemistry – A global perspective, J. Geophys. Res., 86, 7210-7255, 1981.

Lu, K. D., Rohrer, F., Holland, F., Fuchs, H., Bohn, B., Brauers, T., Chang, C. C., Häseler, R., Hu, M., Kita, K., Kondo, Y., Li, X., Lou, S. R., Nehr, S., Shao, M., Zeng, L. M., Wahner, A., Zhang, Y. H., and Hofzumahaus, A.: Observation and modelling of OH and HO2 concentrations in the Pearl River Delta 2006: A missing OH source in a VOC rich atmosphere, Atmos. Chem. Phys. Discuss., 11 (4) 11311-11378, 2011.

Matsumoto, J., Imai, H., Kosugi, N., and Kaji, Y.: In situ measurement of N2O5 in the urban atmosphere by thermal decomposition/laser-induced fluorescence technique, Atmos. Env., 39, 6802–6811, 2005.

Mauldin, R. L., Berndt, T., Sipila, M., Paasonen, P., Petaja, T., Kim, S., Kurten, T., Stratmann, F., Kerminen, V.-M., and Kulmala, M.: A new atmospherically relevant oxidant of sulphur dioxide, Nature, 488, 193–196, doi:10.1038/nature11278, 2012.

McFiggans, G., Alfarra, M. R., Allan, J. D., Bower, K. N., Coe, H., Cubison, M., Topping, D. O., Williams, P. I., Decesari, S., Facchini, M. C., and Fuzzi, S.: Simplification of the representation of the organic component of atmospheric particulates, Faraday Disscuss., 130, 1–22, doi:10.1039/b419435g, 2005.

McNeill, V. F., Geiger, F. M., Loerting, T., Trout, B. L., Molina, L. T., and Molina, M. J.: Interaction of Hydrogen Chloride with Ice Surfaces: The Effects of Grain Size, Surface Roughness, and Surface Disorder, J. Phys. Chem., 111, 6274-6284, 2007.

Miller, T. M, Ballenthin, J. O, Meads, R. F, Hunton, D. E, Thorn, W. F, Viggiano, A. A, Kondo, Y., Koike, M., Zhao, Y. J.: Chemical ionization mass spectrometer technique for the measurement of HNO3 in air traffic corridors in the upper troposphere during the SONEX campaign, J. Geophys. Res. Atmos., 105:3701–3707, 2000.

Mohler O, Arnold F.: Flow reactor and triple quadrupole mass spectrometer investigations of negative-ion reactions involving nitric acid - Implications for atmospheric HNO_3 detection by chemical ionization mass spectrometry, J.Atmos. Chem., 13:33–61, 1991.

Molina, M., and Rowlan, F.: Stratospheric Sink for Chlorofluoromethanes: Chlorine Atomic Catalyzed Destruction of Ozone, Nature, 249, 5460, 810–2, 1974.

Monks, P. S.: Gas-phsae radical chemistry in the troposphere, Chem. Soc. Rev, doi: 10.1039/b307982c, 2005.

Morgan, W. T., Allan, J. D., Esselborn, M., Harris, B., Henzing, J. S., Highwood, E. J., Kiendler-Scharr, A., McMeeking, G. R., Northway, M. J., Osborjne, S., Williams, P. I., Krejci, R, and Coe, H.: Enhancement of the aerosol direct radiative effect by semi-volatile aerosol components: airborne measurements in North-Western Europe, Atmos. Chem. Phys., 10, 8151-8171, 2010.

Mount, G. H., J. W. Brault, P. V. Johnston, E. Marovich, R. O. Jakoubek, C. J. Voppe, J. Harder, and J. Olsen, Measurement of tropospheric OH by long-path laser absorption at Fritz Peak Observatory, Colorado, during the OH Photochemistry Experiment, fall 1993, J. Geophys. Res., 102, 6393– 6414, 1997.

Neuman, J.A., Huey, L. G., Ryerson, T. B., and Fahey.: Study of inlet materials for sampling atmospheric nitric acid. Environ. Sci. Tech., 33(7): p. 1133-1136, 1999.

Neuman, J. A, Gao, R. S, Fahey, D. W, Holecek, J. C., Ridley, B. A,Walega, J.G, Grahek, F.E., Richard, E.C., McElroy, C. T., Thompson, T.L., Elkins, J. W., Moore, F. L., Ray, E. A.: In situ measurements of HNO_3 ,NOy, NO_x and O_3 in the lower stratosphere and upper troposphere, Atmos. Environ., 35:5789–5797, 2001.

Neuman, J. A., Huey, L. G., Dissly, R. W., Fehsenfeld, F. C., Flocke, F., Holecek, J. C., Holloway, J. S., Hubler, G., Jakoubek, R., Nicks D, K., Parrish, D. D., Ryerson, T. B., Sueper, D. T., Weinheimer, A. J.: Fast-response airborne in situ measurements of HNO_3 during the Texas 2000 Air Quality Study, J. Geophys. Res., 107, 4436, 14 PP., 2002.

Norton, R. B.: Measurements of gas phase formic and acetic acids at the Mauna Loa, observatory, Hawaii During the Mauna Lao observatory photochemistry experiment 1988, J. Geophys. Res, 97, D10, 10,389-10,393, 1992.

Nowak, J. B., Neuman, J. A., Kozai, K., Huey, L. G., Tanner, D. J., Holloway, J.S., Ryerson, T. B., Frost, G. J., McKeen, S. A., and Fehsenfeld, F. C.: A chemical ionization mass spectrometry technique for airborne measurements of ammonia, J. Geophys. Res.-Atmos., 112, D10S02, DOI:10.1029/2006JD007589, 2007.

Okawada, N., Mizoguchi, I., and Ishiguro, T.: Effects of photochemical air pollution on the human eye concerning eye irritation, tear lysozyme and tear pH, J. Med. Sci., 41. 9-20, 1979.

Orzechowska, G. E. and Paulson, S. E.: Photochemical sources of organic acids. 1. Reaction of ozone with isoprene, propene, and 2-butenes under dry and humid conditions using SPME, J. Phys. Chem., 109, 5358–5365, 2005.

Osthoff, H., Roberts, J. M., Ravishankara, A. R., Williams, E. J., Lerner, B. M., Sommariva, R., Bates, T. S., Coffman, D., Quinn, P. K., Dibb, J. E., Stark, H., Burkholder, J. B., Talukdar, R. K., Meagher, J., Fehsenfeld, F. C., and Brown, S. S.: High levels of nitryl chloride in the polluted subtropical marine boundary layer, Nat. Geosci., 1, 324–328, doi:10.1038/ngeo177, 2008.

Pepenbrock, T. H, and Stuhl, F.: A laser-photolysisfragment-fluorescence (LPFF) method for the detection of gaseous nitric acid in ambient air, J. Atmos. Chem., 10, pp 451-469, 1990a.

Parrish, D. D., Fehsenfeld, F.C.: Methods for gas-phase measurements of ozone, ozone precursors and aerosol precursors, Atmos. Environ., 34:1921–1957, 2000.

Paulot, F., Wunch. D., Crounse.J. D., Toon.G.C., Millet. D. B., DeCarlo. P.F., Vigouroux. C., Deutcher. N.M., Gonzalez Abad.g., Notholt. J., Warneke. T., Hannigan. J.W., de Gouw. J. A., Dunlea. E.J., De Maziere. M., Griggith. D.W.T., Bernath. P., Jiminez. J. L., and Wennberg. P.O.: Importance of secondary sources in the atmospheric budgets of formic and acetic acids, Atmos. Chem. Phys., 10, 1989–2013, 2011.

Rinsland, C. P., Mahieu, E., Zander, R., Goldman, A., Wood, S. and Chiou, L.: Free tropospheric measurements of formic acid (HC(O)OH) from infrared ground-based solar absorption spectra: Retrieval approach, evidence for a seasonal cycle, and comparison with model calculations, J. Geophys. Res.-Atmos., 109, D18308, DO1:10.1029/2004JD004917, 2004.

Rinsland, C. P., Mahieu, E., Zander, R., Demoulin, P., Forrer, J., and Buchmann, B.: Free tropospheric CO, C_2H_6, and HCN above central Europe: Recent measurements from the Jungfraujoch station including the detection of elevated columns during 1998, J. Geophys. Res., 105, 24235–24249, 2000.

Rinsland, C. P., Goldman, A., Hannigan, J. W., Wood, S. W., Chiou, L. S., and Mahieu, E.: Long-term trends of tropospheric carbon monoxide and hydrogen cyanide from analysis of high resolution infrared solar spectra, J. Quant. Spectrosc. Radiat. Transfer., 104, 40–51, 2007.

Rinsland C. P., Boone C. D. Bernath P. F., Mahieu E., Dufour G. R. Z., Clerbaux C., Turquety S., Chiou L., McConnell J. C., Neary L., & Kaminski J. W.: First space-based observations of formic acid (HC(O)OH): Atmospheric Chemistry Experiment austral spring 2004 and 2005 Southern Hemisphere tropical-mid-latitude upper tropospheric measurements, Geophys. Res. Lett., 33, L23804, 2006.

Roberts, J. M., Osthoff, H. D., Brown, S. S., Ravishankara, A. R., Coffman, D., Quinn, P., and Bates, T.: Laboratory studies of products of N_2O_5 uptake on Cl containing substrates. J. Geophys. Res. Lett., 36, L20808, doi:10.1029/2009GL040448, 2009.

Roberts, J. M., Veres, P., Warneke, C., Neuman, J. A., Washenfelder, R. A., Brown, S. S., Baasandorj, M., Burkholder, J. B., Burling, I. R., Yokelson, R. J., Lerner, B. J., Gilma, J. B., Kuster, W. C., Fall, R. and de Guow, J.: Measurement of HONO, HNCO, and other inorganic acids by negative-ion proton-transfer chemical-ionization mass spectrometry (NI-PT-CIMS): application to biomass burning emissions, Atmos. Meas. Tech., 4, 981-990, 2010.

Roberts, J. M., Veres, P., Cochran, A. K., Warneke, C., Baasandorj, M., Burkholder, J. B., Burling, I. R., Johnson, T. J., Yokelson, R. J., and de Guow, J.: Isocyanic acid in the atmosphere and its possible link to smoke-related health effects, PNAS, 108, 8966-8971, 2011.

Sanhueza, E., Figueroa, L. and Santana, M.: Atmospheric formic and acetic acids in Venezuela, Atmos. Environ., 30, 1861-1873, 1996.

Schneider, J., Burger, V., and Arnold, F.: Methyl cyanide and hydrogen cyanide measurements in the lower stratosphere: Implications for methyl cyanide sources and sinks, J. Geophys. Res., 102, 25501–25506, 1997.

Seeley, J. V., Morris, R. A., Viggiano, A. A.: Rate constants for the reactions of CO_3 - (H_2O), SO_2: Implications for CIMS detection of SO_2, Geophys. Res. Lett., 24:1379–1382, 1997.

Seinfeld, J. H. and Pandis, S. N.: Atmospheric chemistry and physics – from air pollution to climate change, John Wiley & Sons, New York, 1998.

Shim, C., Wang, Y., Singh, H. B., Blake, D. R., and Guenther, A. B.: Source characteristics of oxygenated volatile organic compounds and hydrogen cyanide, J. Geophys. Res., 112, D10305, doi:10.1029/2006JD007543, 2007.

Simon, H., Kimura, Y., McGaughey, G., Allen, D. T., Brown, S. S., Osthoff, H. D., Roberts, J. M., Byun, D., and Lee, D.: Modeling the impact of ClNO2 on ozone formation in the Houston area, J. Geophys. Res., 114, D00F03, doi:10.1029/2008JD010732, 2009.

Simpson, W. R.: Continuous wave cavity ring-down spectroscopy appliedto in situ detection of dinitrogen pentoxide (N_2O_5), Rev. Sci. Instrum., 74:3442–3452, 2003.

Simpson, W. R., von Glasow, R., Riedel, K., Anderson, P., Ariya, P., Bottenheim, J., Burrows, J., Carpenter, L. J., Frieß, U., Goodsite, M. E., Heard, D., Hutterli, M., Jacobi, H.-W., Kaleschke, L., Neff, B., Plane, J., Platt, U., Richter, A., Roscoe, H., Sander, R., Shepson, P., Sodeau, J., Steffen, A., Wagner, T., and Wolff, E.: Halogens and their role in polar boundary-layer ozone depletion, Atmos. Chem. Phys., 7, 4375–4418, doi:10.5194/acp-7-4375-2007, 2007.

Singh, H. B., Salas, L., Herlth, D., Koyler, R., Czech, E., Ciezee, W., Li, Q., Jacob, D. J., Blake, D., Sachse, G., Harward, C. N., Fuelberg, H., Kiley, C. M., Zhao, Y., and Kondo, Y.: In situ measurements of HCN and CH_3CN over the Pacific Ocean:Sources, sinks, and budgets, J. Geophys. Res., 108, NO. D20, 8795, doi:10.1029/2002JD003006, 2003

Slusher, D. L, Pitteri, S. J, Haman, B. J, Tanner, D. J, Huey, L. G. 2001.: A chemical ionization technique for measurement of pernitric acid in the upper troposphere and the polar boundary layer, Geophys. Res. Lett., 28:3875–3878, 2001.

Slusher, D. L., Huey, L. G., Tanner, D. J., Flocke, F. M., and Roberts, J. M.: A thermal dissociation-chemical ionization mass spectrometry (TD-CIMS) technique for the simultaneous measurement of peroxyacyl nitrates and dinitrogen pentoxide, J. Geophys. Res.-Atmos., 109, D19315, DOI: 10.1029/2004JD004670, 2004.

Smith, N., Plane, J. M. C., Nien, C. F., Solomon, P. A.: Nighttime radical chemistry in the San Joaquin valley, Atmos Environ., 29: 2887– 2897, 1995.

Speidel, M., Nau, R., Arnold, F., Schlager, H., and Stohl, A.: Sulfur dioxide measurements in the lower, middle and upper troposphere: deployment of an aircraft-based chemical ionization mass spectrometer with permanent in-flight calibration, Atmos. Environ., 41, 2427–2437, 2007.

Stavrakou, T., Muller, J.F., Peeters, J., Razavi, A., Clarisse, L., Clerbaux, C., Coheur, P.F., Hurtmans, D., De Maziere, M., Vigouroux, C., Deutscher, N.M., Griffith, D.W.T., Jones, N., and Paton-Walsh, C., 2012. Satellite evidence for a large source of formic acid from boreal and tropical forests, Nat. Geosci., 5, 1, 26-30, doi 10.1038/NGEO1354, 2012.

Stedman, D. H., and Niki, H.: Photolysis of nitrogen dioxide in air as measurement method for light intensity, Environ. Sci. Technol., 7 (8), pp 735–739 DOI: 10.1021/es60080a003, 1973.

Taatjes, C. A., Meloni, G., Selby, T. M., Trevitt, A. J., Osborn, D. L., Percival, C. J., and Shallcross, D. E.: Direct observation of the gas-phase Criegee intermediate (CH2OO), J. Am. Chem. Soc., 130, 11883–11885, 2008.

Tanner, D. J, Eisele, F. L.: Ions in oceanic and continental air masses. J. Geophys. Res. 96:1023., 1991.

Talbot, R.W., A.S. Vijgen, and R.C. Harriss, Measuring tropospheric HNO_3: Problems and prospectsf or nylon filter and mist chamber techniques, J. Geophys. Res., 95, 7553-7561, 1990.

Thornton, J. A., Kercher, J. P., Riedel, T. P., Wagner, N. L., Cozic, J., Holloway, J. S., Dube, W. P., Wolfe, G. M., Quinn, P. K., Middlebrook, A. M., Alexander, B., and Brown, S. S.: A large atomic chlorine source inferred from mid-continental reactive nitrogen chemistry, Nature, 464, doi:10.1038/nature08905, 2010.

Twomey, S.: Pollution and Planetary Albedo, Atmos. Environ., 8, 1251–1256, 1974.

Veres, P., Roberts, J. M., Warneke, C., Welsh-Bon, D., Zahniser, M., Herndon, S., Fall, R. and de Gouw, J.: Development of negative-ion proton-transfer chemical-ionization mass spectrometry (NI-PT-CIMS) for the measurement of gas-phase organic acids in the atmosphere, Int. J. Mass Spectrom., 274, 48–55, 2008.

Sanhueza, E., Figueroa, L. and Santana, M., Atmospheric formic and acetic acids in Venezuela, Atmos. Environ., 30, 1861-1873, 1996.

Veres, P. R., Roberts, J. M., Cochran, A. K., Gilman, J.B., Kuster, W.C., Holloway, J.S., Graus, M., Flynn, J., Lefer, B., Warneke, C., and de Gouw, J.: Evidence of rapid production of organic acids in an urban air mass, Geophys. Res. Lett., 38, L17807, 5 PP., 2011.

Von Kuhlmann, R., Lawrence, M. G., Crutzen, P. J. and Rasch, P. J.: A model for studies of tropospheric ozone and nonmethane hydrocarbons: Model evaluation of ozone-related species, J. Geophys. Res.-Atmos, 108, 4729, DOI:10.1029/2002JD003348, 2003.

Wayne, R. P., Barnes, I., Biggs, P., Burrows, J. P., Canosamas, C. E., Hjorth, J., Lebras, G., Moortgat, G. K., Perner, D., Poulet, G., Restelli, G., Sidebottom, H.: The Nitrate Radical - Physics, Chemistry, and the Atmosphere, Atmos. Environ., Part a-General Topics 25:1–203, 1991.

WHO: Air Quality Guidelines for Europe, 2nd edition, 2000.

Wood, E. C., Bertram, T. H., Wooldridge, P. J., and Cohen, R. C.: Measurements of N_2O_5, NO_2, and O_3 east of the San Francisco Bay, Atmos. Chem. Phys., 5, 483–491, 2005.

Wolff, S., Boddenberg, A., Thamm, J., Turner, W. V., and Gab, S.: Gas-phase ozonolysis of ethene in the presence of carbonyloxide scavengers, Atmos. Environ., 31, 2965–2969, 1997.

Worden, H., R. Beer, and C. P. Rinsland.: Airborne infrared spectroscopy of 1994 western wildfires, J. Geophys. Res., 102, 1287– 1299, 1997.

Xu, Z., Zhang, J., Yang, G., Hu, M.: Acyl peroxy nitrate measurements during the photochemical smog season in Beijing, China, Atmos. Chem. Phys. Discuss., 11, 10265–10303, 2011.

Yokelson, R. J., Burling, I. R., Urbanski, S. P., Atlas, E. L., Adachi, K., Buseck, P. R., Wiedinmyer, C., Akagi, S. K., Toohey, D. W., Wold, C. E.: Trace gas and particle emissions from open biomass burning in Mexico, Atmos. Chem. Phys., 11, 6787e6808, 2011.

Zander, R., Duchatelet, P., Mahieu, E., Demoulin, P., Roland, G., Auwera, J. V., Perrin, A., Rinsland, C. P., and Crutzen, P. J.: Formic acid above the Jungfraujoch during 1985–2007: observed variability, seasonality, but no long-term background evolution, Atmos. Chem. Phys., 10, 10047–10065, 2010.

Zhao, Y., Strong, K., Kondo, Y., Koike, M., Matsumi, Y., Irie, H., Rinsland, C. P., Jones, N. B., Suzuki, K., Nakajima, H., Nakane, H., and Murata, I.: Spectroscopic measurements of tropospheric CO, C2H6 , C2H2 , and HCN in northern Japan, J. Geophys. Res., 107, 4343, doi:10.1029/2001JD000748, 2002.

Zheng, J., Hu, M., Zhang, R., Yue, D., Wang, Z., Guo, S., Li, X., Bohn, B., Shao, M., He, L., Huang, X., Wiedensohler, A., and Zhu, T.: Measurements of gaseous H_2SO_4 by AP-ID-CIMS during CAREBeijing 2008 Campaign**,** Atmos. Chem. Phys., 11, 7755-7765, 2011.